Expression and role of Cyclin O in colorectal cancer

Kathi Künnemann

TESI DOCTORAL UPF / 2013

DIRECTOR DE LA TESI

Dr. Gabriel Gil Gómez

TUTOR DE LA TESI

Dr. Pura Muñoz Cànoves (Department of Experimental and Health Sciences, UPF)

Programa de Recerca en Càncer – IMIM Hospital del Mar

Für meine Eltern

Acknowledgements, Danksagung

4 years have gone since I arrived in Barcelona and started the thesis passing through good and not so good moments. Many people contributed to this work and made it possible for me to finally reach the end of this long journey.

First of all, I would like to thank Dr. Gabriel Gil Gómez for incorporating me in his group and letting me work on this project and perform the experiments, for his critical suggestions, for his patience with teaching me and his trust in me with this work. I would like to thank Dr. Pura Muñoz for her help and support in finding a PhD project, the fellowship and in general. I would also like to thank all the members of my PhD committee for having the time to meet and give their support and kind suggestions on this project.

I would like to thank the Generalitat de Catalunya for giving me the FI PhD fellowship in order to finance this thesis during 3 years. Additionally, I would like to thank the IMIM for the financial help in order to publish this thesis.

With Marta, Alex, Marc and Lara, and also Laura O. and Mercè, I could not have had better labmates during these 3 years of the thesis. I would like to thank Marta for the great immunostainings and all your help with the tissue preparations, as well as, all the good moments in the lab, your positivity and support. Also, thank you to Alex and Marc, for the help with experiments, the company to the mouse facility and the interpretations of results. Mostly, thank you for your supporting conversations whenever it was needed and the laughs. Thank you to Lara and Mercè for the conversations during lunch and the activities outside of the lab and Laura for being a great labcompany during the first months of the thesis and for the good times during coffee breaks in the PRBB and in the weekends. Muchisimas Gracias!!!

I would like to thank as well all the people from the Cancer department of the IMIM. I spent a really nice time during and in between experiments and could always find people having a moment for questions, to find a good protocol or a missing antibody when it was needed. Many thanks to Erika for the intestinal discussions ;-) and for sharing experimental techniques and also to Jordina and Erika for being there in the difficult and crazy moments of this thesis.

And thanks as well for all the small talk in between labs, the coffees, the thesis dinners, beer sessions and great volleymatches that I enjoyed so much. Moltes Gràcies a tots ;-)!!!

I would also like to thank people from outside of the IMIM who supported and advised me at some point during the time I spent on this thesis. Thank you to Anna Bigas lab for the gift of the APC min mice (IMIM).Thank you to the people from Pura Muñoz lab, thank you Dr. Cristina López Rodríguez and the people from J. Ayté's lab for helping to make my southern blot work so fast, thanks to the people from the PRBB animal facility for taking care of my mice, thanks to Francesc Alameda and the people from the Pathology unit of the Hospital del Mar for providing the tissue samples and for letting me use the equipment and thanks to Sergio Palomo-Ponce from Eduard Batlle lab for kind suggestions and sharing protocols.

The people from the master classes were the first contacts I made in Barcelona and became good friends during these 4 years. Thanks to Ana, Laura, Ester, Marina, Lorena and Federico for all the dinners and activities. Thanks to Ana Laura for introducing me to the wonderful world of the catalonian mountains and the climbing, and to all friends from the climbing group for the great weekends we spent that helped so well in disconnecting with the labwork. I would also like to thank Stefania for sharing coffees during incubation times in the PRBB and the activities outside of the lab.

Thanks to Sol and Elena, my spanish family replacements, for sharing a great flat and for making me feel like at home in Barcelona.

Zwischendurch auch mal deutsch zu sprechen war immer so entspannend und gut. Danke Sabine! Und Nadine, Danke für die motivierenden Worte wenn es nötig war und für das tolle Unterhaltungsprogramm neben den viel zu langen Schreibtagen in der Bibliothek.

Ich möchte an dieser Stelle ganz besonders und von ganzem Herzen meiner gesamten Familie und im speziellen meinen Eltern danken dafür, dass sie es möglich gemacht haben, dass ich bis hierher gekommen bin und diese Arbeit realisieren konnte und vor allem, dass sie immer für mich da sind, mich in jeder Hinsicht unterstützen und aufbauen wenn immer es nötig ist.

Thank you, Gracias and Danke to everyone!

Abstract

Cyclin O, a novel identified Cdk1 and Cdk2-binding cyclin, has been demonstrated to be required for apoptosis induced by intrinsic apoptotic stimuli. Because proteins implicated in apoptosis are often deregulated in cancer, we aimed to study the expression and role of Cyclin O in Colorectal carcinomas. We demonstrate that Cyclin O is overexpressed in CRC already during early stages of tumour development. Cyclin O expression correlated with a better prognosis of the CRC patients. Furthermore, we could show that loss of one Cyclin O allele leads to a higher adenoma count in a mouse model of CRC, the APC$^{min/+}$ mouse, suggesting that Cyclin O has tumour suppressor functions. Addtionally, we observed Cyclin O expression in the histologically normal APC$^{min/+}$ mouse- and in human peritumoral- intestinal epithelium. Accordingly, we hypothesise that Cyclin O could act as an early indicator of epithelial cell transformation to CRC.

Resumen

La Ciclina O, una ciclina que ha estat identificada recentment i que s'uneix amb Cdk1 i Cdk2, s'ha demostrat ser necessària per a l'apoptosis induïda per estímuls intrinsecs. Donat que les proteïnes implicades en apoptosis solen estar desregulades en el càncer, nosaltres hem volgut estudiar l'expressió i la implicació de la Ciclina O en carcinomes colorectals (CRC). Hem demostrat que la Ciclina O es sobreexpressa en estadis prematurs de CRC. L'expressió de la Ciclina O correlaciona amb una millor pronòstic en pacients amb CRC. A més, hem demostrat que la pèrdua d'un al·lel de la Ciclina O comporta l'aparició d'un major nombre d'adenomes en un model de ratolí de CRC, els ratolin s APC$^{min/+}$. Això ens indica que la Ciclina O funciona com un gen supressor de tumors. També hem observat expressió de la Ciclina O en teixits no tumorals de l'epitel·li intestinal dels ratolins APC$^{min/+}$ i en teixit peritumorals de pacients amb CRC. Amb aquestes observacions hem arribat a formular la hipòtesi de que la Ciclina O podria ser útil com a indicador precoç de la transformació de cèl·lula epitel·lial a tumoral en los pacientes de CRC.

Abstract 1
Abbreviations 7
Introduction 13
I1. The intestine, a short introduction 15
I1.1. Intestinal stem cells 19
I1.2. The Wnt signaling pathway 20
I2. Colorectal cancer 24
I2.1. Inherited colorectal cancer syndromes 24
I2.2. APC mutations in FAP and CRC 26
I2.3. CRC stages 28
I2.4. Animal models for CRC 33
I3. Cyclin O protein and apoptosis 37
I3.1. Cell death criteria 37
I3.2. Apoptosis 37
I3.3 The core biochemical machinery of apoptosis 40
I3.3.1. Caspases 40
I3.3.2. Bcl2 family of proteins 43
I3.4. Apoptotic signalling 45
I3.4.1. Intrinsic apoptotic pathway 45
I3.4.2. Extrinsic apoptotic pathway 46
I3.5. Cell shedding of intestinal epithelial cells 48
I3.6. Cyclin dependent kinases and Cyclins 49
I3.7. Cell cycle and apoptosis 51
I3.8. Cyclin O 53
Objectives 57
Materials and Methods 61
MM1. Anti Cyclin O antibodies 63
MM1.1. ELISA 64
MM1.2. Specificity of the antibody 64
MM2. Other antibodies 66
MM3. Cell culture 67
MM4. Cyclin O somatic knock out in HCT116 cells ... 67
MM4.1. The rAAV targeting construct 67
MM4.2. AAV virus production 69
MM4.3. AAV virus titration 70
MM4.4. AAV virus infection 70
MM4.5. Screening of the targeted clones 71
MM4.6. Cre mediated excision of neo selectable marker 74
MM4.7. Second round of targeting 75
MM4.8. Southern blotting 76
MM4.8.1. Preparation of the radioactive DNA probe 77

MM5. Isolation of genomic DNA and sequencing of the human Cyclin O gene 77
MM6. Subcellular fractionation and western blotting 78
MM6.1. Subcellular fractionation from CRC tissue or cell culture 78
MM6.2. Western blotting 80
MM7. Animals 80
MM8. Human colorectal tissue samples 81
MM9. Immunohistochemistry 84
MM9.1. Alcian blue staining 85
MM10. Statistical analysis 85
MM11. Commercial suppliers 86
Results 89
R1. Expression and clinical implication of Cyclin O in human colorectal cancer 91
R1.1. Expression of Cyclin O in normal human and mouse intestinal tissue 91
R1.2. Cyclin O protein is overexpressed in human colorectal cancer 94
R1.3. Cyclin O expression in fresh samples of CRC patients98
R1.4. Cyclin O expression correlates with a longer cancer specific survival of CRC patients 102
R1.5. Cyclin O overexpression is maintained in the metastasis of CRC 105
R1.6. MOCS2 is a putative target gene of Cyclin O in CRC107
R1.7. The Cyclin O gene is not mutated in human CRCs.. 112
R1.8. Significance of Cyclin O expression in CRC 113
R2. Role of Cyclin O in the mouse intestinal development 117
R2.1. Intestinal crypts are smaller in young Cyclin O deficient mice 117
R2.2. Cyclin O deficient mice have less proliferating intestinal crypt cells 118
R2.3. Cyclin O deficiency has no influence on the appearance of Goblet and Paneth cells in the mouse small intestine ... 121
R3. Implication of Cyclin O deficiency in adenoma formation in a mouse model of CRC, the APC$^{min/+}$ mouse 122
R3.1. Influence of Cyclin O on adenoma number and size in APC$^{min/+}$ mice 122
R3.2. Cyclin O deficient adenomas show more malignant features 126

R3.3. Cyclin O is expressed in the normal superficial intestinal epithelium surrounding the adenomas in APC$^{min/+}$ mice 129
R3.4. Cyclin O is expressed in morphogically normal epithelial cells of APC$^{min/+}$ mice 131

Discussion 135

D1. Expression of Cyclin O in normal human and mouse intestinal tissue 137

D1.1 Cyclin O protein is overexpressed in human CRC 138
D1.2. Cyclin O expression in fresh samples of CRC patients 144
D1.3. Cyclin O expression correlates with a longer cancer specific survival of CRC patients 146
D1.4. Cyclin O expression is maintained during metastasis149
D1.5. MOCS2 is a putative target gene of Cyclin O in CRC150
D1.6. The Cyclin O gene is not mutated in human CRCs.. 152
D1.7. Significance of Cyclin O expression in CRC 154

D2. Consequences of Cyclin O deficiency for mouse intestinal development 156

D2.1. Intestinal crypts are smaller in young Cyclin O deficient mice 156
D2.2. Cyclin O deficient mice have less proliferating intestinal crypt cells 158

D3. Implication of Cyclin O deficiency in adenoma formation in a mouse model of CRC, the APC$^{min/+}$ mouse 161

D3.1. Influence of Cyclin O on adenoma number and size in APC$^{min/+}$ mice 161
D3.2. Cyclin O deficient adenomas show more malignant features 164
D3.3. Cyclin O is expressed in normal epithelial cells surrounding the adenomas and in morphological normal epithelium 165

D4. Concluding remarks 168

Conclusions 173

Bibliography 177

Abbreviations

AAV : Adeno associated virus
ACF : Aberrant crypt foci
AJCC: American Joint Committee on Cancer
AOM : Azoxymethane
APC : Adenomatous Polyposis Coli
ATM : Ataxia Telangiectasia Mutated
Bcl-2 : B-cell lymphoma-2
bp : base pair
BrdU : Bromodeoxyuridine
BSA : Bovine Serum Albumin
C2 : Mouse Cyclin O antibody
CAF : Cancer associated fibroblast
CAK : Cdk Activating Kinase
CARD : Caspase Activation and Recruitment Domain
CBC : crypt based columnar cells
Cdk : Cyclin Dependent Kinase
CRC : Colorectal cancer
DAB : 3, 3’-diaminobenzidine
dCTP : Deoxycytidine triphosphate
DDF : differential detergent fractionation
DDR : DNA damage response
DED : Death Effector Domain
DISC : Death Inducing Signaling Complex
DNA : Deoxyribonucleic acid
DSS : dextran sodium sulphate
DTT : Ditiothreitol
ECM : Extracellular matrix
EDTA : Ethylenediaminetetraacetic Acid
FACS : Fluorescence activated cell sorting
FADD : Fas-associated death domain
FAP : Familial adenomatous polyposis
GFP : Green Fluorescent Protein
GSK3ß : Glycogen Synthase Kinase 3 ß
HC2 : Human Cyclin O antibody
HEOS : Haematoxylin Eosin staining
Het : Heterozygeous
HNPCC : Hereditary Non-Polyposis Colon Cancer
HRP : Horseradish peroxidase
IAP : Inhibitor of Apoptosis
ICE : Interleukin 1 ß Converting Enzyme
IHC : Immunohistochemistry
ISC : Intestinal stem cell
ITR : Inverted terminal repeat
Kb : kilo base pair

KO : knock out
LA : left arm homologous region
LDL : Low Density Lipoprotein
LEF : Lymphoid Enhancing Factor
LN : Lymph node
LOH : Loss of heterozygosity
LRP : LDL Receptor Related Protein
Min : Multiple intestinal neoplasia
MMR : DNA mismatch repair
MOMP : Mitochondrial outer membrane permeabilisation
MSI : Microsatellite instability
PBS : Phosphate buffered saline
PCR : Polymerase Chain Reaction
RA : right arm homologous region
RIPA : radioimmunoprecipitation assay buffer
ROS : Reactive oxygen species
RT : Room temperature
SDS : sodium dodecyl sulfate
SDS PAGE : SDS polyacrylamide gel electrophoresis
SEM : Standard error of mean
SSC : Saline-sodium citrate buffer
ssDNA : Single stranded DNA
SSPE : Saline-sodium phosphate EDTA buffer
TBS : Tris buffered saline
TBS-T : Tris buffered saline Tween 20
TCF : T Cell Factor
TCGA : The Cancer Genome Atlas
TGFß : Transforming Growth Factor ß
TGFBR2 : Transforming Growth Factor Receptor 2
TMA : Tissue micro array
TNF : Tumour Necrosis Factor
TNM : Tumour-Node-Metastasis
TRADD : TNF Receptor Associated Death Domain
TRAIL : TNF Related Tumour Apoptosis Inducing Ligand
WB : Western blotting
WT : wild type
ZFN : Zinc finger nucleases

Introduction

I1. The intestine, a short introduction

The intestine anatomically can be described as a tubular tissue extending from the stomach to the anus. It can be divided into duodenum, jejunum and ileum making up the small intestine, and caecum, colon and rectum, the parts forming the large intestine. The intestinal lumen is the inner part of the intestinal tube where nutrients, such as organic molecules from the diet, water and electrolytes are absorbed when passing through the small intestine and stool is compacted in the colon, two major digestive functions of the intestine. Regarding the tissues' architecture, the most inner layer of the intestine is called mucosa consisting of a monolayer of glandular epithelium, a connective tissue layer called the *lamina propria* and the *muscularis mucosae*, described as a thin layer of smooth muscle. The mucosa is surrounded by a dense layer of connective tissue, the submucosa, where blood vessels, lymphatics and nerves are located passing from the mucosa to the *muscularis externa* (Figure I1). The *muscularis externa* is mainly responsible for peristalsis in order to transport the food through the digestive tract. The submucosa and muscularis externa together make up the outer layers of the intestinal tube only surrounded by another layer of epithelium and connective tissue called serosa or serous membrane.

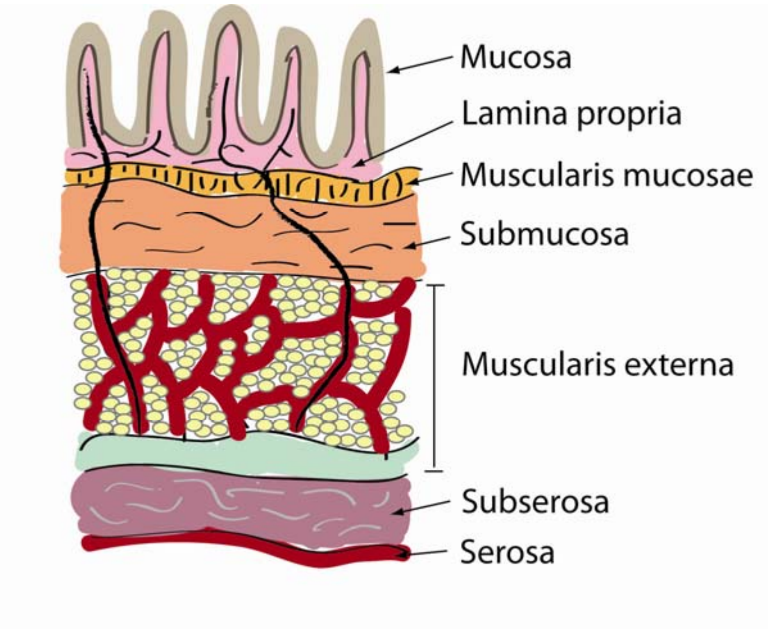

Figure I1. Intestinal tissue layers. Image adapted from AJCC Cancer Staging Manual, 7th edition.

The absorptive function of the small intestinal mucosa is increased by numerous villus and crypt structures. Intestinal villi can be described as protrusions of the epithelial cells into the lumen of the intestine and the so called crypts of Lieberkühn can be seen as invaginations into the submucosa [1]. Intestinal crypts complete their formation around day 7 of the postnatal life from proliferating intervillus regions, which as well as the villus structures, are formed during embryogenesis [2] [3]. Advancing from the adult duodenum towards the colon, the villi morphology changes: they become shorter towards the end of the small intestine and are completely missing in the colon, where they are replaced by a flat epithelial layer called surface epithelium due to functional changes of the intestinal tissue [4].

Epithelial cells of the intestine compared to other epithelial tissues have a relatively short life span. Throughout their life, they are continuously exposed to digestive enzymes and bile acids and suffer from a permanent mechanical stress. In order deal with these aggressions, the intestinal epithelium orchestrates a unique mechanism of constant cell migration starting from the crypts and going upwards to the luminal surface [5] or downwards towards the bottom of the crypts in the case of the Paneth cells [6].

Long-lived multipotent stem cells are present in the intestinal crypts and give rise to transit amplifying progenitors which upon constant upward migration undergo cell cycle arrest and terminally differentiate into the different intestinal cell lineages either when they have left the crypt compartment of the small intestine or when they progress upwards the colonic crypts. Once a differentiated cell has reached the villus tip or the colonic epithelial surface, it undergoes apoptosis and is shed into the lumen [7] [8].

It has been described that mouse small intestinal crypts contain an average of 250 cells supplying the surrounding villus epithelium. Approximately 150 of these cells are actively proliferating and are completing one cell cycle in around 12 – 13 hours [9]. Human crypts are more than 4 times the size of mouse crypts. Human colonic epithelial cells are able to migrate from the crypts bottom to the intestinal surface in around 3 to 8 days [10] [11].

Differentiated intestinal cells can be classified into one type of absorptive cells and four different secretory cell types (Figures I2, I3). The most abundant cells of the small intestine and colon are the absorptive enterocytes and colonocytes respectively [12]. They are able to absorb nutrients and carry characteristic microvilli that form a brush border. Enteroendocrine cells make up around 1 % of the small and large intestinal epithelium, scattered as individual cells which produce and secrete hormones. The most abundant secretory cell type are the Goblet cells, making up around 10 -15 % of the small intestinal and 50 % of the colonic epithelium [13]. They secrete mucus to provide epithelial cells with a protection against destructive contents in the lumen. Another secretory cell type that is believed to share a common progenitor with Goblet cells is the Paneth cell which is able to produce and secrete antimicrobial peptides into the lumen. Paneth cells are absent in the large intestine [2 3 14 15 6].

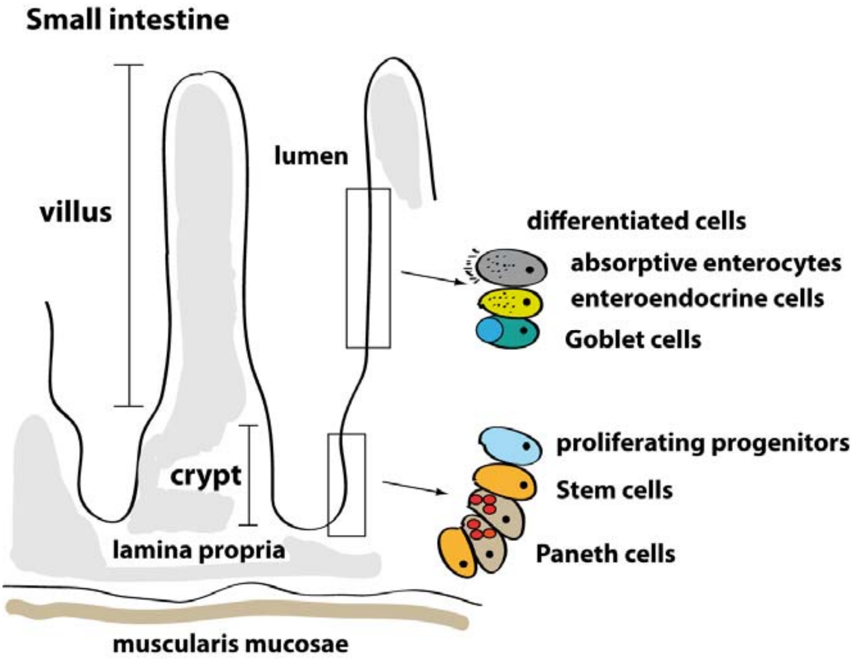
Small intestine
villus
lumen
crypt
lamina propria
muscularis mucosae
differentiated cells
absorptive enterocytes
enteroendocrine cells
Goblet cells
proliferating progenitors
Stem cells
Paneth cells

Figure I2. Scheme of a crypt-villus unit of the small intestine and its cell types.

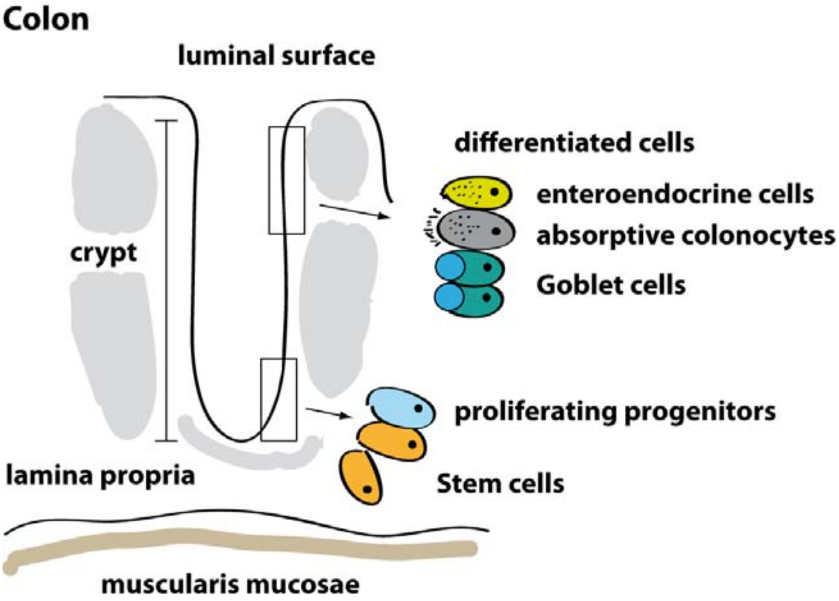
Colon
luminal surface
differentiated cells
enteroendocrine cells
absorptive colonocytes
Goblet cells
crypt
proliferating progenitors
Stem cells
lamina propria
muscularis mucosae

Figure I3. Scheme of a colonic crypt and its cell types.

I1.1. Intestinal stem cells

Important efforts have been made in the field of stem cell research in order to characterise the position and function of the intestinal stem cells, which represent the powerful source within the intestinal epithelium supporting the tissues' self renewing capacity. Nevertheless, the exact identification of this cell population remains controversial [16] [17].

Two different cell positions within the intestinal crypt have been suggested to correspond to the multipotent intestinal stem cells.

Bmi1, a member of the Polycomb Repressing Complex 1 and previously shown to be involved in the self renewal of haematopoietic and neuronal cells, has been used to identify a putative intestinal stem cell population located predominantly at the

+4 position of the crypt. However, the fact that the Bmi1 expression shows a descending gradient expression from the duodenum to the ileum suggests that more than one stem cell population could be present in the intestine [18].

Another group of researchers identified an undifferentiated proliferating cell population located in between the Paneth cells at the base of the crypts with stem cell characteristics. These crypt-based columnar cells (CBC) could be identified by the expression of Lgr5, a G protein-coupled receptor [19 20].

Bmi1 positive cells have been characterised as being slowly cycling stem cells whereas Lgr5 positive cells are described as being cycling fastly. Both cell populations are able to give rise to all the differentiated cell types of the intestine. In order to explain the relationship between those two distinct cell populations, it has been proposed that Lgr5 expressing CBC cells could be responsible for the daily maintenance of the tissue due to their rapid cycling. Slower cycling, Bmi1 expressing cells, could support this population by refilling the Lgr5 cell pool and by compensating for Lgr5 positive cell loss. Nevertheless the connection between these cell populations is still incompletely understood [21 22].

I1.2. The Wnt signaling pathway

Three different pathways are activated upon Wnt receptor activation: the canonical Wnt/β-catenin cascade, the non-canonical planar cell polarity (PCP) pathway, and the Wnt/Ca^{2+} pathway. Of these, the canonical pathway is the best characterized.

The canonical Wnt/β-catenin signaling pathway is conserved in evolution and controls processes including cellular proliferation, differentiation, motility, tissue maintenance, cell fate specification and maintenance of pluripotency [23] [24]. It is known to play a crucial role in normal epithelial homeostasis as well as in CRC (Figure I4) [25] [26] [27]. In the absence of Wnt ligands, a protein complex formed by APC, Axin and the two kinases, Caseine kinase 1 and Glycogen synthase kinase 3 ß (GSK3ß) facilitates the phosphorylation of ß-catenin at its N-terminal residues and in this way markes ß-catenin for ubiquitination and consequential degradation by the proteasome [28]. Upon Wnt activation through binding of Wnt ligands to their transmembrane receptors, the Frizzled proteins and LDL receptor related proteins 5 and 6 (LRP 5/6) [29], the formation of the APC / Axin protein complex is circumvented leading to the cytoplasmic stabilisation and accumulation of ß-catenin [30]. Thus, the stabilised ß-catenin translocates to the nucleus where it binds to the T cell factor / Lymphoid enhancing factor (TCF/LEF) transcription factors [31] leading to the transcription of common Wnt target genes, such as *c-myc* or *cyclin D1* [32] [33] [34].

The importance of the Wnt signalling for the proliferation of intestinal epithelial progenitors can be readily demonstrated by the observed nuclear localisation of ß-catenin in proliferating intestinal crypt cells. Besides, mutations of Wnt pathway proteins such as APC or ß-catenin have shown to cause uncontrolled proliferation and can lead to the development of CRC [35]. Studies on mice lacking Tcf-4, a TCF/LEF family member expressed in the intestinal epithelium, revealed its importance for the maintenance of the intestinal epithelial stem cell compartment. Tcf-4 deficient mice do not show any proliferative activity in the intervillus regions of the developing small intestine. The mice have defects in the intestinal epithelial organisation and die shortly after birth [36].

The Wnt target gene *c-myc* has been identified to participate in the control of proliferation and differentiation in the adult intestine [37]. It has been proposed that expression of c-Myc maintains epithelial proliferating cells in an undifferentiated state whereas the switch to the differentiated state goes along with downregulation of c Myc and upregulation of $p21^{cip/waf}$, a mediator of cell cycle arrest and terminal differentiation. Additionally, Bettess *et al* described a failure of crypt formation upon deletion of *c-myc* in the small intestine of mice [38]. Nevertheless, it has also been described that loss of c-Myc does not change normal intestinal homeostasis [39 40].

Another group of Wnt target genes are EphB receptors (and their ligands, the Ephrins) which represent the largest subfamily of receptor tyrosine kinases [41]. Both, EphB receptors and Ephrin B ligands have been demonstrated to be expressed in inversed gradients within the crypt villus axis with highest EphB receptor expression near the bottom of the crypts and Ephrin B highly expressed at the tip of the villus. They have been described to interact directly from cell to cell frequently resulting in repulsion. It has been suggested that EphB defines the position of epithelial cells within the compartment depending on the expression level of the Ephrin B ligand. EphB2/EphB3 deficient mice show interspersed positions of proliferating and differentiated intestinal cells. Additionally, deficiency in EphB3 mislocates Paneth cells from their usual bottom crypt position to the villus axis. In summary, it has been suggested that cell positioning and migration within the crypt villus compartment of the small intestine is dictated by the

Wnt signaling pathway through control of EphB receptor and EphrinB ligand expression [42] [43] [44].

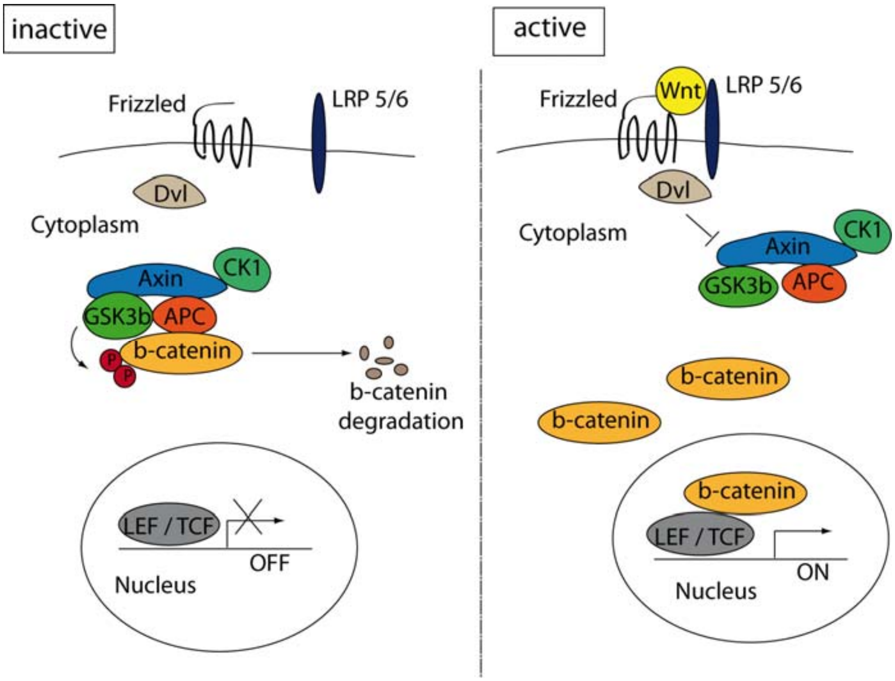
inactive
Frizzled
LRP 5/6
Dvl
Cytoplasm
Axin
CK1
GSK3b
APC
b-catenin
P
P
b-catenin
degradation
LEF / TCF
OFF
Nucleus
active
Wnt
Frizzled
LRP 5/6
Dvl
Cytoplasm
Axin
CK1
GSK3b
APC
b-catenin
b-catenin
b-catenin
LEF / TCF
ON
Nucleus

Figure I4. The canonical Wnt signaling. The APC / Axin complex is active in the absence of Wnt ligands in order to phosphorylate and degrade ß-catenin (inactive). Upon Wnt activation ß-catenin is stabilised and translocates to the nucleus where it participates in the transcription of Wnt target genes (active).

I2. Colorectal cancer

Colorectal cancer (CRC) accounts to one of the four most frequently diagnosed invasive cancers among men and women globally. Even though CRC death rates are declining in the recent years due to continuous improvement in screening methods and treatment it stays one of the most common causes for cancer related death in the United States in 2012. [45-47]

Both, hereditary and environmental factors contribute to the development of CRC. Most colorectal neoplasms develop sporadically. Nevertheless one third of the patients are characterised to have a familial component with a potentially definable genetic basis [48] [49].

Since the early 90's, CRC is thought to arise due to stepwise genetic and epigenetic changes that drive the transformation of normal colonic epithelial cells to cancer. At least four to five gene mutations are believed to be necessary for CRC to appear [50]. A characteristic order in the occurring mutations can be observed even though the total accumulation of changes is most important to reach a full blown tumour stage [51] [52]. A central initiating role is played by the early mutational inactivation of the tumour suppressor gene *APC*. [50] [53] [54]

I2.1. Inherited colorectal cancer syndromes

Around 4 % of the CRC cases contribute to hereditary syndromes. The two main syndromes that account for the majority of these cases are Hereditary Non-Polyposis Colon Cancer (HNPCC, Lynch syndrome) and Familial adenomatous polyposis (FAP) [55]. The two types can be distinguished by the highly increased incidence of development of colonic polyps (polyposis).

Based on available genomic information, they have been demonstrated to be important models to study and understand the mechanisms of inherited as well as sporadic CRC.

HNPCC, also called Lynch syndrome, is mainly caused by autosomal dominant genetic mutations in one of 4 DNA mismatch repair (MMR) genes, *MLH1*, *MSH2*, *MSH6* and *PMS2* respectively, whereupon approximately 90 % of the MMR mutations occur in *MLH1* and *MSH2* [56 57]. Hereditary MMR mutations commonly cause defects in repairing DNA replication errors or a missing DNA proofreading leading to microsatellite instability (MSI) [58]. Microsatellites are DNA regions in which a short nucleotide sequence (from 1 up to 5 nucleotides) is repeated several times. Gain or loss of nucleotides in these regions results in frameshift mutations [59]. Consequently, HNPCC patients carry an elevated risk to accumulate mutations in different somatic genes. Two of the genes that include a microsatellite region within their coding sequence and are frequently mutated in HNPCC are the proapoptotic gene *BAX* and *TGFBR2.* Their mutations favour the development of CRC due to a failure in the apoptosis pathway (*BAX*) or a disrupted function of the tumour suppressor transforming growth factor ß (TGFß, *TGFBR2*) [60 61].

HNPCC patients have an 80 % risk to develop CRC in the proximal colon most likely before the fifth decade of life. At variance with FAP, the development of hundreds of polyps in the colon is not observed. Yet, HNPCC patients hold an increased risk to develop extraintestinal cancers, such as endometrial, gastric, ovarian and urinary cancers [62 63 64].

FAP is one of the best studied and understood autosomal, dominantly inherited colorectal cancer syndromes [65]. It is characterised by germline mutations in the *APC* gene, most of them are nonsense leading to a truncated form of APC [66]. FAP patients develop hundreds to thousands of adenomatous polyps in the colon and rectum. The mostly benign polyps start to appear during childhood and if not treated lead to CRC in 100 % of the cases in the early decades of life (40-50 years) [65] [55]. Apart from colon tumours, FAP patients can also develop extracolonic lesions, such as gastric polyps, osteomas, hepatoblastomas and brain tumours[67].

Attenuated familial adenomatous polyposis (AFAP) is a milder form of FAP characterised by a later appearance of adenomas and cancer and by a fewer number of colorectal polyps (10 – 100) [68].

I2.2. APC mutations in FAP and CRC

APC mutations have been identified in FAP and the majority of sporadic CRC. They appear almost exclusively in tumours of the digestive tract with only few cases of gastric and pancreatic cancers described [69] [70] [52] *APC* mutations in CRC can be roughly divided into frameshift, or nonsense mutations, whereat an overall of 60 % are localised to the central domain of the APC gene, called the mutation cluster region. The mutations produce a truncated form of APC at the carboxyterminal end of its amino acid chain [71] . Whether the missing full length protein or the appearing truncated protein is the main initiator of the disease is still not clear [72] [73] [74].

APC protein acts in the cytoplasmic APC / Axin destruction complex that plays a key role in the canonical Wnt cascade.

Mutations in the Wnt signaling pathway occur commonly in cancer , mostly in tissues which normally depend on wnt for self renewal or repair, such as the intestinal epithelium [27]. APC mutation leads to a circumvented ß-catenin degradation and a subsequently permanent activation of the canonical Wnt pathway that results in continuous activation of Wnt target genes and finally the development of CRC (Figure I5) [75].

Participation of APC in other cellular functions, such as cell adhesion or chromosomal stability has also been described. Therefore, loss of APC function has been suggested to correlate with chromosomal instability (CIN) or deregulation of cell adhesion [67].

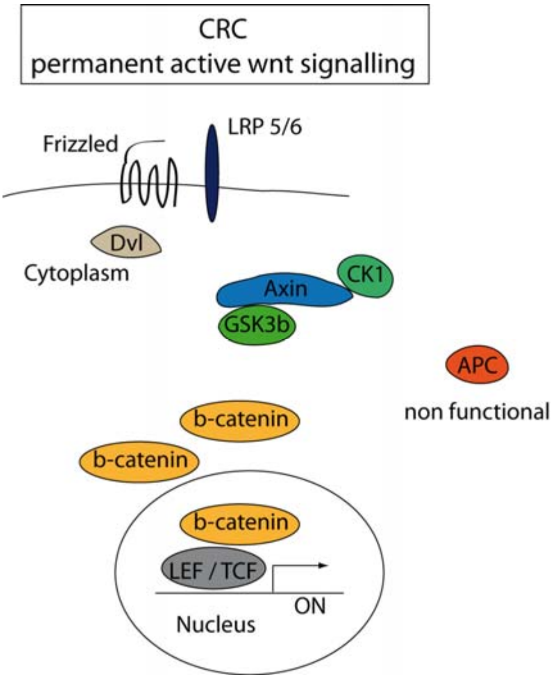
CRC
permanent active wnt signalling
Frizzled
LRP 5/6
Dvl
Cytoplasm
Axin
CK1
GSK3b
APC
non functional
b-catenin
b-catenin
b-catenin
LEF / TCF
ON
Nucleus

Figure I5. The canonical Wnt signalling in CRC. APC mutations in CRC lead to a permanent activation of the Wnt signalling pathway due to a circumvented degradation of ß-catenin.

Other frequent mutations in CRC involve KRAS and p53.

KRAS, a proto oncogene, is a member of the ras family of GTPase proteins involved in the signal transduction of different pathways. *KRAS* mutations occur in 30 – 40 % of CRCs and have been associated with a poorer prognosis and resistance to anti-EGFR antibody therapies [76]. Ras mutations occur during the intermediate stages of adenoma growth rather than early. They generally follow APC mutations [77] [78].

The *p53* tumour suppressor gene encodes a short lived phosphoprotein involved in many cellular functions, such as proliferation, DNA repair and programmed cell death. p53 mutations have been described to occur most likely late in the progression of colorectal cancer and have been associated to mark those neoplasms that tend to behave more agressively. Loss of heterozygosity of *p53* can be found in 30 - 75 % of CRCs and frequently occur after *ras* mutations [79] [65].

I2.3. CRC stages

The American Joint Committee on Cancer (AJCC) designs systems of cancer classification, including staging in order to facilitate medical decisions on cancer treatment, prognosis and other factors.

CRC can be classified using the Tumour-Node-Metastasis (TNM) system, where T describes how far the tumour has grown into the intestine, N describes the extent of spread to the nearby lymph nodes (LN) and M describes whether the cancer has spread to other organs. After having obtained the TNM stage of a cancer, an additional stage group is combined (Figure I6). Hereby describes stage I: the cancer has little outgrowth and has not spread to the LN or distant sites, stage II: the tumour has grown to the outermost layers of colon or rectum, but not further, stage III: the tumour has reached the regional LN, and stage IV: the primary tumour has metastasised to other organs [80] (AJCC Cancer Staging Manual, 7th edition).

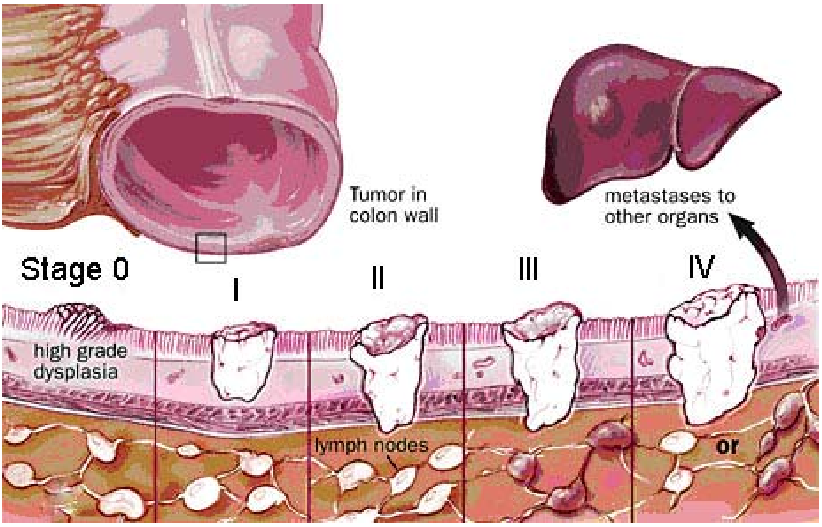
Tumor in colon wall
metastases to other organs
Stage 0
I
II
III
IV
high grade dysplasia
lymph nodes
or

Figure I6. TNM stages of CRC. (adapted from R.C. Donehower M.D., The J. Hopkins White Papers, 2008)

The most common metastatic site for CRC is the liver. Other less frequent sites include the lung, brain and bone [81].

It is widely believed that the earliest lesions that can lead to CRC are adenomatous polyps. A colorectal polyp is an abnormal growth of tissue on the lining of the colon or rectum, usually classified into a premalignant lesion, even though not all polyps will develop into a full blown tumour. An adenoma is a tumor glandular tissue that has not gained yet the properties of a cancer [82]. All adenomas share two main features, a dysregulated proliferation and the failure to fully differentiate. An adenomatous epithelium contains incompletely differentiated Goblet and absorptive cells. However, not all adenomas progress to invasive cancers. Some may stay stable or even regress and disappear (Fenoglio-Preiser, CM, 2007, *Gastrointestinal Pathology*, LWW, USA).

Two different models describe how early neoplastic adenomas form and expand in the colon, representing the earliest premalignant stage of CRC (Figure I7). Shih *et al* propose a “top down morphogenesis” to explain the expansion of adenomatous cells based on their observation that dysplastic cells of the earliest neoplastic lesions could only be localised to the top part of the colonic crypts where differentiated cell types are normally found. They characterised the identified dysplastic cells as actively proliferating and could additionally observe a change of ß-catenin localisation to the nucleus suggesting genetic alterations in the wnt signalling pathway. In contrast to the more common believe that tumours originate from stem cells which in the colon are localised to the bottom of the crypts, Shih *et al* hypothesise that the observed superficial dysplastic precursors migrate laterally and downwards repopulating the normal colonic crypts by pushing the normal crypt cells aside. As a second model, they propose that the identified neoplastic cells originate from the colonic stem cells which transform but initially migrate upwards the crypt in a normal manner. Thus, only later they can be identified as neoplastic [83].

In contrast to the previous model, a second model, the “bottom-up histogenesis”, has been described in order to explain the expansion of earliest lesions in CRC. Here, the first dysplastic cells were found to repopulate an entire single crypt, thus called unicryptal or monocryptal adenoma. Consequently, the dysplastic crypt cells are believed to expand not by lateral migration, but by crypt fission, a crypt division by budding or symmetrically at the crypts’ base. Crypt fission has been observed in sporadic adenomas and for FAP patients. Nevertheless, a later expansion of dysplastic cells by lateral migration or downwards into neighbouring crypts as described in the first model could not be excluded [84].

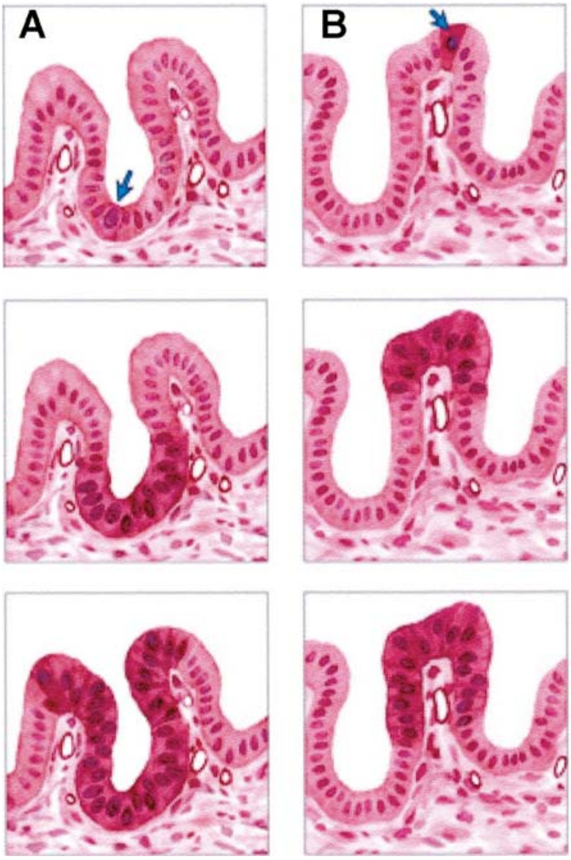

Figure I7. Models of early neoplastic adenoma formation. Two different models are described for the early neoplastic adenoma formation, the “bottom-up histogenesis” (A) and the “top down morphogenesis” (B). (Adapted from Shi *et al*, 2001 [83])

I2.4. Animal models for CRC

The APC$^{min/+}$ mouse, used as a mouse model for CRC, was established by chemical mutagenesis and carries a missense mutation in the *APC* gene at codon 850. Besides, three other APC KO mice have been generated with specific mutations in the *APC* gene. All of these mutations lead to a truncated APC protein at its carboxy-terminal domains [85]. Homozygous APC mutations lead to embryonic lethality. However, heterozygous mice are viable and develop multiple intestinal adenomas several weeks after birth. In detail, It has been described that at around 5 months of age, APC$^{min/+}$ mice develop around 25-75 adenomas in the small intestine and 1-5 in the colon [86] [87]. The adenomas arise most likely due to the loss of heterozygosity of the second *APC* allele. Even though most of the adenomas develop in the small intestine and not in the colon and rectum, the APC$^{min/+}$ mouse has been considered a good CRC model, since it recapitulates some features of human FAP patients [71].

Nevertheless, it has been observed that APC$^{min/+}$ mice can develop small colonic lesions similar to aberrant crypt foci (ACF). ACF have been described as putative preneoplastic lesions in the colon of carcinogen treated mice. They have been studied representing an early stage of colon carcinogenesis even though most of the ACF are hyperplastic and only few of them are able to advance to a colon tumour. The ACF phenotype observed in APC$^{min/+}$ mice could be enhanced by treatment with azoxymethane (AOM), a potent carcinogen [88].

Phenotypes for extra-intestinal organs due to *APC* mutations have also been described. In one study, it has been demonstrated that APC$^{min/+}$ mice develop thymic and lymph node atrophy starting at around 2 months of age. A depletion of lymphocytes has also been observed for sporadic CRC cases [89]. Additionally, it has been described that spleens of APC$^{min/+}$ mice are able to augment the mass and cellularity of the red pulb leading to splenomegaly [90].

Consequently, mice die from severe anaemia and apparent intestinal obstruction [90].

In order to overcome embryonic lethality of homozygous APC mutant mice, in another mouse model two loxP sites were integrated into the *APC* gene. Following infection with a Cre recombinase expressing adenovirus, the adult mice developed adenomas only in their colorectal region [71].

Interesting aspects on adenoma formation in APC$^{min/+}$ mice have been uncovered (Figure I8). A study from Oshima *et al* observed that adenomas of the small intestine expanded underneath the normal villus epithelium without breaking into the intestinal lumen or invading the muscularis mucosae [91]. Cortina *et al* further described that EphB positive proliferating crypt cells are able to accumulate after the loss of heterozygosity (LOH) of *APC* in the mouse' small intestine. The accumulating cells build outpockets from the intestinal crypts ingressing underneath Ephrin-B expressing villus cells. In this way, the growing adenomas get completely surrounded by normal intestinal epithelium while stromal cells are separating both, adenomas and normal epithelium. Due to the fact that colon tissue does not have villus structures, here, APC mutant tumour cells grow from the colonic crypts, repopulating them in continuous contact with normal epithelial cells [92].

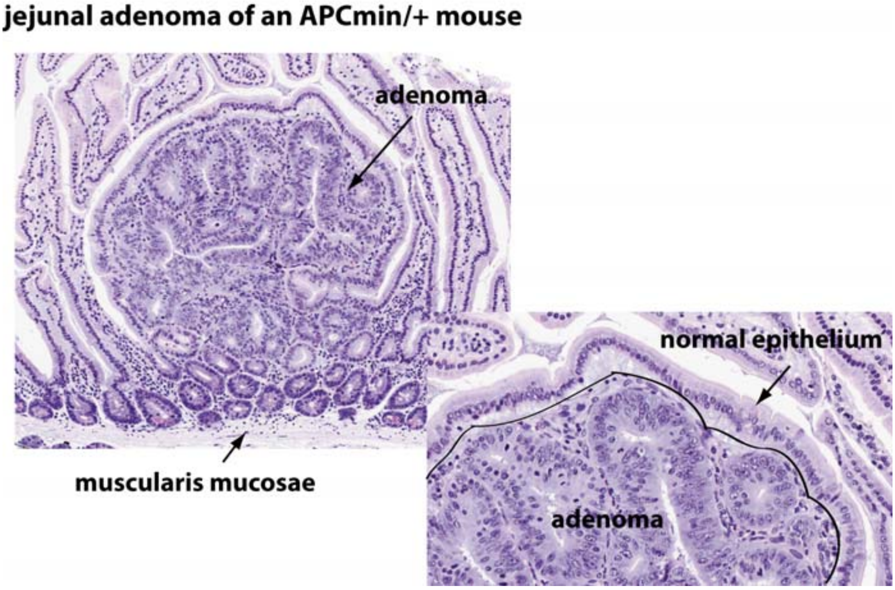

Figure I8. Jejunal adenoma of an APC$^{min/+}$ mouse. The jejunal adenoma grows into the lumen of the small intestine and is surrounded by normal epithelial cells.

Another mouse model confirms the implication of the Wnt signalling pathway in the development of adenomas. Due to the fact that a certain number of CRC cases have been described to carry ß-catenin mutations rather than *APC* mutations, Harada *et al* created a mouse model in which a Lox P flanked ß-catenin protein could be mutated in intestinal tissue by inducing a specific Cre recombinase. Consequently, the mutated ß-catenin protein could not be phosphorylated by the APC / Axin complex and was permanently stabilised [93]. The mice developed intestinal adenomas at a young age. Homozygous germline mutations of ß-catenin lead to embryonic lethality such as described for *APC* [94]

In order to study the effect of the inflammatory processes in the pathology of non-familial CRC, another inflammation-related mouse model has been introduced using azoxymethane, a genotoxic colon carginogen, to induce carcinogenesis. The AOM mouse model is described to develop colonic tumours within 20 weeks after a single administration of AOM followed by a one week exposure to dextran sodium sulphate (DSS) in the drinking water [95]. The administration of AOM and DSS causes inflammation in the colon epithelium and supports the idea that chronic inflammation can lead to CRC. The advantage of this CRC mouse model is its high reproducibility and its relatively easy application to different genetic backgrounds. The model features early stage pathogenic characteristics of human CRC. Colon tumours induced by AOM develop most likely Wnt activating mutations in the *ß-catenin* gene. Mutations in *APC* or *p53* are less frequent [96].

I3. Cyclin O protein and apoptosis

I3.1. Cell death criteria

Different features can be applied in order to distinguish among the different ways a cell can die

Cell death can be classified following to morphological criteria: apoptotic, necrotic and autophagic cell death. In addition to morphology, the involvement of nucleases or of distinct classes of proteases, such as caspases, calpains, cathepsins and transglutaminases are enzymological criteria to classify cell death. Finally, other criteria include functional aspects, such as if the cell death is programmed or accidental, physiological or pathological, and also immunological characteristics (immunogenic or nonimmunogenic) [97] [98].

I3.2. Apoptosis

Apoptosis (Type I cell death) is an ubiquitous physiological process used to eliminate damaged or unwanted cells in multicellular organisms. It is a genetically conserved pathway in all metazoans. The apoptotic mechanism as a form of programmed cell death plays essential roles in organogenesis during embryonic development and for maintenance of cell homeostasis in adult tissues. The term “apoptosis” and its morphological manifestations were defined by Kerr et al in 1972 [99] (Figure I9). The morphological changes of a cell undergoing apoptosis include plasma membrane blebbing while maintaining its integrity until the ultimate cell death, nuclear fragmentation (karyorrhexis), chromatin condensation (pyknosis) and DNA degradation. Apoptotic cells shrink and finally get completely engulfed by phagocytes. Important insights into the molecular mechanisms of apoptosis have been gained by Brenner, Horvitz and Sulston through extensive studies using the model organism *Caenorhabditis elegans* (*C. elegans*) [100] [101] [102]. They initially identified two genes essentially required for cell death, namely *ced-3* and *4* and another gene, *ced-9*, able to prevent cell death. Their mammalian homologs were identified as caspase 1 (ced-3), Apaf-1 (ced-4) and Bcl-2 (ced-9) [103]. Through their important work in this field they uncovered the essential implication of caspases and proteins of the Bcl-2 family in the process of apoptosis [104].

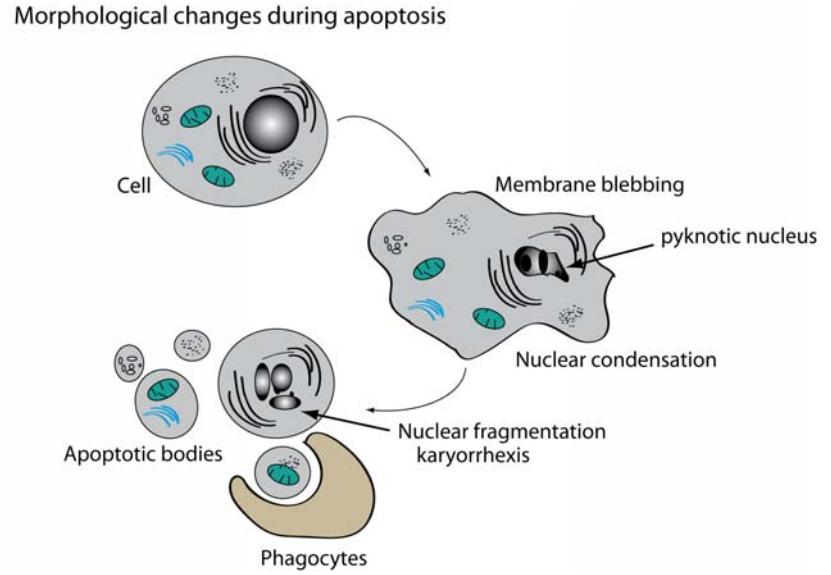
Morphological changes during apoptosis
Cell
Membrane blebbing
pyknotic nucleus
Nuclear condensation
Apoptotic bodies
Nuclear fragmentation
karyorrhexis
Phagocytes

Figure I9. Morphological changes during apoptosis.

Deregulation of the apoptotic pathways, as it has been demonstrated by different genetic loss or gain of function models, can lead to deregulated cell homeostasis and contribute to the outcome of different diseases. Insufficient apoptosis is associated with diseases such as cancer or autoimmune disorders whereas excessive apoptosis is a hallmark of immunodeficiency or neurodegenerative diseases (Alzheimer's, Parkinson and others) [103].

Other forms of programmed cell death include autophagy and necrosis.

Autophagy (Type II cell death) is an intracellular regulated process by which unwanted cell organelles or parts of the cytoplasm are engulfed by two-membrane autophagic vacuoles and subsequently degraded by fusion with lysosomes. Autophagy can be seen as a mechanism of adaptation to cellular stress or starvation and can ultimately lead to cell death when autophagic vacuoles accumulate massively [105]. It can be distinguished from apoptosis attending to molecular and morphological aspects, such as caspase independence and preservation of the cytoskeleton until the late stage of autophagic cell death [106] [107] [108].

Necrosis (Type III cell death) is another form of controlled cell death and has been described to be implicated in physiological as well as pathophysiological processes. It is regulated by different signal transduction pathways and catabolic mechanisms, such as death domain containing kinases (RIPK1, RIPK3) - or Toll like – receptors. Necrosis is morphologically characterized by cytoplasmic swelling, an early plasma membrane rupture and breakdown of cytoplasmic organelles. At variance with apoptosis, the uncontrolled release of parts of cellular components into the extracellular matrix during necrosis can lead to inflammation [109] [110].

I3.3 The core biochemical machinery of apoptosis

I3.3.1. Caspases

Caspases are **c**ysteinyl **asp**artate protein**ases** belonging to the family of cysteine proteases which cleave their substrates after an aspartic acid (asp) residue and are known to participate essentially in the processes of programmed cell death and inflammation.

In the 90s, the mammalian Interleukin 1 ß Converting Enzyme (ICE) was identified and later named Caspase-1, the first member of the caspase family. ICE cleaves the IL-1 ß precursor to active IL-1 ß dependent on an asp residue. [111] [104].

Up to know, 14 different mammalian caspases have been identified. Whereas most of these caspases are involved in apoptosis, some are implicated in inflammation. Therefore, caspases can be functionally classified into 3 groups: inflammatory caspases, apoptotic initiator caspases and apoptotic effector caspases (Figure I10).

The inflammatory caspases include human caspase -1, -4, -5 and mouse caspase -1, -11 and -12. The human inflammatory caspases 4 and 5 have no known counterparts in mice, similar to murine caspases 11 and 12 in humans, even though the *caspase -12* sequence is present in humans and *caspases -4* and *-5* are likely to have originated from a duplication of *caspase -11* [112]. *Caspase -10* does not exist in mice.

The Caspases 2, 8, 9 and 10 account to the group of apoptotic initiator caspases. They contain N-terminal adaptor domains and are activated by formation of caspase-activating complexes, which function as a platform to recruit caspases, providing proximity for self-activation. Well-known initiator caspase-activating complexes include the DISC Death Inducing Signaling Complex (DISC), which activates caspases-8 and 10; the apoptosome, which activates caspase-9; and the PIDDosome, which activates caspase-2 [113].
The effector or executioner caspases (caspase-3, 6, 7) lack the N-terminal adapter domains and are cleaved and activated by initiator caspases.

Caspases are synthesized as inactive proenzymes (zymogens) and only when they are cleaved at specific sites they become active enzymes during the induction of apoptosis [114]. Structurally, caspases contain a prodomain followed by a large p20 and small p10 subunit. Apoptotic initiator caspases have long prodomains containing either a Death Effector Domain (DED) (Caspase -8 and -10) or a Caspase Activation and Recruitment Domain (CARD) (Caspase -2 and -9). Activation of initiator caspases require oligomerisation of their monomeric inactive precursors. Formation of specific multimeric platforms such as the Death Inducing Signaling Complex (DISC) for caspase -8 and -10[115], the PIDDosome for caspase -2[116] and the apoptosome for caspase -9[117], facilitates the oligomerisation of the initiator caspase leading to its activation by bringing multiple caspase molecules in close proximity forming a multiprotein complex called aggregosome. In this way, only when these platforms are present it is likely that activation of the caspase cascade is triggered [114]. Initiator caspases cleave and activate apoptotic effector caspases -3, -6 and -7, characterized by having very short prodomains. The effector caspases execute the downstream processes of apoptosis, such as the degradation of chromosomal DNA [118]. The Caspase-Activated DNase (CAD) is responsible for this process. CAD builds cytosolic complexes with its inhibitor ICAD in order to keep it inactive. During apoptosis, active Caspase 3 cleaves ICAD at 2 positions and CAD is consequently released from the complex and able to cleave the chromosomal DNA in the nucleus. Active CAD can only be synthesized in the presence of ICAD and alone has no DNase function [119].

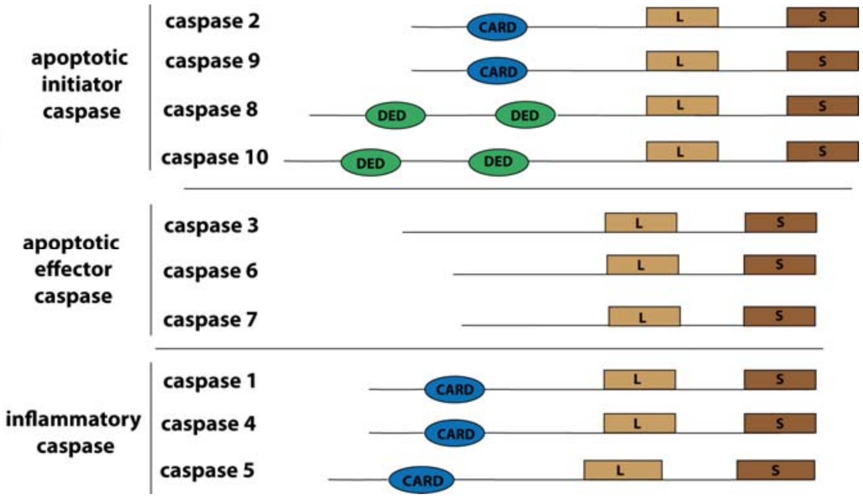
apoptotic initiator caspase
caspase 2
caspase 9
caspase 8
caspase 10
apoptotic effector caspase
caspase 3
caspase 6
caspase 7
inflammatory caspase
caspase 1
caspase 4
caspase 5
CARD
DED
L
S

Figure I10. Classification of mammalian caspases. L is the p20 subunit, S the p10 subunit. (Adapted from Jin *et al* 2005 [120])

The inhibitors of apoptosis (IAPs) are proteins first identified in insect viruses where they prevent the infected cell from killing themselves by apoptosis. IAPs bind to activated caspases in order to inhibit their function. Some of them are able to mark the activated caspases for their destruction by the proteasome. Because of the presence of RING domains in their sequence mammalian IAPs include X-linked IAP (XIAP), cIAP-1, cIAP-2, Neuronal Apoptosis Inhibitory Protein (NAIP), Survivin and Livin. IAPs are regulated by anti-IAP proteins which are released from the mitochondrial intermembrane space during the induction of the intrinsic apoptotic pathway. Anti-IAP proteins include Second Mitochondrial Activator of Caspases / Direct IAP Binding Protein with Low pI (Smac / DIABLO) and Omi / HtrA2 (High temperature requirement protein 2) [121] [122] [123].

I3.3.2. Bcl2 family of proteins

Proteins of the Bcl2 family regulate the mitochondrial outer membrane permeabilisation and have either pro- or anti-apoptotic functions. They characteristically contain 1 up to 4 Bcl2 homology domains (BH) that are important for establishing homo- and heterodimeric interactions between the different family members (Figure I11). There are 2 types of pro-apoptotic proteins that can be distinguished functionally and by the number of BH domains. The pro-apoptotic effector proteins Bax and Bak contain BH domains 1, 2 and 3. They undergo activation first by conformational change and then by mitochondrial translocation and by oligomerisation, getting integrated into the outer mitochondrial membrane leading to its permeabilisation [124]. Other pro-apoptotic proteins such as Bid, Noxa or Bim contain only the BH3 domain and are thus called BH3-only proteins. They seem to function upstream of Bax and Bak in order to regulate apoptosis [125] [126]. The anti-apoptotic Bcl2 proteins such as Bcl2 or Bcl-X_L contain all 4 BH domains and are able to inhibit apoptosis mainly by binding and inhibiting pro-apoptotic Bcl2 proteins. Upon apoptosis induction, 2 different models explain the inhibition of the anti-apoptotic Bcl2 proteins. Following one model, they are inhibited by BH3-only proteins while Bax and Bak function independently promoting Cytochrome C release from the mitochondria. Following the other model, one class of BH3-only proteins inhibits the anti-apoptotic Bcl2 proteins while another class of BH3-only proteins activates Bax and Bak [127] [128]. The Bcl2 family of proteins regulates the release of mitochondrial proteins that are normally located at the intermembrane space of these organelles, such as Cytochrome C, endonuclease G, AIF, Smac/Diablo and HtrA2.

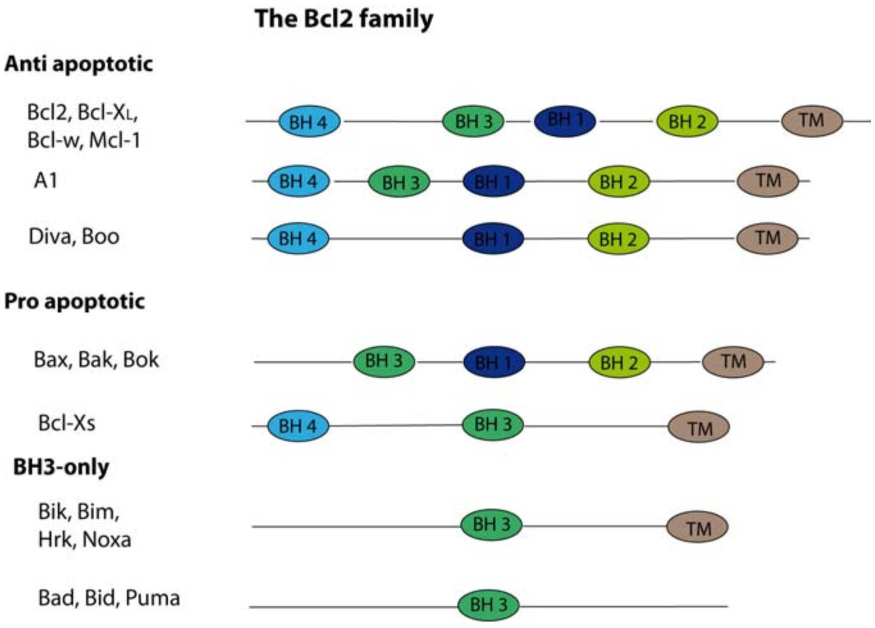
The Bcl2 family
Anti apoptotic
Bcl2, Bcl-XL, Bcl-w, Mcl-1
BH 4
BH 3
BH 1
BH 2
TM
A1
Diva, Boo
Pro apoptotic
Bax, Bak, Bok
Bcl-Xs
BH3-only
Bik, Bim, Hrk, Noxa
Bad, Bid, Puma

Figure I11. The Bcl2 family of proteins. Members of the Bcl2 family include anti-apoptotic, pro-apoptotic and BH3-only proteins.

I3.4. Apoptotic signalling

Caspase activation is a requirement to classify cell death as apoptosis. Activation of caspases can occur by two distinct pathways: an extrinsic, death receptor-mediated pathway and an intrinsic, mitochondrial-mediated pathway. In either of these pathways, initiator caspases are activated by oligomerization following an apoptotic signal. Initiator caspases cleave and activate effector caspases which then cleave diverse cellular proteins resulting in apoptosis.

I3.4.1. Intrinsic apoptotic pathway

The intrinsic apoptotic pathway signals apoptosis from inside the cell through the permeabilisation of the mitochondrial outer membrane permeabilisation (MOMP). This process is regulated by the Bcl2 family of proteins and induces the release of different mitochondrial intermembrane proteins such as Cytochrome c. Once Cytochrome c is released into the cytosol it participates in forming the apoptosome, a wheel-like heptamer of Apaf1 and Cytochrome C proteins. Once it is formed, the apoptosome recruits and activates initiator caspase 9 leading to the cleavage and activation of downstream executioner caspases, such as caspase -3, -6 and -7 and consequently, to the induction of apoptosis [129] [130].

I3.4.2. Extrinsic apoptotic pathway

The extrinsic apoptotic pathway is triggered by extracellular proteins that bind to cell-surface death receptors, belonging to the superfamily of the Tumour Necrosis Factor (TNF) receptors. Receptors from the TNF superfamily include Fas/CD95L/Apo-1, Tumour Necrosis Factor α receptor (TNF-αR) and DR4 and DR5, two TRAIL receptors. Ligands for the induction of this pathway include TNF-α, Fas ligand (CD95L) and TNF-Related Apoptosis Inducing Ligand (TRAIL). Binding of the trimerised ligand to the trimerised receptor triggers the recruitment of intracellular adaptor proteins to their cytosolic part via homotypic interaction of death domains (DD) which are found on the receptor as well as on the adaptor protein [131]. The Fas Associated Death Domain protein (FADD) and the TNF Receptor Associated Death Domain protein (TRADD) are the two main DD-containing adaptor proteins binding to the different death receptors, FADD mainly to Fas and TRAIL-R1 and -2, while TRADD preferentially binds to TNFR1, DR3 and DR6 [132] [133]. Additionally, the adaptor proteins contain a Death Effector Domain (DED) another homotypic protein-protein interaction domain necessary to recruit DED-containing procaspases -8, -10 or the caspase inhibitor c-FLIP to the aggregosome, in this case called Death-Inducing Signaling Complex (DISC).

Binding FasL to the Fas receptor triggers DISC formation containing FADD and Procaspase 8. Oligomerisation and proteolytic cleavage of Procaspase 8 molecules due to their close proximity in the DISC leads to their activation. The consequently activated initiator caspases signal by either direct cleavage of effector Procaspase 3 or indirectly by cleavage of the BH3-only protein Bid generating truncated Bid (tBid). tBid is able to permeabilise the mitochondrial outer membrane leading to the formation of the apoptosome and hence, activation of the effector caspases -3, -6 or -7. Whether truncation of Bid is involved in enhancing the Fas-mediated extrinsic apoptotic pathway has been described to be dependent on the specific cell type [134 135 136].

FADD-like Interleukin-1 Converting Enzyme (FLICE) Inhibitory Protein (c-FLIP) is a catalytically inactive homolog of caspase 8 that inhibits the activity of the DISC. One long and two shorter isoforms of c-FLIP are described, all containing 2 DED domains. The short isoforms bind through their DED domain to the DISC and inhibit the activation of Procaspase 8 and, consequently, inhibit death receptor-mediated apoptosis [137 138].

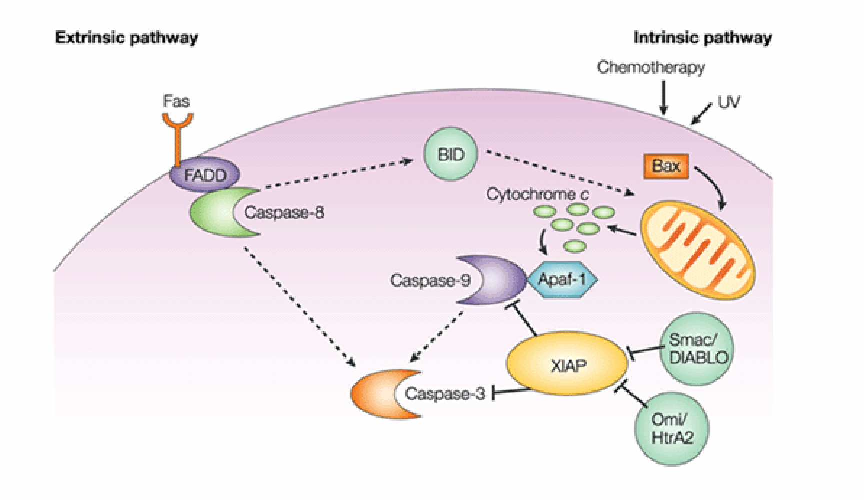
Extrinsic pathway
Intrinsic pathway
Chemotherapy
UV
Fas
FADD
Caspase-8
BID
Bax
Cytochrome c
Caspase-9
Apaf-1
XIAP
Smac/
DIABLO
Omi/
HtrA2
Caspase-3

Figure I12. Overview of the intrinsic and extrinsic apoptotic pathways. Adapted from Salvesen *et al*, 2002 [123] .

I3.5. Cell shedding of intestinal epithelial cells

The intestinal epithelium is a continuously self-renewing tissue. An intestinal epithelial cell migrates from the bottom of the crypts along the crypt-villus axis to the tip of the villus, where it is finally shed into the lumen. In mice it has been described that approximately 1400 epithelial cells are shed per villus and day [139]. This type of apoptosis is called anoikis and is triggered by the loss of the cell-matrix and cell-cell contacts of the epithelial cell.

Anoikis has been proposed to be regulated via both the intrinsic and extrinsic pathways [140]. Different studies have indicated that anoikis proceeds through the proapoptotic proteins Bax and Bak that are activated following the detachment of cells from the ECM. It can be blocked by overexpression of antiapoptotic Bcl-2 proteins [141]. Furthermore, the detachment-induced activation of Caspase 8 was inhibited by Bcl-2 overexpression, suggesting that Caspase 8 activation occurs as a consequence of activating the intrinsic pathway [142].

However, some studies in epithelial cells have also suggested that the initiating event is the activation of an extrinsic apoptotic death receptor, as overexpression of a dominant-negative form of FADD, which blocks caspase 8 recruitment to the DISC, inhibits anoikis. However, extracellular inhibitors of some death receptors failed to inhibit anoikis [143].

I3.6. Cyclin dependent kinases and Cyclins

Cyclin dependent kinases (Cdks) are members of a family of serine and threonine protein kinases. Some of the Cdks are described to be involved in the control of the cell cycle progression, but others have other functions such as transcrictional regulation or cell differentiation. Based on sequence similarity, the human genome contains 21 genes encoding Cdks and five additional genes encoding a more distant group of proteins known as Cdklike (CdkL) kinases. According to the current nomenclature for Cdk proteins, there are 11 classical Cdks (Cdk 1-11), 2 newly proposed members (Cdk12 and 13) and Cdk-like kinases based on the presence of cyclin binding elements (PFTAIRE and PCTAIRE) or on their sequence similarity to the original Cdks (Cdc2-like kinases or cell cycle related kinases). In order to be activated, Cdks require binding to cyclins [144] [145].

At least 29 human genes are identified to contain a cyclin box domain, the common feature to all the cyclin family members. This domain is involved in the binding to specific Cdks.

It has been described that progression through the cell cycle occurs by different combinations of Cdks and their specific cyclin partners that build the Cdk-cyclin complex. In early G1 phase, Cdk4 and / or Cdk6 are activated by D-type cyclins leading to phosphorylation of members of the retinoblastoma protein family and consequent activation of E2F transcription factors. Transcription of E2F target genes is required for later cell cycle progression since for instance Cyclin E- and A are E2F target genes [146]. In the late G1 phase, Cdk2 is activated by E-type cyclins leading to S phase initiation. Later, Cdk2 builds complexes with A-type cyclins in order to further progress through the S phase.

Finally, Cdk1 binding to cyclin A and later cyclin B leads to G2 / M transition and completing mitosis [147] (Figure I13).

Apart from their function in the cell cycle, Cdk-cyclin complexes have been described to be involved as well in other functions, such as in neuronal development, the regulation of transcription (Cdk7-Cyclin A, Cdk8-cyclin C, Cdk9-cyclin T, Cdk9-cyclin K) or DNA damage repair [148].

Even though Cdk activity is regulated by their specific binding to cyclins, other regulatory mechanisms have also been described. Proteins of the INK4 family ($p16^{INK4a}$, $p15^{INK4b}$, $p18^{INK4c}$, $p19^{INK4d}$) and proteins of the Cip / Kip family ($p21^{Cip1}$, $p27^{Kip1}$, $p57^{Kip2}$) are able to bind and inhibit different Cdks. INK4 proteins inhibit mainly Cdk4 and 6 complexes whereas Cip / Kip proteins bind to all Cdk / cyclin complexes [149] [150] [151].

In order to be fully activated, Cdk-cyclin complexes require phosphorylation by another Cdk activating kinase (CAK) causing a conformational change to the complex. The kinase contains three subunits, Cdk7, cyclin H and MAT1 and is necessary for full activation of Cdk1, -2, -4 and -6 [152].

Another protein kinase, Wee1, a tyrosine kinase, has been described to inhibit Cdk activity by phosphorylating the residue of Tyrosine 15 in the Cdk protein. Cdc25 phosphatases (Cdc25A, B and C), on the other hand can dephosphorylate the same residues in order to activate the Cdk-cyclin complex [145] [153].

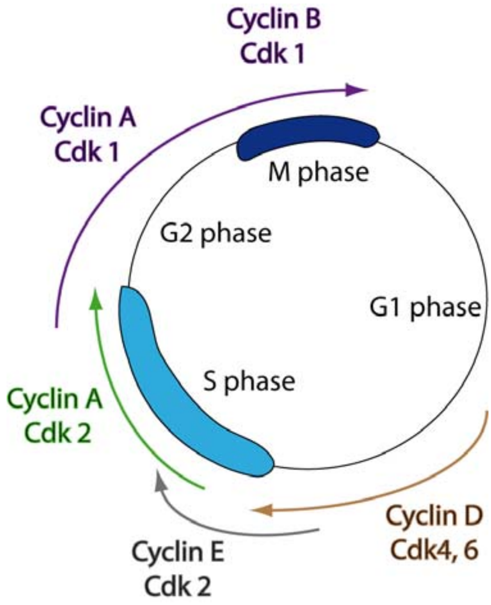

Figure I13. Cdk-cyclin complexes during cell cycle progression.

I3.7. Cell cycle and apoptosis

Cyclin dependent kinases together with cyclins play essential roles in the regulation of the cell cycle progression, whereas a role for Cdks in apoptosis is not well defined due to the lack of clear genetic evidence [154]. Different experimental approaches have been performed in order to demonstrate Cdk functions in apoptosis, such as use of chemical and protein inhibitors or genetic approaches [155]. The selection of a good experimental model in order to distinguish between Cdk functions in the cell cycle and apoptosis has been shown to be challenging.

Thymocytes have been used for the study of Cdks in apoptosis, because 90 % of the normal cells of the thymus are quiescent and do not go back into the cell cycle *in vitro*. In this way, any cell cycle-related Cdk activation in these cells will not be related to a cell cycle function. Using thymocytes, Cdk2 has been shown to increase its activity during dexamethasone and γ-irradiation induced apoptosis. However, the extrinsic apoptotic pathway via CD95/Fas does not activate it. Additionally, inhibition of Cdk2 has been demonstrated to abrogate thymocyte apoptosis induced by intrinsic stimuli in thymocytes [156 157].

We and others have demonstrated that overexpression of the apoptosis regulatory proteins Bax and Bcl-2 in T cells of transgenic mice leads to perturbations in the dividing population of thymocytes. It has been demonstrated that overexpression of Bax can increase the cell cycle progression in activated T cells whereas Bcl-2 delays the process [158]. The degradation of the negative regulator of cdk activity $p27^{kip1}$ is delayed in activated T cells when Bcl-2 is overexpressed. Furthermore, a linear relationship between $p27^{kip1}$ degradation, Cdk2 activation and thymocyte apoptosis which is modulated by p53, Bax and Bcl-2 could be demonstrated [157 159].

Our laboratory has proven that Cdk2 activation in apoptosis happens very early and is followed by Caspase-8 activation, changes in mitochondrial permeability and cytochrome c release mediated by the proapoptotic proteins Bax and Bid. We also demonstrated that gene transcription is needed downstream of Cdk2 activation in order to trigger apoptosis [156].

De novo protein synthesis has shown to be required for Cdk2 activation during thymocyte apoptosis since cycloheximide, an inhibitor of protein synthesis, abolishes the increase in Cdk2 activity and can block thymocyte apoptosis in response to treatment with dexamethasone or γ-irradiation. Cyclins A and E bind to Cdk2 during cell cycle progression, whereas during apoptosis we suggested that Cdk2 is activated by an unknown

Apoptosis Related Cdk2 Activator (ARCA). Using *in silico* analysis of the human genome we identified several non-characterised Cyclin-like proteins, from which preliminary results encouraged us to further characterise one of them, located in human chromosome 5 in a region sintenic with mouse chromosome 13, named Cyclin O.

I3.8. Cyclin O

Studying Cyclin O, we could demonstrate that it is able to bind and activate Cdk2 in response to intrinsic apoptotic stimuli such as glucocorticoids and DNA damaging agents (Figure I14). We could also show that *de novo* synthesis of Cyclin O precedes apoptosis induction whereas its downregulation abrogates DNA damage and dexamethasone-induced apoptosis. This lack of apoptotic response after Cyclin O downregulation is due to a failure in the activation of apical Caspases and is not a consequence of defective signalling in the DNA damage or glucocorticoid pathways.

Taken all these observations, Cyclin O is the most likely candidate to be the ARCA.

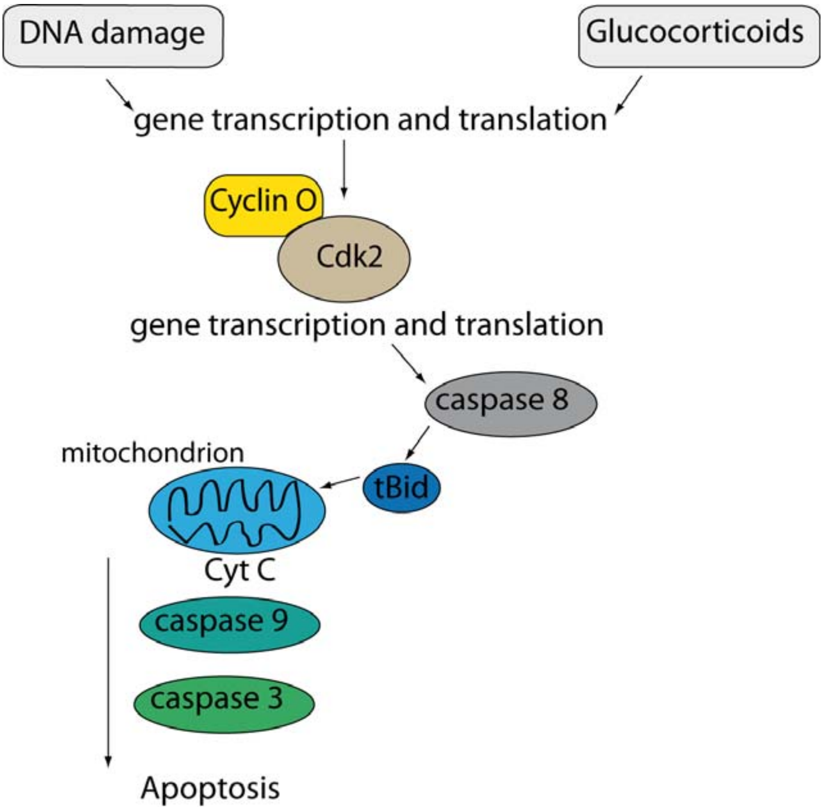
DNA damage
Glucocorticoids
gene transcription and translation
Cyclin O
Cdk2
gene transcription and translation
caspase 8
mitochondrion
tBid
Cyt C
caspase 9
caspase 3
Apoptosis

Figure I14. Cyclin O in the intrinsic apoptotic pathway. Upon induction of apoptosis by intrinsic stimuli Cyclin O binds to Cdk2 and induces caspase 8 activation by an unknown mechanism, the release of Cytochrome C results in the formation of the apoptosome and activation of downstream caspases 9 and 3.

The Cyclin O gene is highly conserved and is present in all the vertebrate genomes sequenced until now. It encodes for 3 different transcripts, product of the use of two alternative promoters and alternative splicing. Cyclin Oα from now on Cyclin O shares 28 % identity with human Cyclins A2 and B1 and two thirds of the Cyclin O sequence encompass a highly conserved cyclin box located at its C-terminal end. Cyclin O has been identified as a cytosolic protein of around 40 kDa and 350 amino acids.

Cyclin Oγ and δ are human and mouse (respectively) specific long non coding RNAs partially overlapping with Exons 1 (mCyclin O δ) or exons 2 and 3 (hCyclin O γ) of the gene encoding Cyclin O [160].

Tumorigenesis is a multistep process that requires genetic alterations that drive the progressive transformation of normal cells to malignant cancer cells. For a mutated cell to survive in a highly controlled tissue environment, it has to be able to overcome anti-cancer defense mechanisms and acquire new capabilities in order to grow a tumour. Evasion of programmed cell death counts to one of the six essential alterations in cell physiology to cause tumour development [161].

Cyclin O has been shown to be required for the induction of the intrinsic apoptotic pathway and has been suggested to have a putative functional role in the DNA damage response (DDR). Alterations in Cyclin O’s function could give an advantage to the tumour cell to overcome apoptosis and accumulate mutations.

Therefore, we aimed to study its expression and to understand the possible functional alterations of Cyclin O in CRC.

Objectives

Our **first objective** was to study the expression of Cyclin O in human colorectal adenocarcinomas and its clinical implication.

Our **second objective** was to study the role of Cyclin O in mouse intestinal development.

Our **third objective** was to study the consequences of Cyclin O deficiency in the formation of adenomas in a mouse model of colorectal carcinoma, the $APC^{min/+}$ mouse.

Materials and Methods

MM1. Anti Cyclin O antibodies

The anti mouse Cyclin O antibodies C2, N1 and alpha1 were generated previously in our laboratory, C2 and N1 were described in Roig *et al* [160], alpha1 in Ortet, L., *Signalling of Cyclin O complexes through eIF2alpha phosphorylation,* doctoral thesis, 2010. The anti human Cyclin O antibody HC2 was generated in rabbits using a peptide corresponding to the C-terminal end of the human Cyclin O as antigen. The peptide H-LRAPVKKSRRPC-NH_2 was coupled with 3-maleimidobenzoic acid N-hydroxysuccinimide ester (MBS, Sigma-Aldrich) to Keyhole Lympet Haemocyanine (KLH). Peptides were synthesised by Dr. David Andreu (Grup de Recerca en Proteòmica I Química de Proteïnes, UPF). New Zealand Rabbits were used for immunisation and were kept at the animal facility of the Facultat de Farmàcia, Universitat de Barcelona.

The HC2 serum was affinity purified using the corresponding peptide bound to an EAH-sepharose 4B column according to the manufacturer (GE Healthcare). The HC2 serum and affinity purified antibody were titrated by ELISA and Bovine Serum Albumin (BSA) (Sigma-Aldrich) was added to a final concentration of 1mg/ml and the affinity purified antibody was aliquoted and kept at -20 ºC until use.

MM1.1. ELISA

The antigens used to coat the ELISA plates were crosslinked to the carrier ovoalbumin (OVA) using glutaraldehyde. 96-well Maxisorp microtiter plates (Nunclon) were coated with peptide-OVA conjugate at a concentration of 20 µg / ml. Reactive sites were blocked with 1% gelatine for 30 minutes. For competitive ELISA, the affinity purified antibody was pre-incubated with the HC2 peptide at a final concentration of 300 µg / ml for 1h at room temperature (RT). The blocked antibody was then serially diluted in PBS containing 1% BSA and incubated for 1 hour at 37 ºC in the antigen-coated wells. After washing three times with PBS-Tween 0.1%, alkaline phosphatase-conjugated swine anti-rabbit immunoglobulins (DAKO) were added and then plates were incubated for 1 hour at 37 ºC. Reactions were developed using 4-methylumbelliferyl-phosphate disodium salt (Sigma-Aldrich) at 1 mg / ml diluted in 1M triethanolamine pH 9.5 for 30 minutes at RT, and fluorescence was determined using an Infinite M200 fluorimeter (TECAN).

MM1.2. Specificity of the antibody

The human anti-Cyclin O antibodies N1, HC2 and alpha1 were compared in the same tissue area of 2 different CRC tumour samples (Figure MM1). N1 and HC2 show the same punctuate staining pattern in tumour 1 suggesting a cytoplasmic location of Cyclin O protein in the CRC tumour cells. In tumour 2, N1 and alpha1 show a diffuse staining pattern for Cyclin O in the cytoplasm of the tumour cells. The different staining pattern shown by N1 suggests that Cyclin O can be expressed differently in different tumour samples.

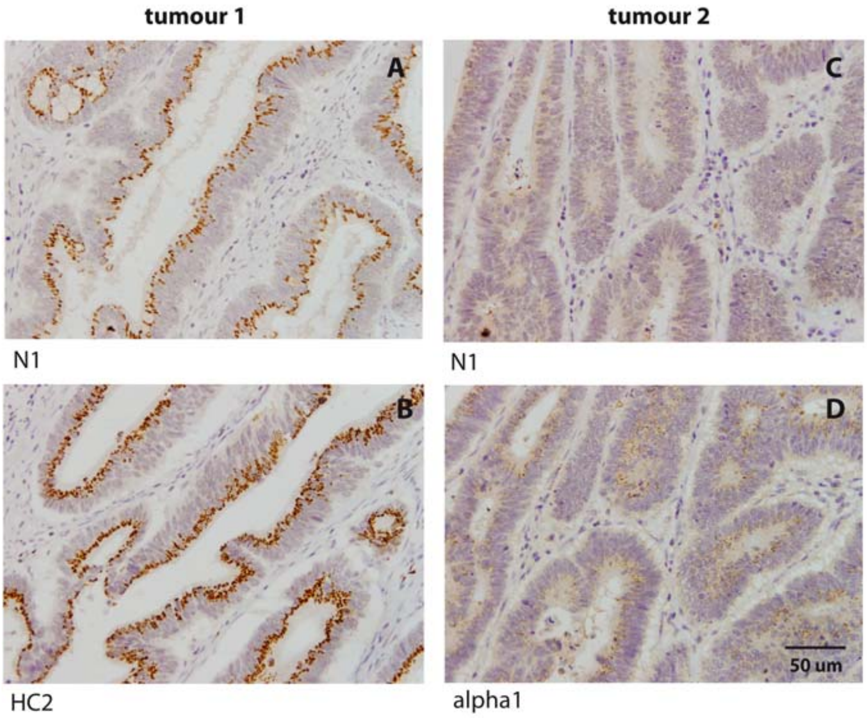

Figure MM1. Specificity of human anti-Cyclin O antibodies. Two different human CRCs (06/7750 tumour 1 and 07/1449 tumour 2) were stained by IHC for Cyclin O protein using the human anti-Cyclin O antibodies N1 (A, C), HC2 (B) and alpha1 (D). Staining patterns were compared in the same tissue area and were similar indicating the specificity of the antibodies.

Anti Cyclin O antibody	Antigen
HC2	TSLTHMLPVQICEKC
N1	LRAPVKKSRRPR
alpha1	ESRSKLLSWLIPVHRQFGLSC

Table MM1. Anti-Cyclin O antibodies and their corresponding peptides.

MM2. Other antibodies

Protein	Antibody	Source	Supplier	Technique used
ß-catenin	Clone 14	Mouse monoclonal	BD Transduction laboratories	IHC
BrdU	3D4	Mouse monoclonal	BD Pharmingen	IHC
E-cadherin	Clone 36	Mouse monoclonal	BD Transduction laboratories	IHC
MOCS2	FL 188	Rabbit polyclonal	Santa Cruz	IHC
MOCS2	F 9	Mouse monoclonal	Santa Cruz	WB
Lysozyme	EC 3.2.1.17	Rabbit polyclonal	Dako	IHC
B220	RA3-6B2	Rat monoclonal	Supernatant from the hybridoma	IHC
ß actin	BA3R	Mouse monoclonal	Sigma	WB
Pyruvate kinase	Ab1235	Goat Polyclonal	Chemicon	WB

Table MM2. Primary antibodies used

Antibody	Supplier	Technique used
Polyclonal Goat Anti-rabbit Immunoglobulins/HRP	DAKO	WB, IHC
Polyclonal Goat Anti-Mouse Immunoglobulins/HRP	GE Healthcare	WB, IHC
Polyclonal Goat Anti-rat Immunoglobulins/HRP	GE Healthcare	IHC
Powervision^{TM} Anti-mouse	Leica Biosystems	IHC
Powervision^{TM} Anti- rabbit	Leica Biosystems	IHC

Table MM3. Secondary antibodies used

MM3. Cell culture

The cell lines used were obtained from American Type Culture Collection (ATCC) and were the following: HCT116, a human colorectal carcinoma cell line with a near diploid stemline chromosome number (6,8 % polyploids) and HEK 293, a human embryonic kidney cell line. Cells were grown in Dulbecco's modified Eagle's medium (DMEM) (Invitrogen) supplemented with antibiotics and 10% foetal calf serum (Biological Industries). Cells were maintained at 37 ºC with a humid atmosphere of 5% of CO_2. The mouse T cell lymphoma cell line WEHI 7.2 (obtained from Dr. Roger Miesfeld, University of Arizona, Tucson, Arizona, USA) was grown in low glucose (1 g/L) DMEM supplemented with antibiotics and 10% foetal calf serum. WEHI7.2 cells that stably express shRNA against GFP (shGFP) or shRNA against Cyclin O (shCyclinO), have been described[160]. WEHI7.2 cells overexpressing Cyclin O were generated by Roset, R., *Study of the regulation and signalling of CDK2-Cyclin O complexes during apoptosis*, doctoral thesis, 2008.

MM4. Cyclin O somatic knock out in HCT116 cells

MM4.1. The rAAV targeting construct

In order to study the effects of Cyclin O deficiency in CRC-derived cancer cells, we intended to knock out the Cyclin O gene in HCT116 CRC cells by homologous recombination. Because of the relatively small size of the Cyclin O gene, we aimed to knock out the whole coding region of the gene using a recombinant adeno-associated virus (rAAV) construct. We chose the HCT116 cell line because of its pseudo-diploidy, making necessary only two rounds of targeting to inactivate the Cyclin O gene. The rAAV construct contains a *neo* selectable marker cassette (TK-*neo*) flanked by two LoxP sites and the inverted terminal repeats (ITRs). The homologous recombination sites were cloned into two multiple cloning sites (MCS) flanking the selectable marker cassette (Figure MM2). The size of the targeting construct is limited by the packaging capacity of the rAAV. Therefore, each of the homologous recombination arms should be around 1 kb [162] [163].

For the first round of targeting we reached a targeting efficiency of 3,3 %.

Regions of homology flanking the human Cyclin O gene locus were cloned into the pAAV TK acceptor vector, first a 1009 bp left arm homologous sequence using XbaI and BamHI upstream and a 917 bp right arm homologous sequence using ClaI and ApaI downstream of the TK-neo cassette.

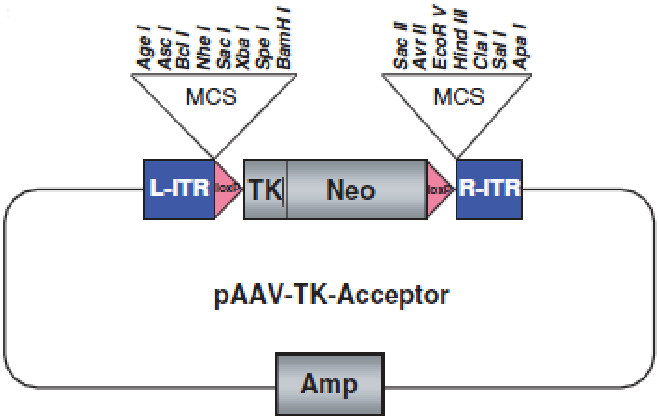
Age I
Asc I
Bcl I
Nhe I
Sac I
Xba I
Spe I
BamH I
Sac II
Avr II
EcoR V
Hind III
Cla I
Sal I
Apa I
MCS
MCS
L-ITR
loxP
TK
Neo
loxP
R-ITR
pAAV-TK-Acceptor
Amp

Figure MM2. Scheme of the pAAV TK acceptor vector.

MM4.2. AAV virus production

The pAAV-TK acceptor vector was used for the production of Adeno-associated virus in order to target the Cyclin O gene. The pAAV hrGFP, containing the sequence for human recombinant green fluorescent protein (hrGFP), was only used for estimation of the virus titer and the corresponding packaging vectors (obtained from Indiana University National Gene Vector Biorepository (NGVB) and University of Washington, Seattle, USA (pRepCap2)) [162]).

The AAV virus containing the targeting construct and the AAV hrGFP virus were prepared by cotransfecting HEK 293 cells with the vector pXX6-80, containing the adenovirus accessory proteins that are required for an efficient rAAV replication, and the vector pXR2, containing the *rep* and *cap* sequences that are required for the rAAV replication and packaging [162], in equal proportions using the lipofectamine method (Invitrogen). After 4 hours of transfection the medium was removed and cells were fed with fresh medium. 48 hours post-transfection cells were scraped into 1 ml of phosphate-buffered saline followed by 3 cycles of freezing and thawing. The lysate was clarified by centrifugation and the supernatant containing the AAV virus was divided into aliquots and stored at – 80 ºC until further use.

MM4.3. AAV virus titration

In order to estimate the titer of the AAV virus, the AAV hrGFP virus was produced in parallel and under same conditions as the AAV virus carrying the targeting construct. The virus titer was determined measuring GFP positive cells by FACS analysis. HCT116 cells were seeded in a 24-well plate and the next day serial dilutions of the virus were added to the cells. After 24 hours, the medium was changed. 48 hours post-infection, cells were trypsinised, washed, resuspended in 250 µl of PBS and analysed by flow cytometry using a FACScan cytometer (Beckton Dickinson).

In order to calculate the virus titer the following formula was used: *Virus titer= (F * C / V) * D* where F = % of GFP positive cells / 100, C = total number of seeded cells, V = volume of the virus dilution added to each well, D = dilution factor [164].

In this way, a virus titer of 10^4 particles / ml was estimated for the AAV-hrGFP virus.

MM4.4. AAV virus infection

HCT116 cells were grown in a T75 flask until 75 % of confluency and infected with the AAV recombinant virus in 4 ml of medium. After 3 hours of incubation another 8 ml of medium were added and the cells were further incubated. After 48 hours, the infected cells were trypsinised and replated in ten 96-well plates in medium containing G418 (Invitrogen) at a final concentration of 0,5 mg / ml [163].

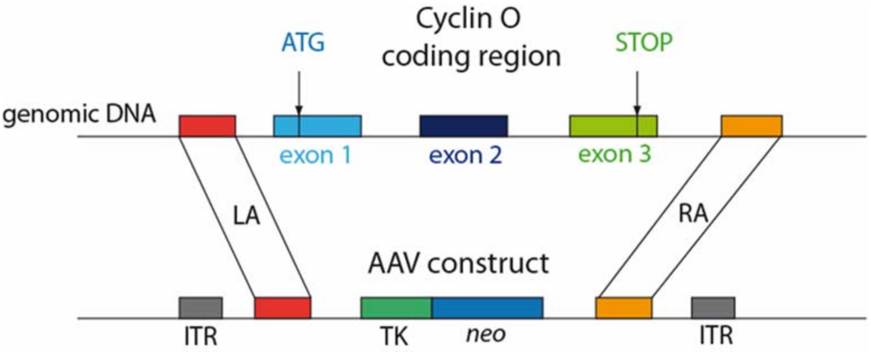

Figure MM3. Scheme for AAV targeting of the Cyclin O gene. LA = left arm homologous region, RA = right arm homologous region, ITR = inverted terminal repeat, TK = thymidine kinase promoter.

MM4.5. Screening of the targeted clones

Drug resistant colonies were grown for 4 weeks. At the end of the selection period, single clones from 96-well plates were replated separately in 24-well plates. When cell confluency was reached, clones were harvested, genomic DNA isolated and locus-specific integration was assessed by PCR for each clone (tables MM4, 5, 6). Correctly targeted clones after the first round of infection were selected for treatment with Cre recombinase in order to remove the *neo* selectable marker cassette.

To identify Cyclin O targeted HCT116 cells the following PCR experiments were performed.

First round targeting

In order to confirm integration of the targeting construct by homologous recombination into one allele of the Cyclin O gene locus, primer pairs were designed one into the upstream genomic region flanking the left arm homologous DNA sequence of the targeted region and the other one inside the neo cassette of the AAV construct (OligoF 1 + OligoR 2; OligoF 3 + OligoR 4) (Figure MM4). Only clones giving the expected PCR product of 1000 bp were selected for the second test. In order to exclude random integration of the AAV construct, primer pairs were positioned one into the left / right arm and the other one inside the AAV-based vector's ITR (Figure MM5). Only the clones positive for the first screening test were tested, clones giving a PCR product for random integration were excluded and one positive clone was chosen for the second round of targeting.

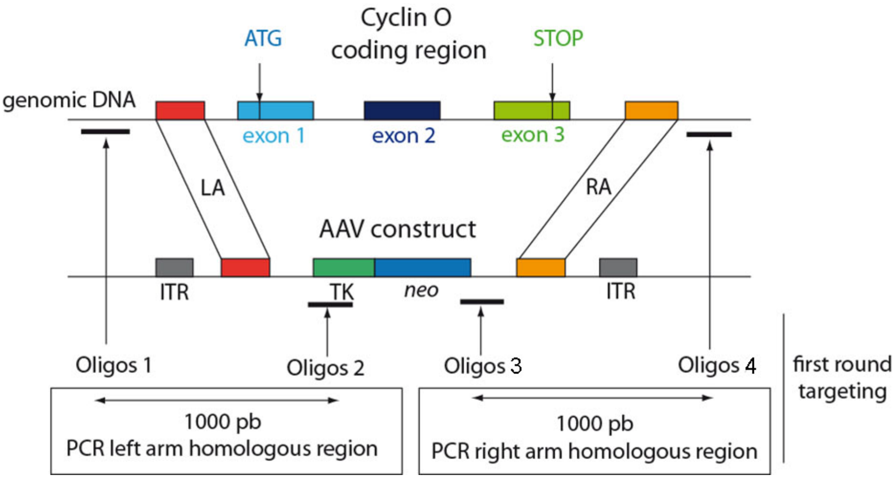
Cyclin O
coding region
ATG
STOP
genomic DNA
exon 1
exon 2
exon 3
LA
RA
AAV construct
ITR
TK
neo
ITR
Oligos 1
Oligos 2
Oligos 3
Oligos 4
first round
targeting
1000 pb
PCR left arm homologous region
1000 pb
PCR right arm homologous region

Figure MM4. Scheme of oligo positions for AAV construct integration PCRs. LA homologous region oligo 1 was positioned into the LA flanking genomic DNA and its corresponding oligo 2 into the AAV construct. RA homlogous region oligo 1 was positioned into the AAV construct and its corresponding oligo 2 into the RA flanking genomic DNA. Both PCRs give a 1000 bp product.

PCR Cyclin O targeting

94 ºC	2 min	
94 ºC	30s	40 cycles
55 ºC	30s	
72 ºC	1.20 min	
72 ºC	5 min	

Table MM4. PCR conditions for Cyclin O targeting in HCT116 cells

left arm homologous region	
different primers for the OligoF 1 position	**different primers for the OligoR 2 position**
5'-tgctcagagttatggggaaatagg-3'	5'-ctcttgcaaaaccacactgc-3'
5'-gttgagggtacctgagctttc-3'	5'-gtttgctcgacattgggtggaaac-3'
5'-gcagccccttctcctatagg-3'	5'-gcttcctcttggcaaaaccac-3'

Table MM5. Oligos used for first round targeting on left arm integration site.

right arm homologous region	
different primers for the oligoF 3 position	**different primers for the oligoR 4 position**
5'-cgtgctttacggtatcgccgctc-3'	5'-gattcctgtaacgtgactgag-3'
5`-gccttctatcgccttcttgacgag-3'	5'-cgtaacagtgagactgaagac-3'

Table MM6. Oligos used for first round targeting on right arm integration site.

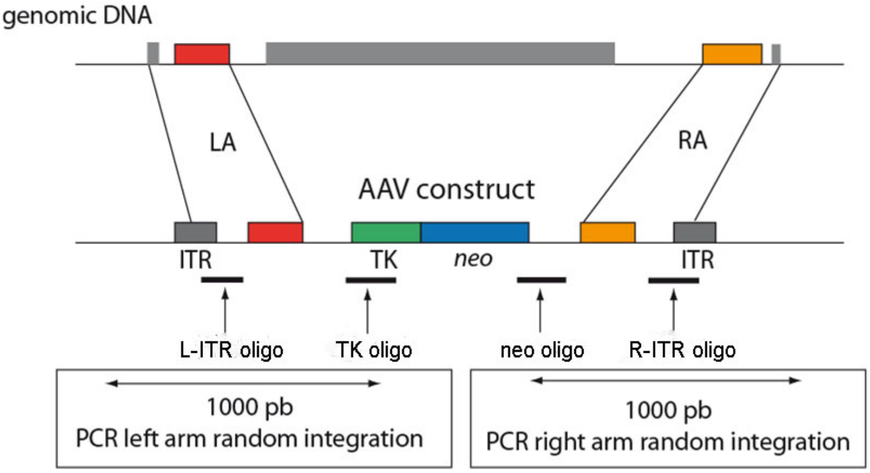
genomic DNA
LA
RA
AAV construct
ITR
TK
neo
ITR
L-ITR oligo
TK oligo
neo oligo
R-ITR oligo
1000 pb
PCR left arm random integration
1000 pb
PCR right arm random integration

Figure MM5. Scheme of oligo positions for random integration PCRs.

random integration left arm homologous region	
L-ITR oligo	**TK oligo**
5'-cctgatcaacgcgtgctagc-3'	5'-gcggcaccggagccgcgatt-3'

random integration right arm homologous region	
neo oligo	**R-ITR**
5'-aaacagatccttcgtttcc-3'	5'-ccatcactaggggttcctgcg-3'

Table MM7. Oligos used for exclusion of random integration.

MM4.6. Cre mediated excision of neo selectable marker

In order to excise the *neo* selectable marker cassette, the chosen HCT116 targeted cell clone was seeded into a 6-well dish and the following day cells were treated with purified cell penetrating fusion protein TAT-Cre (2,3 µM) (kind gift from Dr. C. López-Rodríguez, UPF) for 3 hours at 37 ºC [165]. Treated cells were then washed and further incubated in cell medium. After 48 hours, cells were reseeded in order to isolate single cell colonies. After 7 days, well separated colonies were harvested and reseeded. Excision of the selectable marker was confirmed by the gain of sensitivity to G418.

MM4.7. Second round of targeting

In order to confirm correct targeting of the second allele of the Cyclin O gene locus, we took advantage of the availability of the oligos designed for the human Cyclin O sequencing in order to amplify a WT fragment of the Cyclin O gene (see table MM8. Fragment B). In the case of correct knock out of both Cyclin O alleles, clones giving no PCR product for the WT fragment would be selected (Figure MM6).

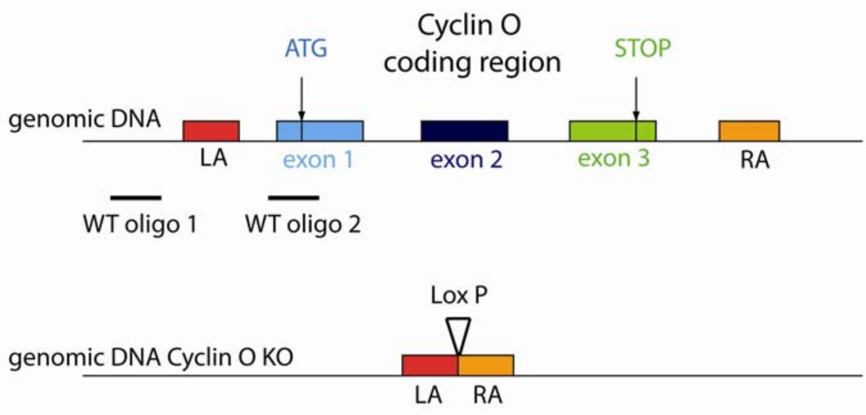
Cyclin O coding region
ATG
STOP
genomic DNA
LA
exon 1
exon 2
exon 3
RA
WT oligo 1
WT oligo 2
Lox P
genomic DNA Cyclin O KO
LA
RA

Figure MM6. Scheme of oligo positions for second round targeting.

MM4.8. Southern blotting

Southern blot analysis was performed using genomic DNA from a candidate HCT116 clone after the first round of targeting of the Cyclin O gene, from a clone carrying a random integration and from the parental HCT116 cells.

20 µg of EcoRV digested genomic DNA were run on an agarose gel and transferred into a nylon membrane (Hybond XL, GE healthcare) overnight. The membrane was prehybridised with 100 µg / ml single stranded salmon sperm DNA in prehybridation solution (12,5 x SSPE, 10x Denhardts solution (1% Ficoll (type 400), 1% polyvinylpyrrolidone, and 1% bovine serum albumin in H_2O), 1,6 % SDS) overnight at 63 ºC under constant agitation.

The membrane was then hybridised with the single stranded radioactive DNA probe (1,5 x 10^6 cpm / ml) diluted in hybridation solution (12,5 x SSPE, 10x Denhardts solution, 1,6 % SDS, 20 mM EDTA pH 8, 100 µg / ml salmon sperm ssDNA) overnight at 63 ºC under constant agitation. Afterwards, the membrane was prewashed with washing buffer 1 (2x SSC pH 7, 0,1 % SDS in H_2O) and then washed 2x with washing buffer 2 (2x SSC pH 7, 0,5 % SDS in H_2O) for 30 min at 45 ºC., followed by 2 washes in washing buffer 3 (0,2x SSC pH 7, 0,8 % SDS in H_2O) for 15 min at 65 ºC and a last wash in washing buffer 4 (0,2x SSC pH 7 in H_2O). The membrane was afterwards exposed to X-ray films.

MM4.8.1. Preparation of the radioactive DNA probe

A 500 bp DNA fragment was amplified from the left arm homologous region (OligoF 1: 5’-ttatcaccctgaaggagc-3’, oligoR 2: 5’-gtctgatcctgagttccaaac-3’) by PCR. The DNA fragment was used as a template for random labelling (Roche) using alpha ^{32}P dCTP (3000 Ci / mmol) and purified using microspin columns (GE Healthcare). The prepared radioactive DNA probe for southern blotting was stored at -20 ºC until used.

MM5. Isolation of genomic DNA and sequencing of the human Cyclin O gene

Genomic DNA was obtained from HCT116 cells or human CRC tumour tissue performing a proteinase K (500 µg / ml) digest overnight at 55 ºC [166].

In order to sequence the Cyclin O gene locus in genomic DNA from HCT116 cells or CRC tumour tissue, DNA fragments were amplified by PCR using Platinum pfx DNA polymerase (Invitrogen) from 100 ng of genomic DNA / reaction in a final volume of 50 µl. The purified PCR product was sequenced using the BigDye® Terminator v3.1 cycle sequencing kit (Invitrogen). The sequencing was performed at the Genomics Core Facility of the Universitat Pompeu Fabra.

PCR DNA amplification

94 ºC	2 min	
94 ºC	30 s	
55 ºC	30 s	35 cycles
68 ºC	40 s	
68 ºC	5 min	

PCR Sequencing

96 ºC	1 min	
96 ºC	10 s	
50 ºC	5 s	25 cycles
60 ºC	4 min	

Table MM8. PCR conditions

hCyclin O gene fragment	OligoF 1	OligoR 2
A	5'-gtggagctccaatctattcc-3'	5'-ctccttctctctaccacacc-3'
B	5'-aatcgcggctccggtgccgc-3'	5`-aaggtctgtagatctagctgcg-3'
C	5'-cgggagactccggcatttgc-3'	5'-acttgcccgggagttcggtagg-3'
D	5'-tagacggcttgagggacttg-3'	5'-agctggaagcagtctgcagc-3'
E	5'-ctgtaagctgctcagctggc-3'	5'-gttgatctaactactgtcc-3'
F	5'-tggcacctctagtctagcc-3'	5'-aaggggagtagctggtgaag-3'
G	5'-cctggagcatttcacgcacg-3'	5'-agctgaccaagcaggtcctg-3'
H	5'-aaacagatccttcgtttcc-3'	5'-atagaggttctattcgaggg-3'

Table MM9. Oligos used for sequencing of the human Cyclin O gene.

MM6. Subcellular fractionation and western blotting

MM6.1. Subcellular fractionation from CRC tissue or cell culture

In order to prepare the normal colon tissue samples for the subcellular fractionation, we separated carefully the submucosa from the mucosa part of the tissue piece, only the colon mucosa part was used for the fractionation procedure. The tumour and mucosa tissue samples used for immunoblotting were processed using subcellular fractionation buffer 1 (1 x DDF (300 mM sucrose, 100 mM NaCl, 10 mM PIPES pH 6,8, 3 mM $MgCl_2$ in H_2O), 5 mM EDTA pH 8) containing Digitonin (0,015 %) an all glass Dounce type tissue homogenizer in order to get a coarse homogenate. The homogenate was incubated at 4 ºC for 10 min under constant agitation, centrifuged at 500 rcf for 10 min at 4 ºC and the supernatant was kept as cytosolic protein fraction at -80 ºC until used. The remaining pellet was resuspended in cell fractionation buffer 2 (1 x DDF, 3 mM EDTA pH 8) containing Triton-X 100 (0,5 %) and reextracted for 30 min at 4 ºC under constant agitation, centrifuged at 5000 rcf for 10 min at 4 ºC and the supernatant was kept as membrane / organelle protein fraction at -80 ºC until used [167]. The remaining pellet was resuspended in RIPA buffer (10 mM Tris-HCl pH 7.4, 1% NP-40, 0.1% SDS, 1% sodium deoxycolate and 0.15 M NaCl) and reextracted for 10 min at 4 ºC, centrifuged at 10000 rcf for 10 min at 4 ºC and the supernatant was kept as nuclear protein fraction at -80 ºC until used.

Cells from cell culture used for immunoblotting were washed with cold PBS and either frozen at -80 ºC when whole protein lysates using RIPA buffer were needed or immediately processed for subcellular fractionation using the same procedure as described above.

Protease and phosphatase inhibitors were added (2 µg/ml aprotinin, 2 µg/ml leupeptin, 2 µg/ml antipain, 20 µg/ml soybean trypsin inhibitor, 1 mM DTT, 1 M NaF, 0.5 M β-glycerol phosphate, 0.1 M sodium pyrophosphate, 1 mM Pefablock™ and 20 mM sodium ortovanadate) to all buffers used for protein extractions.

Protein samples were quantified using the Bradford reagent (BioRad).

MM6.2. Western blotting

Equal amounts of protein were loaded on each lane (20 to 70 µg / lane), resolved by SDS-Polyacrylamide Gel Electrophoresis (SDS PAGE) and transferred into a nitrocellulose membrane (Protran). Membranes were blocked with 5 % non-fat milk prepared in TBS-T (20 mM Tris HCl pH 7.6, 137 mM NaCl, 0.1% Tween 20) either for 1 hour at RT or overnight at 4 ºC under constant agitation. Primary antibodies were diluted in TBS-T containing 2% BSA and were incubated for 1h at RT or overnight at 4 ºC. After extensive washing with TBS-T, membranes were incubated for 1 hour with the corresponding secondary HRP (Horseradish Peroxidase)-conjugated antibody. Membranes where then incubated with either ECL chemiluminiscent substrate (Pierce) or SuperSignal West Pico (Pierce). For stripping the antibody, membranes were incubated for 30 minutes at 50 ºC with 62.5 mM Tris-HCl pH 6.8, 2% SDS, 100 mM β-mercaptoethanol.

MM7. Animals

Apc$^{Min/+}$ mice (Jackson Laboratories) were kept in a homogenous inbred C57BL/6J background. Cyclin O -/- mice (kept in pure C57Bl/6J background) were crossed with *Apc*$^{Min/+}$ mice. All mice were genotyped by PCR. Animals were kept under pathogen-free conditions and all procedures were approved by the Animal Care Committee.

genotyping *Ccno*

471bp KO
652 bp WT

Oligo 1	**Oligo 2**
5'-tcattctcagtattgttttgcc-3'	5'-ggaactcagcctcctgactg-3'
Oligo 3	
5'-ctgtgaccttttcgagtccc-3'	

Table MM10. Oligos for genotyping of *Ccno* from mouse tail DNA. The expected sizes for the WT band is 652 bps and the KO band 471 bps.

genotyping *APC*

471 bp KO
652 bp WT

Oligo 1	**Oligo 2**
5'-gccatcccttcacgttag-3'	5'-ttccactttggcataaggc-3
Oligo 3	
5'-ttctgagaaagacagaagtta-3'	

Table MM11. Oligos for genotyping of APC from mouse tail DNA. The expected sizes for the WT band is 652 bps and the KO band 471 bps.

For analysis of proliferating cells, mice were injected intraperitoneally with 0,5 ml of BrdU in sterile PBS (125mg/kg mice) 2 hours before sacrifice.

MM8. Human colorectal tissue samples

For the tissue microarrays (TMA) 334 CRC patients were selected who underwent surgery of the primary tumour between January 1995 and December 2009 at the Hospital del Mar, Barcelona. Clinical data and follow-up were obtained from the review of the patient's medical records and from the Tumour Registry.

Postoperative adjuvant chemotherapy with 5-fluorouracil was performed for all stage III and IV patients. All patients were followed under the same protocol for at least eight years after surgery. Microscopic confirmation of diagnosis, tumour type and histological grade was carried out by pathologists of Servei de Patologia, Hospital del Mar. Patient staging was classified according to the International Union against Cancer Tumour-Node Metastasis criteria. The analysis of the samples was approved by the Ethical Committee for Clinical Experimentation of the Parc de Salut Mar and the Banc teixits, Barcelona, Spain. Cancer-specific survival was calculated from time of the surgery for the primary tumour until patient death secondary to colorectal cancer recurrence or metastasis.

In order to prepare the TMAs, formalin-fixed, paraffin-embedded tissue blocks of colorectal tumours were retrieved from the archives of the Servei de Patologia from Hospital del Mar. Multiple areas of invasive carcinoma and different histological patterns of those tumours (cribiform, mucinous, poorly-differentiated, “signet ring cell”), adenomatous lesions from the same surgical sample, and normal mucosa, far from the infiltrating tumour, were identified on corresponding haematoxylin-eosin-stained slides, and the tissue blocks were transferred to a recipient “master” block using a Tissue Microarrayer. Each core is 0.6-mm wide spaced 0.7-0.8 mm apart. Five different TMAs were made with the tumours selected. Sample duplicates were randomly distributed over the TMAs.

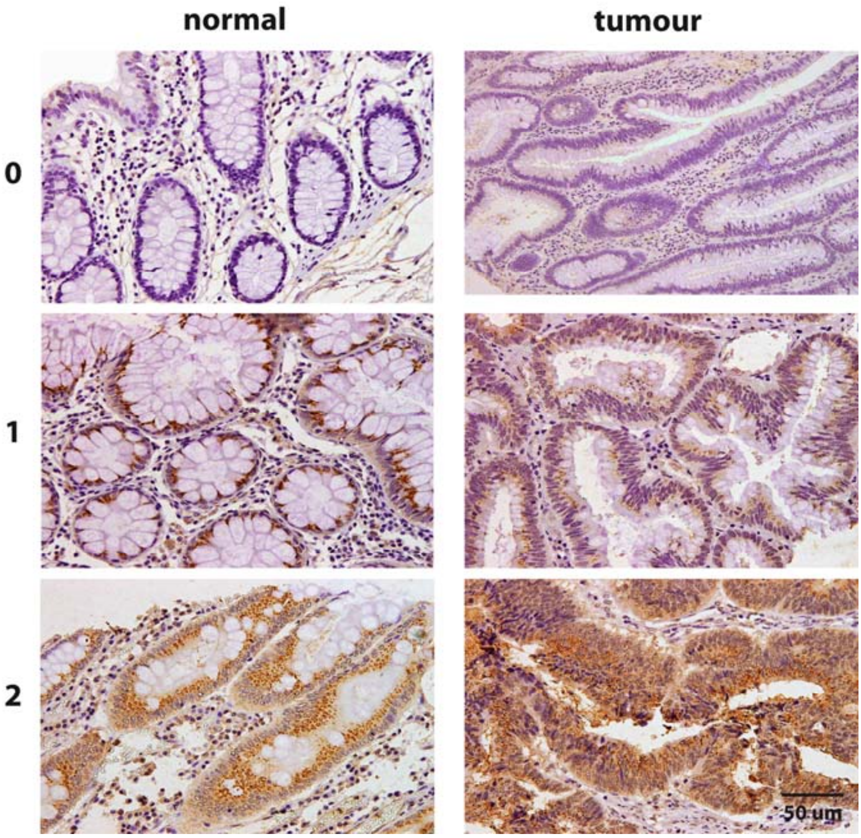

Figure MM7. Cyclin O IHC staining intensity for the evaluation of the TMAs. The intensity of Cyclin O staining was evaluated using a scale from 0 to 2, being 0 negative or low Cyclin O expression and 2 high Cyclin O expression.

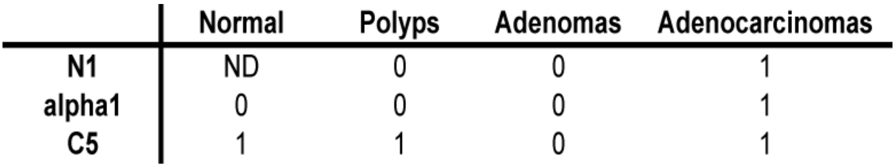

	Normal	Polyps	Adenomas	Adenocarcinomas
N1	ND	0	0	1
alpha1	0	0	0	1
C5	1	1	0	1

Table MM12. Correlation of the IHC using the HC2 antibody with other anti-Cyclin O antibodies. The correlation between the IHC of TMA1 with HC2 and the N1, alpha1 and C5 anti-Cyclin O antibodies was analysed using the X^2 square method. A p-value < 0,05 is indicated with 1 (statistically significant), a p-value > 0,05 is indicated with 0 (not statistically significant) ND = not done.

MM9. Immunohistochemistry

Immunohistochemical analysis was performed using 4 µm sections of paraformaldehyde-fixed, paraffin-embedded mouse or human tissue blocks. The tissue sections were hydrated and endogenous peroxidase blocking was performed using 1,5 % H_2O_2 in PBS incubating the tissue sections for 20 min at RT. Antigen recovery and blocking was performed depending on the primary antibody used for the staining (see table MM13.). Primary antibodies were diluted in PBS + 1 % BSA (table MM13.) and incubated for 90 min at RT (HC2) or overnight at 4 ºC. A secondary antibody coupled to HRP was applied depending on the primary antibody and incubated for 1 hour at RT. The colorimetric substrate was used for visualisation. Sections were counterstained with haematoxylin, dehydrated and mounted.

Primary antibody	**Antigen recovery**	**Blocking**	**Dilution**
Cyclin O (HC2, C2)	citrate buffer pH 6	5 % non-fat milk in PBS (0,04 % Tween 20)	1:3 (HC2), 1:20 (C2)
beta catenin	Tris EDTA pH 9	PBS + 1 % BSA	1:100
BrdU	citrate buffer pH 6	PBS + 0,05 % BSA	1:100
E cadherin	citrate buffer pH 6	Goat serum blocking solution	1:50
lysozyme	Tris EDTA pH 8	PBS + 1 % BSA 0,3 % Triton X 100	1:2500
MOCS2 (rabbit)	citrate buffer pH 6	5 % non-fat milk in PBS (0,04 % Tween 20)	1:400

Table MM13. Conditions for IHC depending on the primary antibody.

MM9.1. Alcian blue staining

Tissue sections were stained with a 1 % Alcian blue solution (in 3 % acetic acid pH 2) for 30 min at RT, sections were washed, a HEOS staining was performed and sections dehydrated and mounted.

MM10. Statistical analysis

Data were expressed as the mean ± S.E.M. (Standard Error of the Mean). Data were evaluated statistically by Student's t-test.

Survival data were analyzed according to the method of Kaplan-Meier and tested for significance between the groups with the log rank test. The associations between Cyclin O expression and other clinicopathologic variables were assessed by the chi-square test used with categorical variables. All statistical analyses were carried out using SPSS20.

Significance levels: P=0.05, *; 0.05 >p>0.01,**; 0.01>p>0.005, ***; 0.005>p>0.001, **** and 0.001>p>0.0005, *****.

MM11. Commercial suppliers

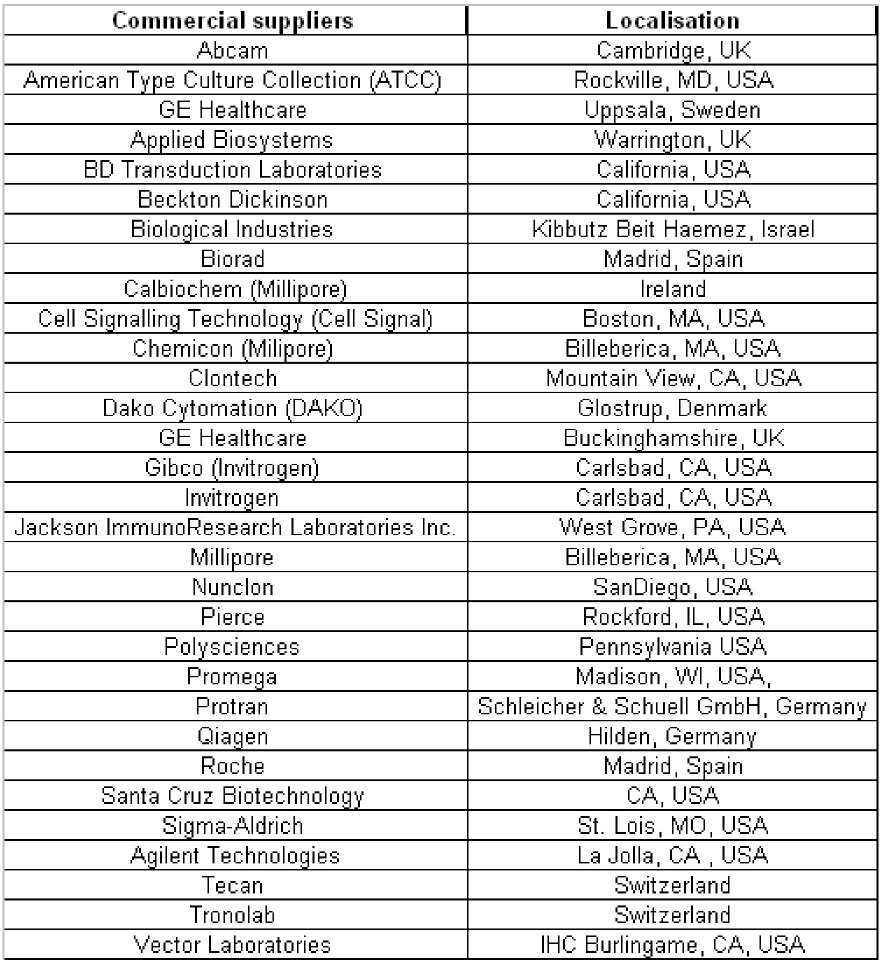

Commercial suppliers	Localisation
Abcam	Cambridge, UK
American Type Culture Collection (ATCC)	Rockville, MD, USA
GE Healthcare	Uppsala, Sweden
Applied Biosystems	Warrington, UK
BD Transduction Laboratories	California, USA
Beckton Dickinson	California, USA
Biological Industries	Kibbutz Beit Haemez, Israel
Biorad	Madrid, Spain
Calbiochem (Millipore)	Ireland
Cell Signalling Technology (Cell Signal)	Boston, MA, USA
Chemicon (Milipore)	Billeberica, MA, USA
Clontech	Mountain View, CA, USA
Dako Cytomation (DAKO)	Glostrup, Denmark
GE Healthcare	Buckinghamshire, UK
Gibco (Invitrogen)	Carlsbad, CA, USA
Invitrogen	Carlsbad, CA, USA
Jackson ImmunoResearch Laboratories Inc.	West Grove, PA, USA
Millipore	Billeberica, MA, USA
Nunclon	SanDiego, USA
Pierce	Rockford, IL, USA
Polysciences	Pennsylvania USA
Promega	Madison, WI, USA,
Protran	Schleicher & Schuell GmbH, Germany
Qiagen	Hilden, Germany
Roche	Madrid, Spain
Santa Cruz Biotechnology	CA, USA
Sigma-Aldrich	St. Lois, MO, USA
Agilent Technologies	La Jolla, CA , USA
Tecan	Switzerland
Tronolab	Switzerland
Vector Laboratories	IHC Burlingame, CA, USA

Table MM 14. Commercial Suppliers.

Results

R1. Expression and clinical implication of Cyclin O in human colorectal cancer

R1.1. Expression of Cyclin O in normal human and mouse intestinal tissue

As a first approach to study the implication of Cyclin O protein in CRC, we aimed to know if the protein is expressed in the normal intestinal epithelium. Because it is difficult to obtain human samples of normal healthy intestinal epithelium, in order to study the expression of Cyclin O in the human intestine, we first took advantage of the Oncomine database that is constantly updated by collecting microarray data results from different sources, such as published data or other gene expression databases. In this way facilitates the “in silico” analysis of the expression pattern of a wide range of genes in different human cancer types and normal tissues [168].

Among the Oncomine significant search results, we found a study from Sabates-Bellver *et al* which revealed statistically significant differences in Cyclin O mRNA expression between normal colon and colonic adenoma tissue [169] (Figure R1). The dataset contains a total of 57 samples, which are divided into 32 normal samples taken from different parts of the colon and 25 colonic adenomas. We could observe that Cyclin O mRNA is not expressed in the majority of normal colon samples (Figure R1 , light blue bars), with only 6 out of 32 samples showing low levels of Cyclin O mRNA, indicating that Cyclin O mRNA is expressed at very low levels in normal human colon tissue. In contrast, all the adenoma samples showed elevated Cyclin O mRNA levels. Comparing normal and colon adenoma samples, these findings indicate that Cyclin O mRNA levels are upregulated in colon adenomas ($p = 1,29 * 10^{-14}$).

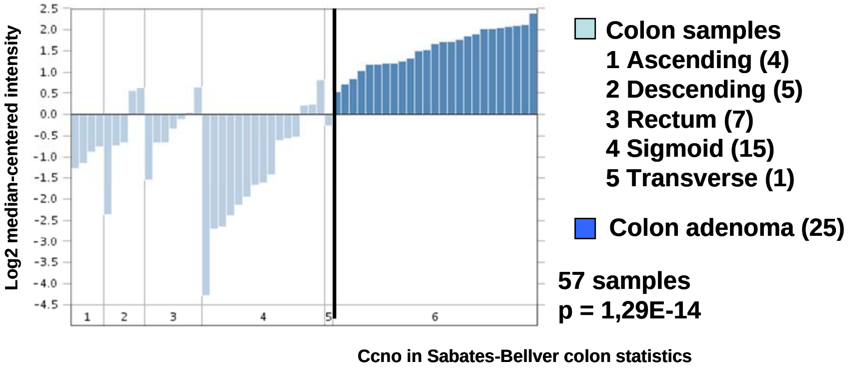

Figure R1. Comparison of the expression of the Cyclin O gene in normal colon versus colon adenomas. Samples from different parts of normal colon (light blue bars) and colon adenomas (dark blue bars) are shown. The p value indicates statistically significant difference between the two groups. (Graph was adapted from the Oncomine database).

We also analysed the results of a second dataset from The Cancer Genome Atlas (TCGA) containing 123 samples, divided into normal colon (19 samples) and rectum (3 samples) and 101 colorectal adenocarcinoma samples (Figure R2). In agreement with the results shown before, Cyclin O mRNA expression levels were found to be very low in normal human colorectal tissue, whereas the majority of adenocarcinoma samples were found to have elevated Cyclin O mRNA levels ($p = 9,3 * 10^{-14}$).

From the two microarray datasets, we can conclude that the Cyclin O gene is not detected in normal human colorectal tissue, but it is expressed in premalignant lesions such as adenomas and in full blown colorectal adenocarcinomas. This indicates that the Cyclin O gene is deregulated along the transit from normal tissue to adenoma and from adenoma to adenocarcinoma.

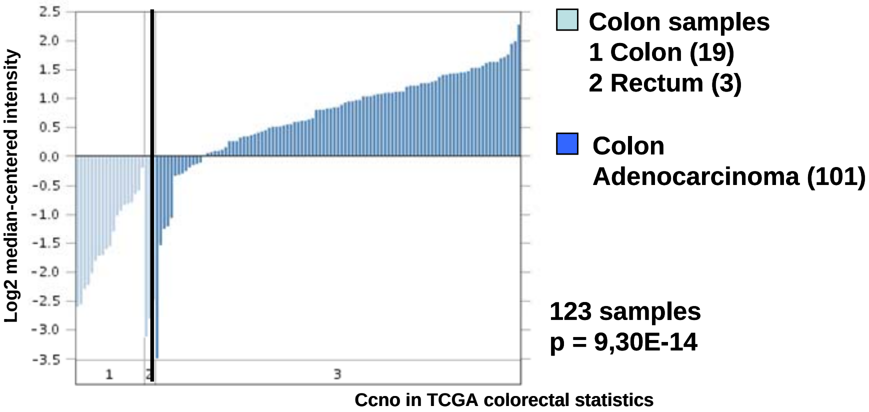

Figure R2. Expression of Cyclin O gene in normal colorectal and adenocarcinoma samples. Normal colorectal tissue samples (light blue bars) and colon adenocarcinomas (dark blue bars) are shown. The p value indicates statistically significant difference between the 2 groups. (Graph was adapted from the Oncomine database)

In order to study the role of Cyclin O in CRC, we also aimed to how Cyclin O is expressed in normal mouse intestine. For this reason, the expression pattern of Cyclin O in different WT mouse tissues was analysed by semi-quantitative RT-PCR in our laboratory (Figure R3). The highest levels of Cyclin O mRNA expression were observed in the mouse brain and testis. In mouse small intestine and colon, we could detect very low levels of Cyclin O mRNA. This suggests that Cyclin O is expressed at very low levels in normal mouse intestine and colon, resembling what has been observed in the case of the normal human colon.

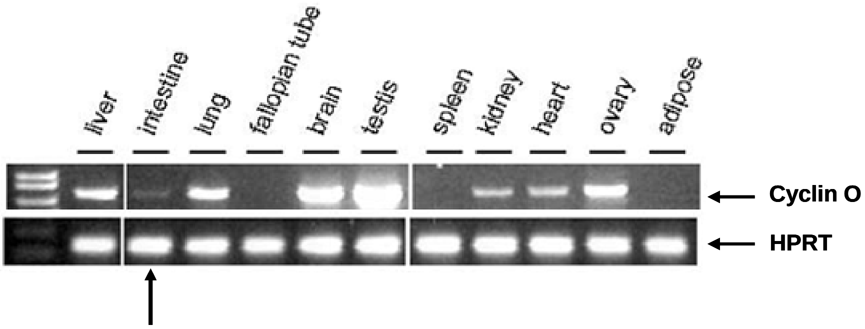

Figure R3. Cyclin O expression in different mouse tissues. Expression of Cyclin O mRNA was measured by semi-quantitative RT-PCR in mouse tissues. As a loading control, HPRT levels were measured. Figure adapted from Ortet, L., *Signalling of Cyclin O complexes through eIF2alpha phosphorylation*, doctoral thesis, 2010.

Additionally, we could not detect any endogenous Cyclin O protein by IHC neither in the small intestine nor in the colon of WT mice (data not shown), confirming the mRNA results.

R1.2. Cyclin O protein is overexpressed in human colorectal cancer

In order to validate the results of the Cyclin O mRNA expression analysis from the Oncomine database, we analysed tissue micro arrays (TMA) for the expression of human Cyclin O protein using IHC (Figure R4). The TMAs gave us the opportunity to estimate the Cyclin O expression in a wide range of CRC-related samples. They included samples of normal colon mucosa, polyps, adenomas and adenocarcinomas taken from a total of 319 CRC patients.

We found moderate expression levels of Cyclin O protein in 60 % of the adenocarcinomas, 37 % of the adenomas and 43 % of the polyp samples. In addition to this, high expression levels could be observed in 10 – 15 % of each of these groups.

Our results confirm that Cyclin O protein is expressed in human colorectal adenocarcinomas, in agreement with the results from the database analysis. The deregulated expression seems to appear at an early stage of epithelial transformation since in about 50 % of the premalignant lesions (polyps and adenomas), the Cyclin O protein is detected (Figures R5, R6).

However, we could also detect positive Cyclin O expression in about 50 % of the normal mucosa samples. This finding does not agree with the microarray expression studies in normal colorectal tissue.

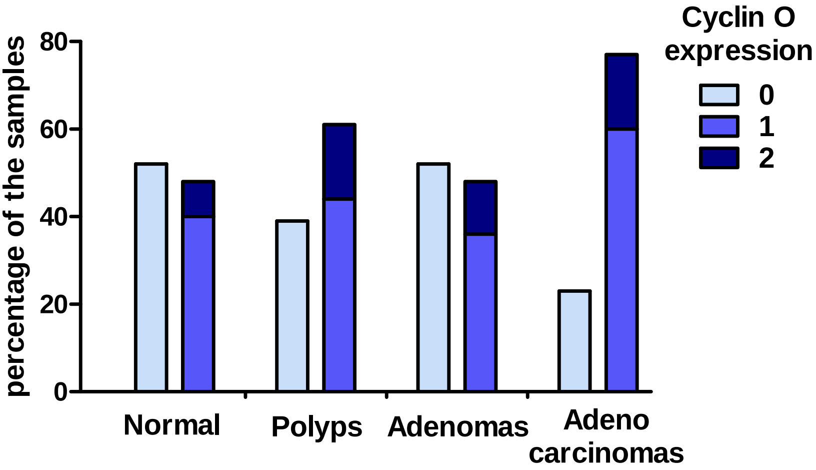

Figure R4. Cyclin O protein is overexpressed in CRC. TMAs containing samples of the morphologically normal margins of the tumour (Normal), polyps, adenomas and adenocarcinomas from 319 CRC patients were evaluated for Cyclin O expression levels by 3 independent observers using a scale of 0 to 2, being 0 low or no expression (light blue), 1 moderate expression (blue) and 2, high expression (dark blue).

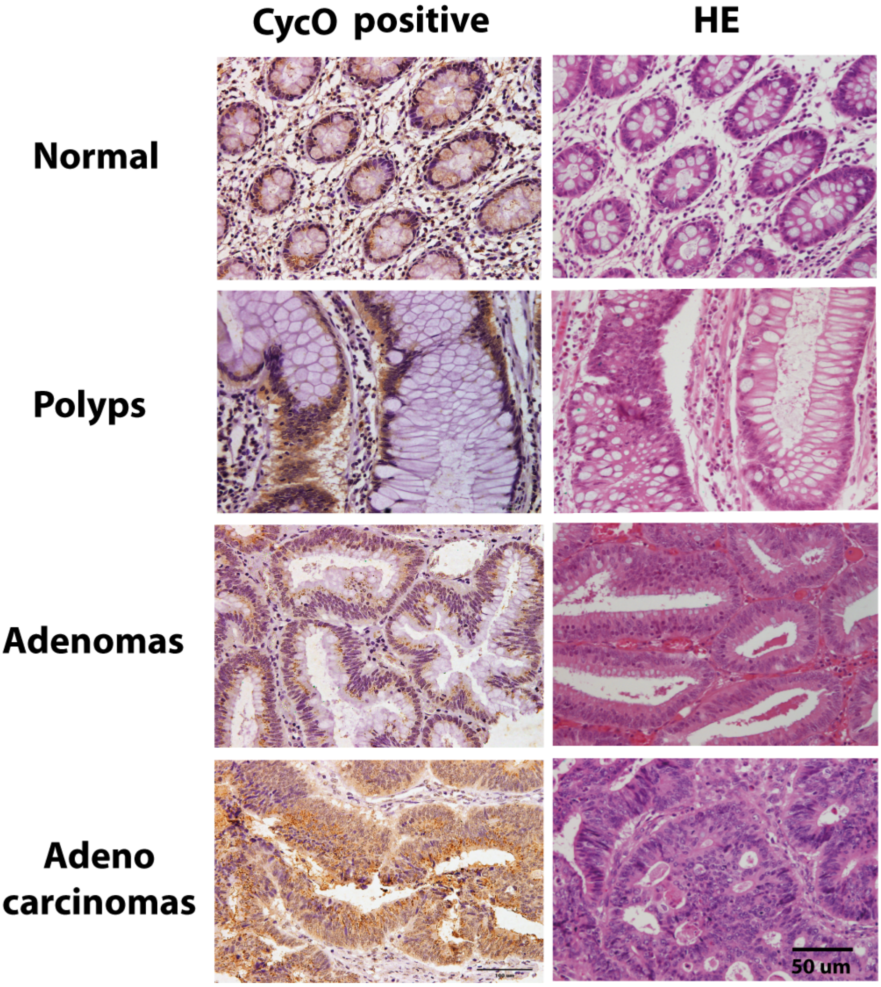
CycO positive
HE
Normal
Polyps
Adenomas
Adeno carcinomas
50 um

Figure R5. Cyclin O expression in the TMA tissues. Cyclin O is expressed (CycO positive) in tissues from normal mucosa (normal), polyps, adenomas and adenocarcinomas. IHC was performed using the HC2 antibody and the colorimetric substrate DAB. The corresponding HEOS staining is also displayed (HE).

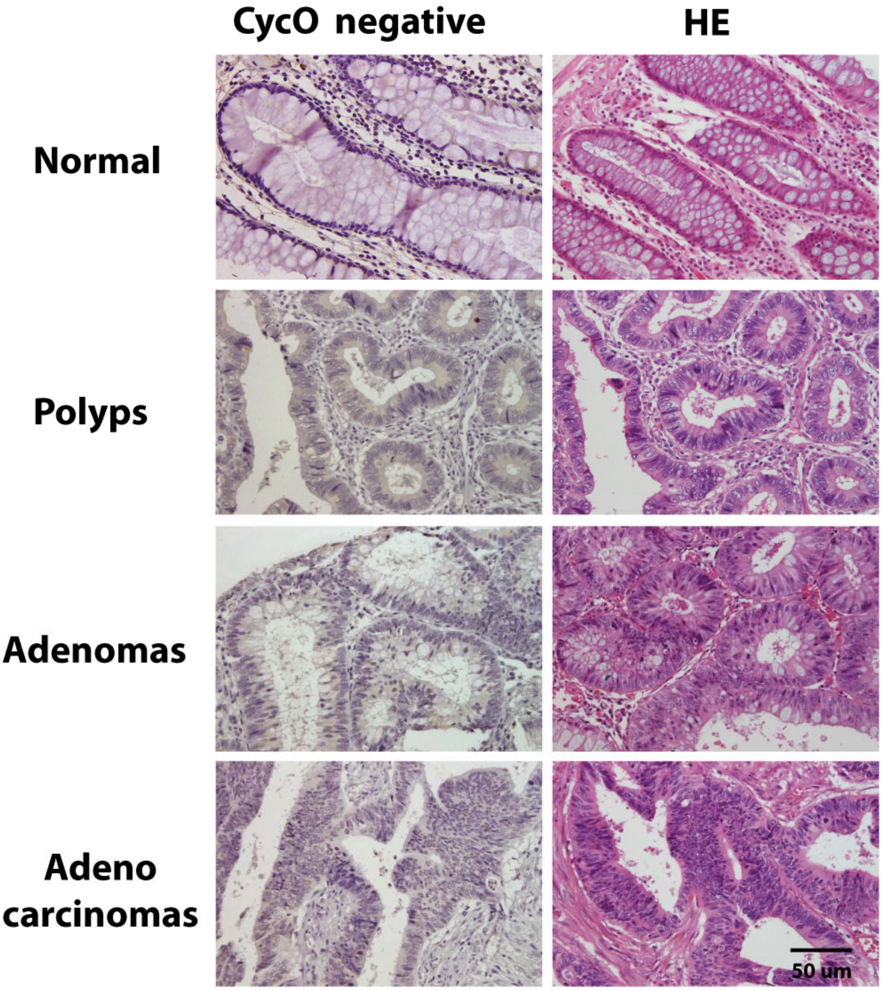
CycO negative
HE
Normal
Polyps
Adenomas
Adeno carcinomas
50 um

Figure R6. Negative Cyclin O expression in the TMA tissues. Negative Cyclin O expression (CycO negative) in tissues from normal mucosa (normal), polyps, adenomas and adenocarcinomas. IHC was performed using the HC2 antibody and the colorimetric substrate DAB. The corresponding HEOS staining is also displayed (HE).

R1.3. Cyclin O expression in fresh samples of CRC patients

The analysis of CRC samples by IHC using the TMAs allowed us to study the Cyclin O expression in a high throughput manner. However, we sought to confirm our expression analysis using IHC and additionally a different experimental technique. Western blotting allowed us to quantify and compare protein expression levels in fresh tissue samples from CRC patients.

In order to be able to quantify Cyclin O protein levels in the obtained tissues, we separated the colon mucosa from the submucosa in the normal samples, processed the fresh tumours and normal mucosa samples from the CRC patients and analysed by western blotting the levels of Cyclin O in subcellular fractions of the tissues. We transfected HEK293T cells, which do not express Cyclin O protein, with a human Cyclin O expressing plasmid and used the cell lysate as a positive control for the western blotting.

We could observe different normal / tumour ratios of Cyclin O expression in 5 CRC cases analysed (Figure R7). Cases 1 and 3 showed higher Cyclin O protein levels in the normal colon samples than in the corresponding CRC tumour samples. Case 2 showed about the same Cyclin O protein levels in both samples, case 4 showed higher Cyclin O protein levels in the CRC tumour than in the corresponding normal colon and case 5 showed very low (Normal) or not detectable Cyclin O protein levels (Tumour) in the samples. The corresponding nuclear fractions of the cases were negative for Cyclin O expression (data not shown).

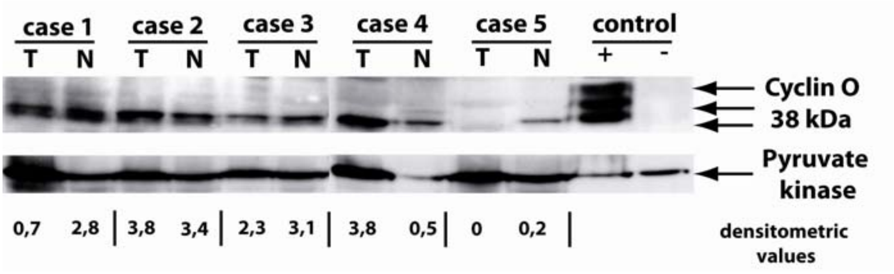

Figure R7. Cyclin O expression in the cytoplasmic fraction of fresh samples of CRC patients. Cytoplasmic tissue fractions were obtained from fresh tumour (T) and normal mucosa (N) samples coming from the same surgical specimen of 5 different CRC patients after subcellular fractionation. Fractions were analysed for Cyclin O protein by western blotting using the HC2 antibody. Whole lysates from Cyclin O transfected (control +) and not transfected (control -) HEK293T cells were used as positive and negative control respectively. Arrows indicate the 38 kDa Cyclin O protein and its phosphorylated forms (present only in Cyclin O transfected HEK293T lysate control). Pyruvate kinase was used as a loading control for the cytoplasmic fraction. The ratio Cyclin O / pyruvate kinase measured by densitometry is shown under each lane as calculated using ImageJ in arbitrary units.

Since both in the case of the tumours and in the normal samples the cell lysates contain proteins coming from non-epithelial cells, we aimed to compare the differences observed in the levels of Cyclin O protein by western blotting to the expression levels detected by IHC. From the western blotting result, we chose 3 different cases for IHC analysis (Figure R8). We chose case 2 as an example for high Cyclin O protein levels in both tumour and normal tissue. We selected case 4 as an example for higher protein levels in the CRC tumour than in the normal colon sample. Additionally we chose case 5 as an example for higher Cyclin O protein levels in the normal colon sample than in the CRC tumour sample. For CRC case 2, we could confirm Cyclin O expression in the cytoplasm of normal mucosa tissue taken from the distant margins of the tumour and in the CRC tumour by IHC. CRC case 4 shows high Cyclin O protein expression in both samples, normal mucosa and tumour, without considerable differences in expression levels. Finally, in the CRC case 5 we could detect Cyclin O protein in the normal mucosa sample but tumour cells were also positive for Cyclin O expression. Additionally, we could observe a highly desmoplastic appearance of this tumour sample. The cellular composition of this sample could explain the difficulties to get a reliable quantification of Cyclin O levels by western blotting.

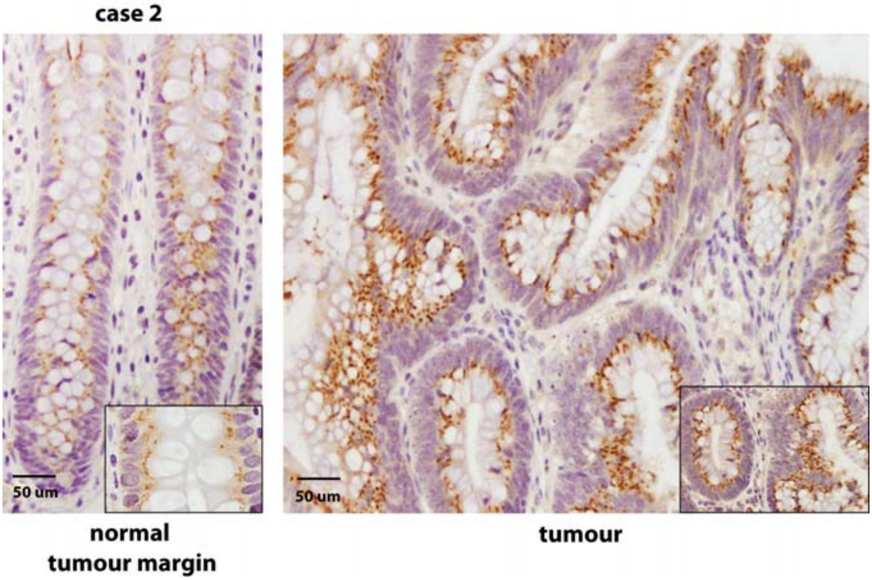

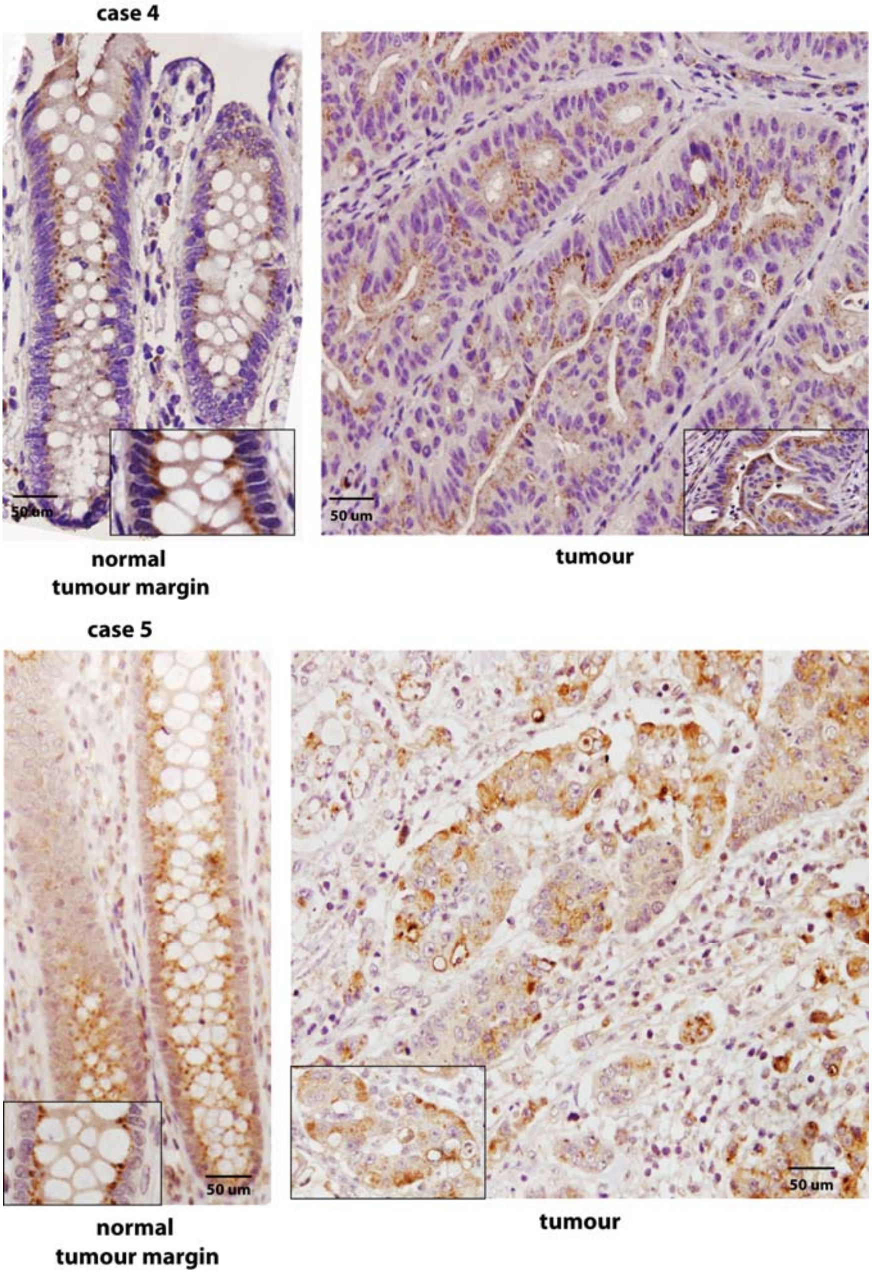
case 4
50 um
50 um
normal
tumour margin
tumour
case 5
50 um
50 um
normal
tumour margin
tumour

Figure R8. Cyclin O expression in fresh CRC tissue. For CRC cases 2, 4 and 5, a normal mucosa sample taken from the distant tumour margins and a tumour tissue sample with their corresponding inserts are displayed. Cyclin O protein has been detected using the HC2 antibody and the Powervision® system with the colorimetric substrate DAB.

To gain further insight into the meaning of the Cyclin O expression in morphologically normal peritumoral epithelium, we intended to study the Cyclin O expression in normal colon at increasing distances from the neoplastic lesion. We expected to find a border between histologically normal appearing colon samples expressing Cyclin O which could represent transformed tissue in a very early stage and cyclin O negative samples. We were unable to find a normal colon sample without Cyclin O expression, neither by western blotting nor by IHC. We suggest from this observation that either the normal samples could not be taken far enough from the tumour or, more likely, that secondary changes in the resected tissue as a consequence of the surgery (i. e. caused by anoxia) would trigger basal expression levels of Cyclin O.

R1.4. Cyclin O expression correlates with a longer cancer specific survival of CRC patients

In order to study the clinical significance of the Cyclin O expression in CRC samples detected in the TMA analysis, we aimed to correlate the Cyclin O protein expression with different clinical parameters from the CRC patients. We studied the correlations between the expression of Cyclin O in the TMA adenocarcinoma samples with the cancer specific survival of the CRC patients according to the TNM staging of the tumour (Figure R9). In the case of CRC stages III and IV, we could observe a statistically significant longer cancer specific survival of the patients whose tumour was positive for Cyclin O protein expression compared to patients with no detectable Cyclin O protein in the adenocarcinoma samples. Additionally, a Cox’s regression analysis indicated that

Cyclin O expression in the adenocarcinoma samples is a prognostic factor for the cancer specific survival independent of the TNM staging of the cancer (p=0,0005, R=0,368).

The same holds true for the Cyclin O expression in the polyp and adenoma samples from CRC patients with stages III and IV. We could also find a statistically significant longer cancer specific survival of the patients with Cyclin O expression compared to patients with negative Cyclin O expression (p=0,02, data not shown).

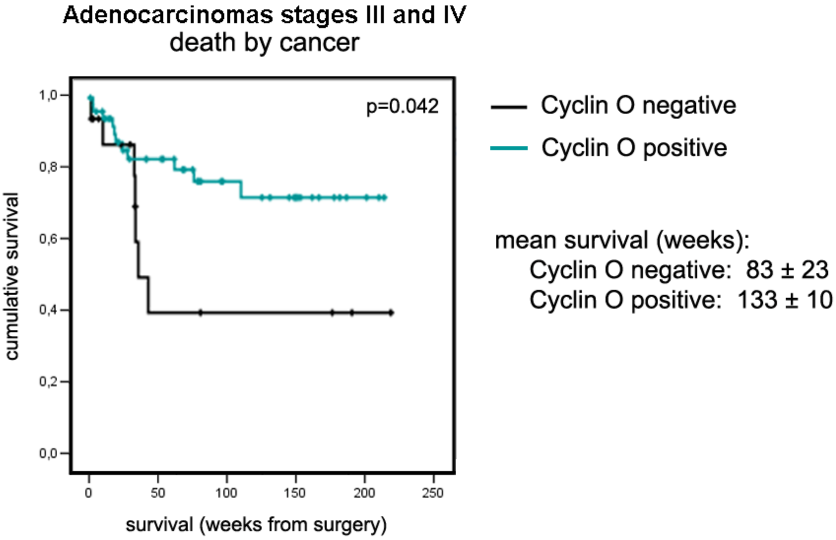

Figure R9. Correlation of cancer specific survival of the CRC patients in stages III and IV and the Cyclin O protein levels in their adenocarcinoma samples. The Kaplan-Meier survival plot shows the cancer specific survival of CRC patients with positive Cyclin O protein expression (blue line) and no Cyclin O protein expression (black line) in their adenocarcinoma samples.

We next explored putative correlations between Cyclin O expression in the peritumoral normal colon mucosa samples and the cancer specific survival of the CRC patients. We could observe that CRC patients with tumours in stages I and II and no Cyclin O expression in the normal mucosa samples have a tendency to have a longer cancer specific survival than CRC patients with Cyclin O expression in these samples. No statistical significance was reached for this correlation (Figure R10).

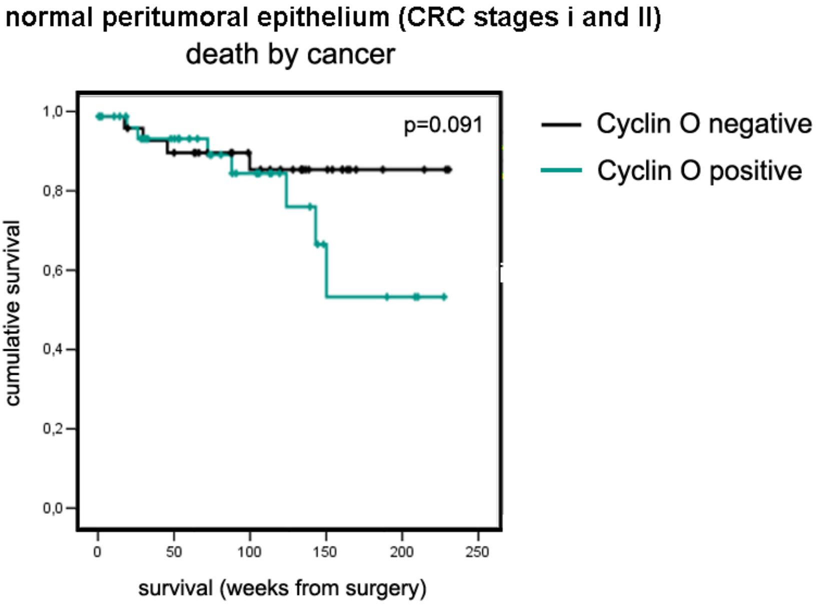

Figure R10. Correlation of cancer specific survival of patients with CRC stage I or II and Cyclin O protein levels in their normal peritumoral colon mucosa samples. Kaplan-Meier survival plot shows the cancer specific survival of CRC patients stage I or II with Cyclin O protein expression (blue line) and no Cyclin O protein expression (black line) in their normal peritumoral colon mucosa samples.

Our results indicate that Cyclin O expression in the tumour favors the survival of CRC patients with tumours of stages III and IV. We hypothesise that the presence of Cyclin O protein in CRC cells might have influence on the success of the adjuvant cancer treatment or that the tumours with positive levels of Cyclin O would show common histopathological features that slow their progression (i. e. a more differentiated phenotype).

In order to investigate our hypothesis, we aimed to correlate the expression of Cytokeratin 20, a putative differentiation marker, in the same TMA samples with the survival of CRC patients, but we could not find the same correlation as previously observed for Cyclin O (data not shown).

R1.5. Cyclin O overexpression is maintained in the metastasis of CRC

Because of the deregulated Cyclin O levels in primary colorectal tumours, we wondered if Cyclin O expression is maintained when the primary tumour spreads to distant sites. We then performed IHC for Cyclin O in the primary adenocarcinoma sample and in its metastatic sites in two cases where material was available (Figure R11). In the two CRC cases shown, we could detect the Cyclin O protein both in the cytosol of the normal epithelial cells of the normal colon intestinal cells taken from the margins of the tumour and in the cytoplasm of the cells of the primary tumour. In CRC case 1, we could find Cyclin O positive metastatic cells in the regional lymph nodes (Figure R11, C). In case 2, Cyclin O expressing metastatic cells could be detected in the liver (Figure R11, F). In both cases, the metastatic cells show the same cytoplasmic localisation of Cyclin O protein as already observed in the primary tumours and normal peritumoral mucosa.

We can conclude that Cyclin O expression is maintained in metastasis originated from a primary colon adenocarcinoma.

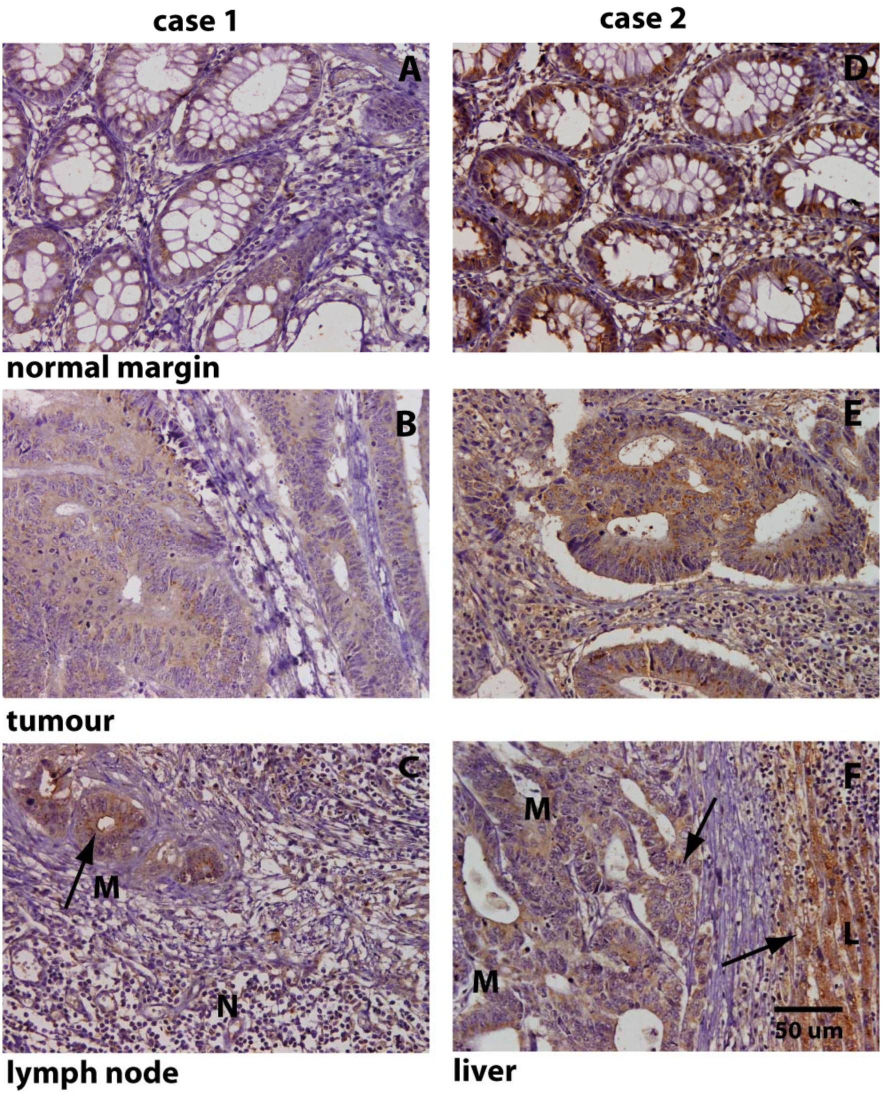
case 1
case 2
A
D
normal margin
B
E
tumour
C
M
N
F
M
M
L
50 um
lymph node
liver

Figure R11. Cyclin O expression is maintained during CRC metastasis. IHC of human Cyclin O protein in normal tumour margin **(A, D)**, CRC tumour **(B, E)**, metastasis to the regional lymph node **(C)**, metastasis to the liver **(F).** M, metastatic cells, N, lymph node lymphocytes and L, liver cells.

R1.6. MOCS2 is a putative target gene of Cyclin O in CRC

From a microarray analysis previously performed in our laboratory, we identified Molybdenum Cofactor Synthesis Protein 2A and B (*MOCS2*) as a gene induced by γ-radiation in a Cyclin O dependent manner and a putative downstream target gene of Cyclin O (Balsiger, Roset, Ortet and Gil-Gomez, unpublished data). We chose to include MOCS2 in this study, because of its potential role in the resistance of cancer cells to different chemotherapeutic treatments.

The MOCS2 enzyme is known to be involved in the synthesis of molibdopterin which is a cofactor for many enzymes, such as Xanthine oxidase or Aldehyde oxidase involved in the detoxification of xenobiotics [170] [171]. Increased activity of these enzymes could be related to the resistance of colorectal tumours to some chemotherapeutic drugs.

In order to get further insight of *MOCS2* as a putative downstream target gene of Cyclin O, we treated a empty vector control and Cyclin O overexpressing WEHI7.2 cells with γ-radiation as previously described in [160], the same conditions that were used to get the samples analysed by microarray analysis (Figure R12). We could observe a transient induction of MOCS2 protein in the control cells. However, in the Cyclin O overexpressing cells, the basal levels were higher and the peak of induction lasted longer.

Our result are in agreement with *MOCS2* being a putative downstream target gene of Cyclin O.

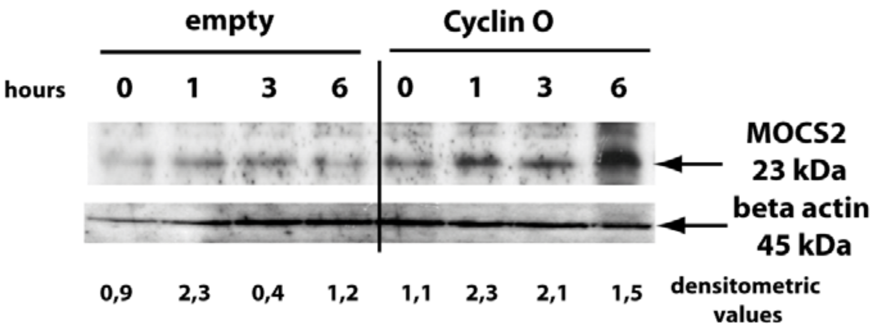

Figure R12. MOCS2 is regulated by Cyclin O. WEHI7.2 cells stably transfected with an empty vector control or a vector expressing Cyclin O protein were exposed to 10 Gy of γ-radiation and whole cell lysates were obtained at the indicated time points. MOCS2 protein levels were measured by western blotting. ß actin was used as a loading control. Densitometric values were measured with the ImageJ program and the ratio MOCS2 / ß-actin calculated. Results are displayed underneath in arbitrary units 0, 1, 3 and 6 hours after gamma irradiation.

Next we aimed to correlate the expression levels of MOCS2 protein to those of Cyclin O by means of IHC using the CRC samples included in TMA1 and TMA3, previously used in the analysis of Cyclin O expression. The MOCS2 protein is expressed in the cytoplasm of normal intestinal epithelium as well as in the tumour cells. We could observe a positive correlation in MOCS2 and Cyclin O protein expression in normal mucosa samples, polyps and adenocarcinomas (Figure R13).

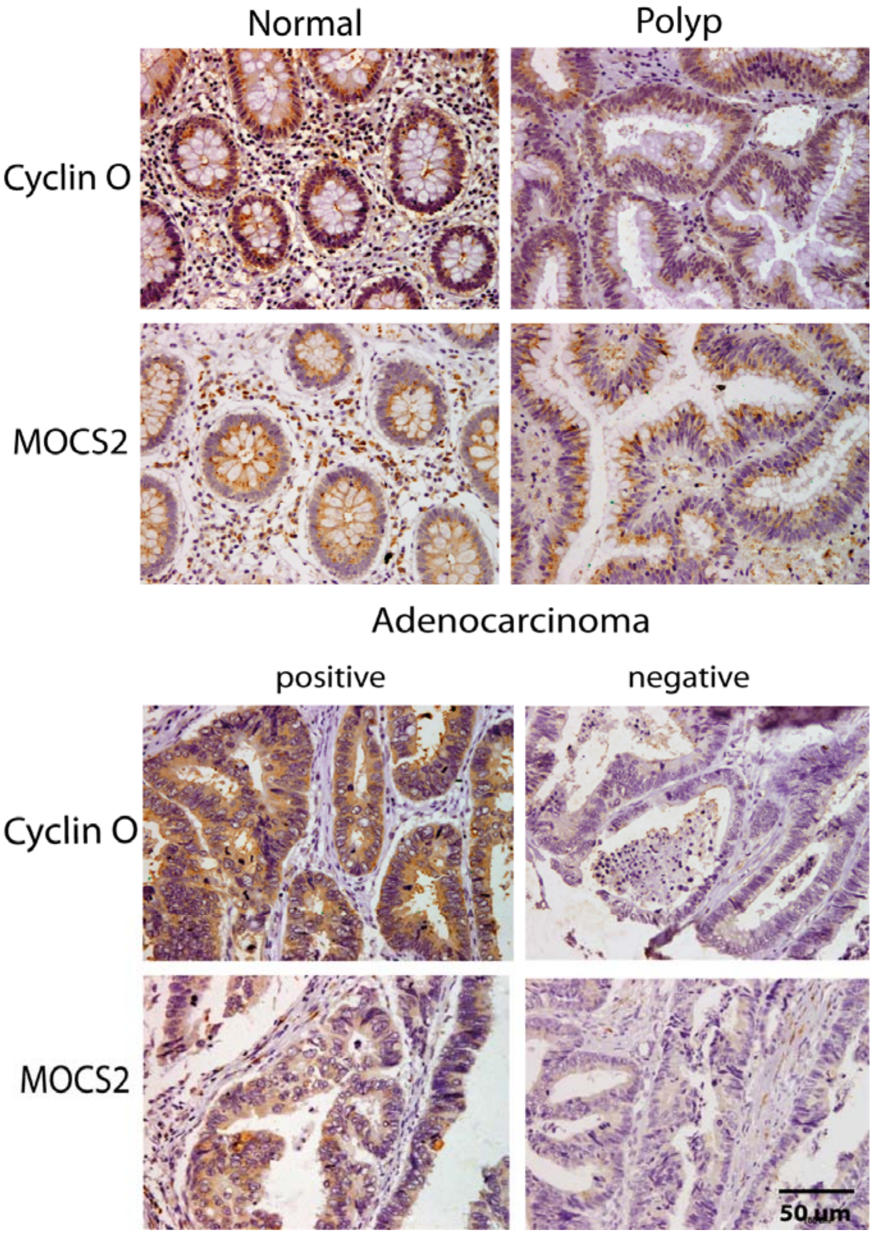
Normal
Polyp
Cyclin O
MOCS2
Adenocarcinoma
positive
negative
Cyclin O
MOCS2
50 µm

Figure R13. Correlation of Cyclin O to MOCS2 expression. IHC for Cyclin O and MOCS2 from a normal, polyp and adenocarcinoma sample were selected from the TMAs.

We correlated MOCS2 expression in the samples included in TMA1 (100 cases) to the cancer specific survival of patients following CRC. Although perhaps due to the limited number of samples analysed we did not reach statistical significance, the analysis of MOCS2 expression in the adenocarcinoma and normal epithelium samples showed a trend towards a better cancer specific survival for the CRC patients when MOCS2 was not expressed in the tissue (Figure R14).

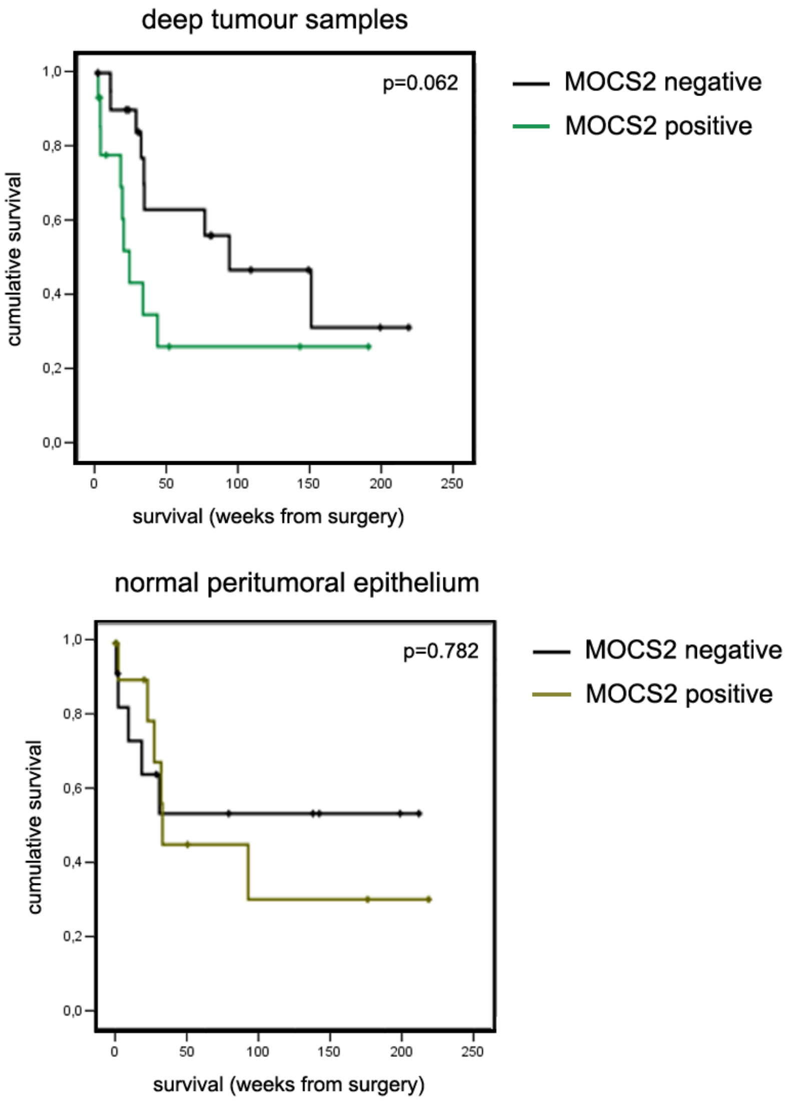

Figure R14. Correlations of MOCS2 to the cancer specific survival of the CRC patients. The graphs show the correlation between the MOCS2 expression in the adenocarcinoma samples (upper graph) or in the normal peritumoral epithelial samples (lower graph) and the cancer specific survival of the CRC patients.

R1.7. The Cyclin O gene is not mutated in human CRCs

For a cancer cell to gain and maintain its malignant properties, it accumulates mutations. A wide number of genes in cancer have an impaired or absent function because they are mutated. Because of its overexpression in CRC cells, we wondered if the *CCNO* gene encoding for Cyclin O is also mutated and therefore the apoptotic inducing function of the protein would be impaired.

The analysis by IHC of colon adenocarcinoma samples using polyclonal antibodies directed against epitopes present at the beginning (antibodies N1 and C1), middle part (antibody alpha1) and the end of the coding region (antibody HC2) suggested that the protein present in the tumours was full length. However, it could contain mutations that impair its normal function. The *CCNO* locus spans a length of only about 3,3 kb (including 0,5 kb of 5’ and 3’ flanking regions in addition to the gene). Taking this into account we intended to sequence the whole gene locus from genomic DNA isolated from the CRC cell line HCT116 and from a fresh tumour sample (Figure R15). In both samples, Cyclin O is detected by IHC. However, we did not detect any mutation in either the pseudodiploid HCT116 cells nor in the adenocarcinoma DNA sequenced, indicating that the Cyclin O protein expressed in CRC samples corresponds to the WT form.

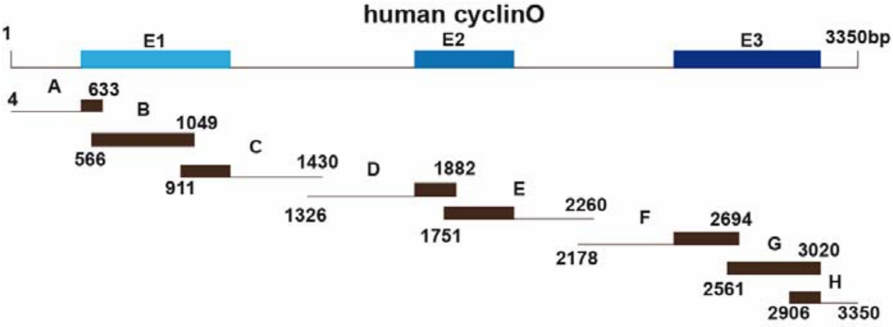

Figure R15. Sequencing strategy of the human Cyclin O gene locus. Scheme of human Cyclin O gene fragments which were amplified by PCR. The different PCR products were sequenced and compared to the WT human Cyclin O sequence.

R1.8. Significance of Cyclin O expression in CRC

Up to know, we have observed Cyclin O overexpression in CRC tissues. Next, we wondered if the downregulation of Cyclin O could return the cancer cell to a less malignant phenotype or resensitise them to chemotherapeutic drugs. Therefore, in order to gain further insight into the function of Cyclin O in CRC cells, we first intended to downregulate Cyclin O in CRC cell lines by the mean expression of specific shRNAs. Unfortunately, using different shRNAs we could only marginally downregulate the Cyclin O mRNA expression levels in the cell. Therefore, we decided to change the experimental technique.

We then intended to knock out the Cyclin O gene in the pseudodiploid CRC cell line HCT116 by homologous recombination using a recombinant AAV containing a *CCNO* targeting construct [163]. After the first round of targeting we selected a candidate HCT116 heterozygote clone. The candidate clone was transduced with TAT-Cre recombinant protein [165] to delete the *neo* cassette then we checked the candidate clones by PCR and by regaining the sensitivity to G418. The parental cell line and the clone prior and after Cre transduction were analysed by southern blotting [165]. The genomic DNA was digested with EcoRV, transferred to a nitrocellulose membrane and probed with a random-primer labeled probe corresponding to the left arm of the construct.

For the WT allele we expected to detect a DNA fragment of 11002 bp, for the *neo* allele 8952 bp and for the Cre deleted allele 7778 bp (Figure R16) As expected, we detected the WT allele in all the samples. Additionally a clone with random integration of the targeting construct identified by PCR as targeted incorrectly and that we used as a control, showed a band of 5000 bp that did not correspond to any of the expected bands. However, we could not detect the expected bands for the *neo* allele and Cre-deleted allele in the candidate clone. Both bands were approximately 4600 bp smaller than expected, suggesting that a rearrangement of the genomic locus had taken place during the targeting process (Figure R17). Due to the positive result of the diagnostic PCR for targeting it is likely that a recombination took place at some point during the process outside of the targeted region.

During the first round of targeting, we reached a targeting efficiency of 3,3 %. We continued working with the selected candidate clone in order to target the second Cyclin O allele. We proceeded as described in MM4.4. and 4.5. and checked the G418 resistant clones obtained in 2 independent targeting experiments for the loss of the second Cyclin O allele. However, we could not identify any Cyclin O knockout homozygote clone.

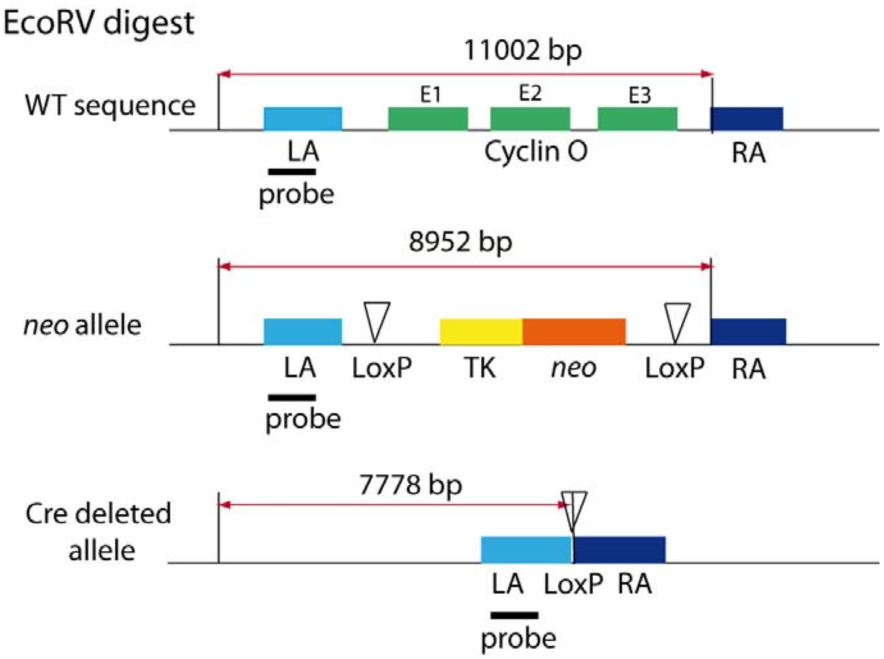
EcoRV digest
11002 bp
WT sequence
E1
E2
E3
LA
Cyclin O
RA
probe
8952 bp
neo allele
LA
LoxP
TK
neo
LoxP
RA
probe
7778 bp
Cre deleted allele
LA
LoxP
RA
probe

Figure R16. EcoRV restriction map of HCT116 targeted clone genomic DNA. After digestion with EcoRV and southern blotting using a 500 bp probe recognizing the left arm (LA), we expect the following DNA fragments (red arrows), for the WT sequence 11002 bps, for the targeted clone including the *neo* cassette 8952 bps, for the TAT-Cre treated clone 7778 bps.

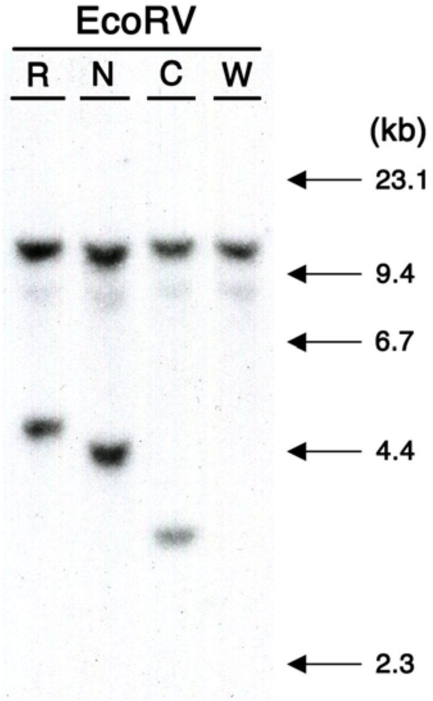

Figure R17. Southern blot of heterozygous Cyclin O deletion in HCT116. HCT116 cells were targeted for deletion of one allele of the Cyclin O gene using an AAV based virus containing a targeting construct including a floxed *neo* marker. Genomic DNA of a targeted HCT116 clone with random integration (R), a HCT116 targeted candidate clone with one Cyclin O allele replaced by the *neo* allele (N), the HCT116 targeted candidate clone after TAT-Cre treatment (C) and WT HCT116 cells were digested with EcoRV and transferred to a nitrocellulose membrane. Membranes were probed using a 500 bp ^{32}P labelled probe recognizing the LA of the construct.

R2. Role of Cyclin O in the mouse intestinal development

R2.1. Intestinal crypts are smaller in young Cyclin O deficient mice

In our laboratory we are currently characterising the phenotype of Cyclin O knock out mice. Cyclin O deficient mice are viable and are born with a mendelian ratio.

Studying the physiological functions of Cyclin O in the intestine is important for understanding of the reasons of its deregulation in CRC. In order to monitor morphological differences in the small intestine in different groups of age-matched WT and Cyclin O deficient mice we first compared the sizes of the villi and the crypts. To do this, we calculated the ratio between the crypt depth and the villus length in each part of the small intestine. We could find statistically significant lower crypt to villus ratios in the jejunum and ileum of 3 weeks old Cyclin O deficient mice compared to WT mice (Figure R18). We observed that most likely these differences are due to reduced crypt depths in Cyclin O KO mice, while the lengths of the villi are comparable between both groups of mice.

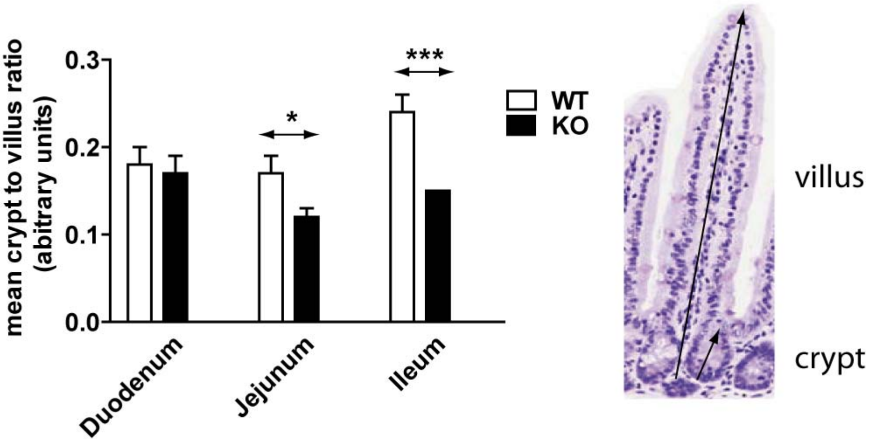

Figure R18. Smaller intestinal crypts in young Cyclin O deficient mice. The length of the villus and depth of the crypt were measured on an Olympus BX61.microscope using the cellSense standard program and the crypt / villus (c/v) ratio was calculated. The mean ± SEM of 5 different measures per intestinal segment from 20 days old WT littermates (white bars) were compared to age matched Cyclin O KO mice (black bars). Asterisks indicate statistically significant differences determined by Student’s t test.

However we can only observe this phenotype in young mice. Older Cyclin O deficient mice seem to overcome this deficiency. Due to the limited number of mice of this age group that have been analysed our finding can only represent a preliminary result until more data will be collected.

R2.2. Cyclin O deficient mice have less proliferating intestinal crypt cells

Our observation of the fact that young Cyclin O KO mice have smaller intestinal crypts led us to question if this deficiency can be due to a defect on the proliferating cells located in the crypt compartment. In order to detect intestinal crypt cells in S phase, we injected BrdU i.p. into two different groups of age matched Cyclin O

WT and Hom mice and sacrificed them after 2 hours. We then processed the intestines for histology, stained the sections with an anti-BrdU antibody and counted the number of BrdU positive cells per half crypt in each segment of the intestines.

We found a statistically significant lower number of BrdU positive crypt cells in the ileum and colon of two-months old Cyclin O Hom mice compared to age matched WT mice (Figure R20). Additionally, we could also notice a tendency towards having lower numbers of proliferating cells in the jejunum of the same mice.

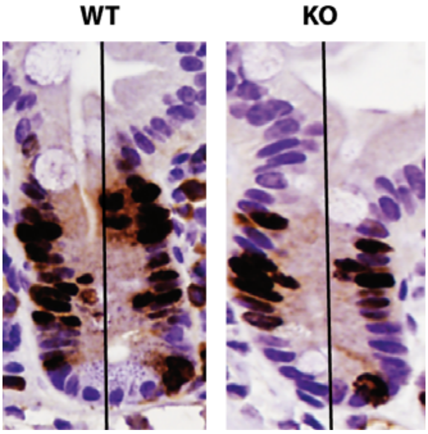

Figure R19. BrdU positive proliferating crypt cells. BrdU positive cells were counted per half crypt (separated by the middle line) of wild type (WT) and Cyclin O deficient (KO) mice. Crypts of the intestinal jejunum of the 6 months old mice group are shown.

We obtained the same results from a group of six months old mice (Figure R20). Here we could find statistically significant lower number of proliferating crypt cells in the jejunum, ileum and colon of Cyclin O deficient mice compared to WT mice.

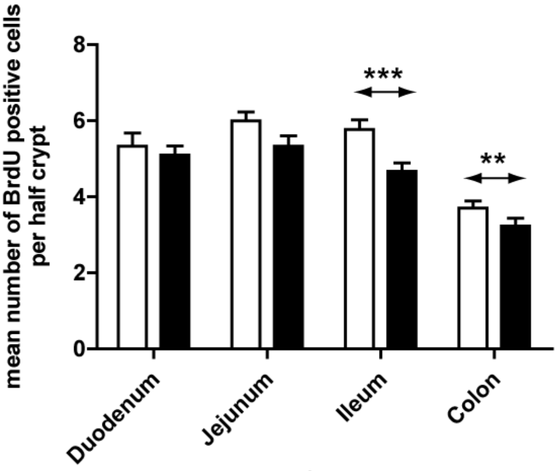

2 months

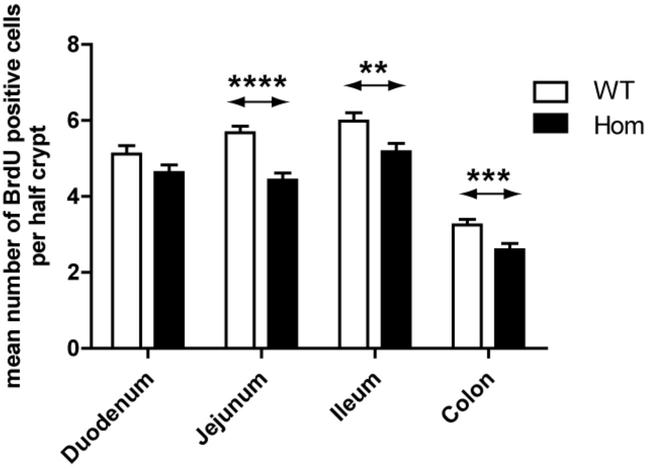

6 months

Figure R20. Less proliferating intestinal crypt cells in 2 and 6 months old Cyclin O KO mice. BrdU positive cells were counted for each intestinal part in 60 half crypts of 2 and 6 months old littermates. Mean numbers ± SEM of BrdU positive cells in WT mice (white bars) were compared to Cyclin O KO mice (black bars). Asterisks indicate statistically significant differences determined by the Student's t test.

Moreover, in the six months old group we compared the total number of cells of the crypt between Cyclin O deficient and WT mice and could not find any difference, indicating that the decreased number of proliferating cells in Cyclin O KOs is not a consequence from a reduced total crypt cell count.

In summary, from our observations we can conclude that Cyclin O deficient mice show a decreased number of proliferating cells in the crypts of the distal parts of the small intestine and in the colon.

R2.3. Cyclin O deficiency has no influence on the appearance of Goblet and Paneth cells in the mouse small intestine

The observed defect in the number of proliferating cells in the intestinal crypts led us to quantitate also the generation of the differentiated cell types of the intestine. We counted the number of Goblet cells (alcian blue positive) per villus along the small intestine, but we could not find any significant difference between Cyclin O deficient and WT mice. We also performed IHC for Lysozyme in order to check for the position of the Paneth cells in the small intestine. In Cyclin O deficient mice, we could observe that the Paneth cells are located at the bottom of the crypts, where they are normally positioned.

From these results we conclude that there is no defect in the generation of Goblet and Paneth cells in the small intestine of Cyclin O deficient mice. However, we did not check for other differentiated cell lineages such as the absorptive cells or enteroendocrine cells.

R3. Implication of Cyclin O deficiency in adenoma formation in a mouse model of CRC, the APC$^{min/+}$ mouse

R3.1. Influence of Cyclin O on adenoma number and size in APC$^{min/+}$ mice

We did not observe the development of intestinal tumours in Cyclin O deficient mice, up to 20 months of life, suggesting that the absence of Cyclin O alone in a physiologically normal intestine is not sufficient to induce tumour growth.

We investigated if partial loss of Cyclin O could sinergize with the loss of APC in the development of intestinal neoplasms by crossing Cyclin O deficient mice to APC$^{min/+}$ mice, a standard mouse model that recapitulates the first steps in the generation of CRCs. The APC$^{min/+}$ mouse is one of the most widely used CRC models, resembling some characteristics observed in FAP patients. The APC$^{min/+}$ mice carry a heterozygous point mutation in their *Apc* gene which leads to the development of multiple adenomas, mostly in the small intestine. We took advantage of this model to investigate the influence of Cyclin O deficiency on the development of adenomas in a dynamic *in vivo* environment.

We counted intestinal adenomas for Cyclin O$^{+/-}$ and Cyclin O$^{+/+}$ APC$^{min/+}$ mice and found that Cyclin O$^{+/-}$ APC$^{min/+}$ mice develop a statistically significant higher number of adenomas (Figure R21).

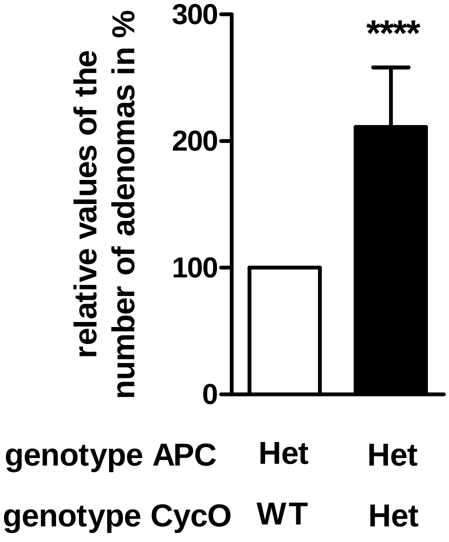

Figure R21. Cyclin O heterozygosity influences the adenoma number of APC$^{min/+}$ mice. Swiss roll processed intestine slices were obtained and a representative slice was stained with HEOS and the number of adenomas counted under the microscope. The relative values of the adenoma numbers were compared between Cyclin O$^{+/+}$ APC$^{min/+}$ and Cyclin O$^{+/-}$ APC$^{min/+}$ littermates. 6 littermates of each genotype were analysed. Mean age of mice was 26 ± 6 weeks.

We then compared the surface occupied by adenomas within a swiss roll section. Although the difference was not statistically significant the adenomas arising in Cyclin O$^{+/-}$ APC$^{min/+}$ mice show a tendency to be bigger compared to Cyclin O$^{+/+}$ APC$^{min/+}$ mice (Figure 22).

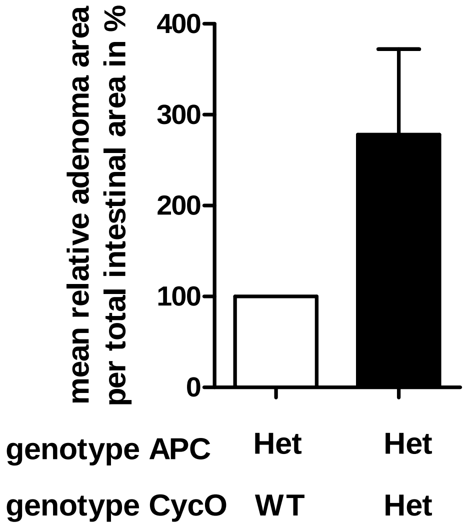

Figure R22. Cyclin O heterozygosity does not influence adenoma size in APC$^{min/+}$ mice. Swiss roll processed intestine slices were obtained and a representative slice was stained with HEOS and the number of adenomas counted under the microscope using the CellSense standard program and related to the total area of the intestine in the swiss roll preparation. Calculated values were compared between Cyclin O$^{+/+}$ APC$^{min/+}$ and Cyclin O$^{+/-}$ APC$^{min/+}$ mice, n=6. Mean age of mice was 26 ± 6 weeks.

We classified the size of the adenomas in groups of micro-, intermediate- and macro-adenomas and compared the different genotype groups with respect to the adenoma size groups (Figure R23). We could not observe any significant difference in the size distribution of adenomas from Cyclin O$^{+/-}$ APC$^{min/+}$ mice compared to control mice. Again, the Cyclin O$^{+/-}$ APC$^{min/+}$ mice show a slight tendency to develop bigger adenomas compared to control mice.

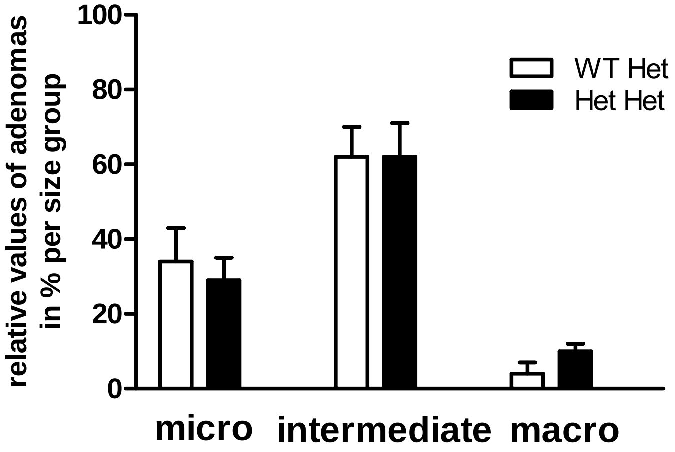

Figure R23. Influence of Cyclin O heterozygosity on the size distribution of adenomas in APC$^{min/+}$ mice. The adenoma areas in swiss roll prepared, HEOS stained intestines were measured and categorized in 3 different size groups (micro, intermediate, macro). Relative value of adenomas for each size group was compared between Cyclin O$^{+/+}$ APC$^{min/+}$ mice (n = 6, white bars) and Cyclin O$^{+/-}$ APC$^{min/+}$ mice (n = 6, black bars). Mean age of mice was 26 weeks. (microadenomas, smaller than 10^5 µm^2; intermediate adenomas in between 10^5 µm^2 and 1,5 * 10^6 µm^2; macro-adenomas bigger than 1,5 * 10^6 µm^2)

In summary, we can conclude from these results that Cyclin O heterozygosity does increase the adenoma number but only seem to increase marginally the adenoma growth in APC$^{min/+}$ mice.

Due to the perinatally development of hydrocephalus in Cyclin O homozygous mice, we could not obtain enough Cyclin O$^{-/-}$ APC$^{min/+}$ mice reaching the age when adenomas appear to draw conclusions about the effect of the complete lack of Cyclin O on the adenoma development in APC$^{min/+}$ mice.

R3.2. Cyclin O deficient adenomas show more malignant features

The adenomas arisen in Cyclin $O^{+/-}$ $APC^{min/+}$ mice show differential characteristics in number and size compared to Cyclin $O^{+/+}$ $APC^{min/+}$ mice. In order to explore histological differences, we aimed to compare different histopathological parameters between the adenomas arisen in Cyclin $O^{+/-}$ and Cyclin $O^{+/+}$ $APC^{min/+}$ mice. Both groups of mice show mostly cytoplasmic ß-catenin expression with higher levels in some areas of the adenomas and with low content of cells showing nuclear staining. Between 50 and 100 % of the adenomatous cells are proliferating according to the PCNA IHC (Fig R25 and 26).

Dysplasia is characterised by unequal sized or abnormally shaped cells and the presence of mitotic figures. In the adenomas from both genotypes, we could only find areas with low levels of dysplasia. Low grades of desmoplasia could be observed in the adenomas.

Vimentin is a type III intermediate filament and has been described to be among the genes differentially expressed in tumours with more invasive features. It is a marker for mesenchymal cells from the connective tissue, but has also been described to be expressed in tumour cells adopting to a more mesenchymal phenotype [172 173]. We performed IHC stainings for vimentin in both groups of intestines and semiquantitated the IHC results relating the stromal area of positive vimentin staining to the total area of each adenoma (Figure R24). We could observe a tendency to a higher mean percentage of vimentin positive areas of tumour stroma in the adenomas of Cyclin $O^{+/-}$ $APC^{min/+}$ mice compared to Cyclin $O^{+/+}$ $APC^{min/+}$ mice. Accordingly, most of the adenomas of Cyclin $O^{+/-}$

APC$^{min/+}$ mice showed a higher number of mesenchymal cells compared to Cyclin O$^{+/+}$ APC$^{min/+}$ mice adenomas. We could also observe less ß-catenin positive cells in adenomas with high numbers of mesenchymal cells in Cyclin O$^{+/-}$ APC$^{min/+}$ mice.

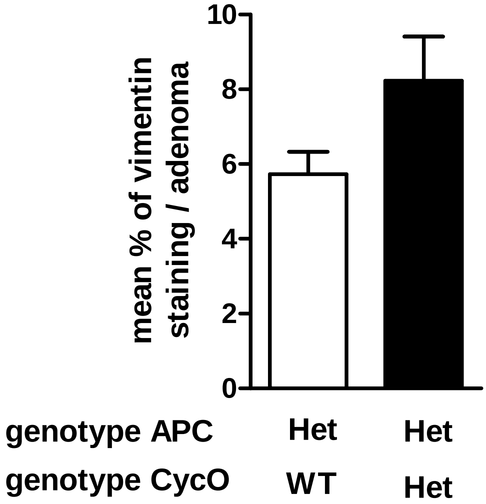

Figure R24. Vimentin in the adenomas. IHC of vimentin was performed and the area of the staining was quantified and related to the total area of each adenoma using the ImgaeScope program. The values are displayed as mean % of the vimentin staining / adenoma for the Cyclin O$^{+/+}$ APC$^{min/+}$ mice (white bar, n = 15) and Cyclin O$^{+/-}$ APC$^{min/+}$ mice (black bar, n = 15).

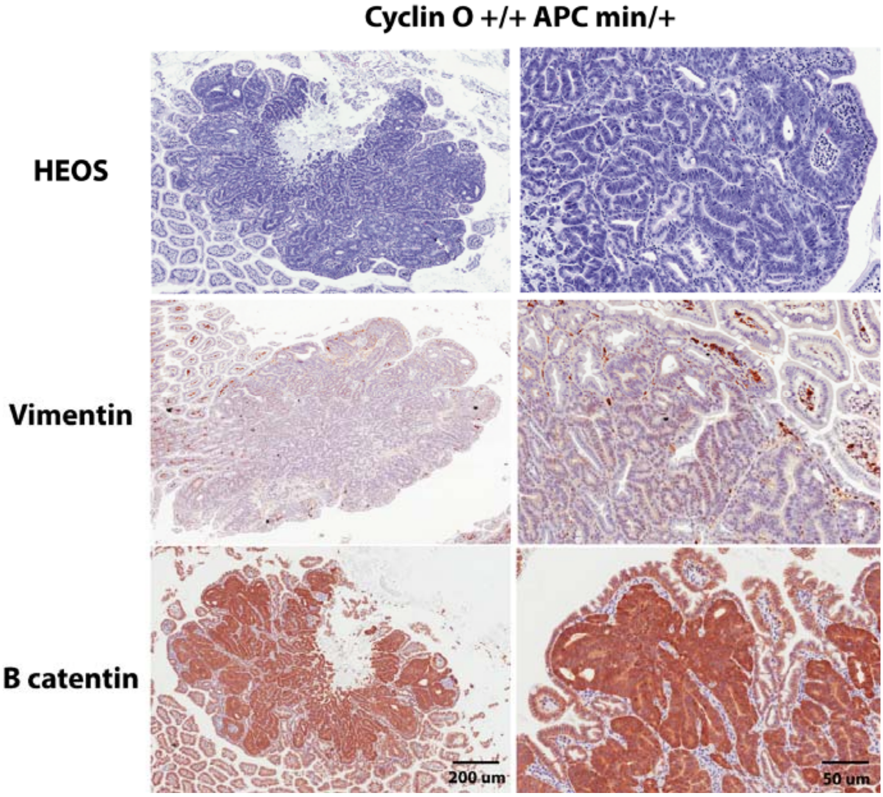
Cyclin O +/+ APC min/+
HEOS
Vimentin
B catentin
200 um
50 um

Figure R25. Vimentin expression in a adenoma of a Cyclin O$^{+/+}$ APC$^{min/+}$ mouse. A representative adenoma from a Cyclin O$^{+/+}$ APC$^{min/+}$ mouse shows HEOS and IHC for vimentin and ß-catenin in 2 magnifications.

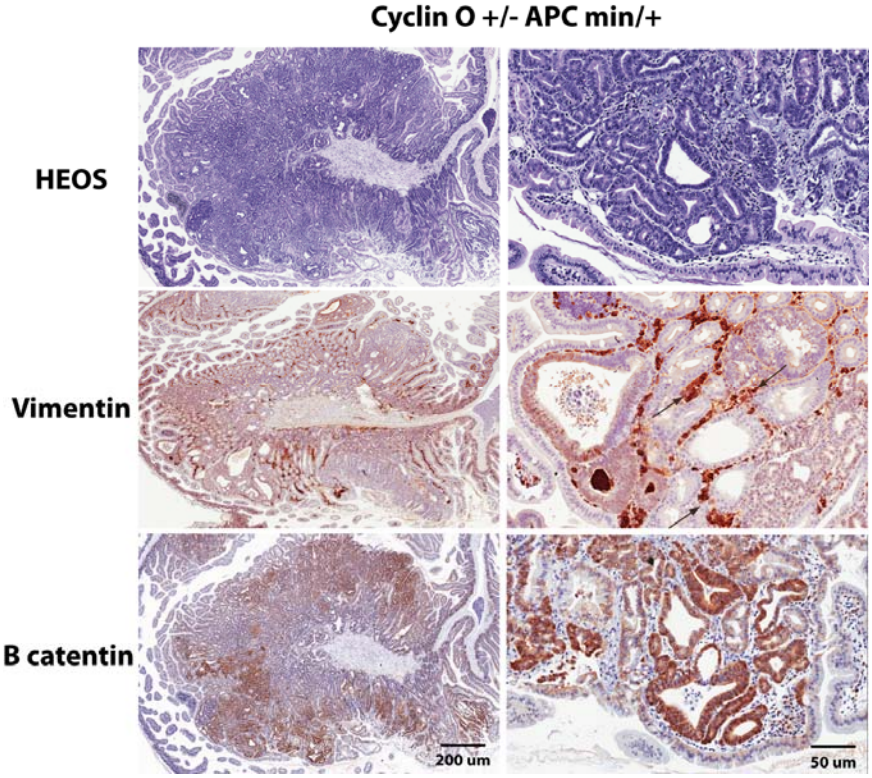

Figure R26. Vimentin expression in a adenoma of a Cyclin O$^{+/-}$ APC$^{min/+}$ mouse. . A representative adenoma from a Cyclin O$^{+/-}$ APC$^{min/+}$ mouse shows HEOS and IHC for vimentin and ß-catenin in 2 magnifications. The arrows indicate vimentin positive stromal cells.

R3.3. Cyclin O is expressed in the normal superficial intestinal epithelium surrounding the adenomas in APC$^{min/+}$ mice

We showed in sections R1.1. that Cyclin O is not expressed in the normal intestinal epithelium of the mouse. In human CRC, however we could observe increased expression of the protein. Next we wanted to know, if Cyclin O expression is also deregulated in adenomas arisen in APC$^{min/+}$ mice.

We performed IHC for Cyclin O protein in Cyclin O$^{+/-}$ and Cyclin O$^{+/+}$ APC$^{min/+}$ mice. In both groups of mice, we could detect Cyclin O in the outer most cell layer surrounding the intestinal adenomas, corresponding to a monolayer of normal superficial intestinal epithelium (Figure R27). We could find Cyclin O protein expressed with its typical punctuate pattern in the cytoplasm of these cells. We also stained the same tissue samples for E-cadherin and ß-catenin. In the cell layer where Cyclin O is expressed, E-cadherin and ß-catenin are located in the cell membrane, just like in the normal epithelial cells of the intestine.

From our results we show that Cyclin O is expressed in the intestine of APC$^{min/+}$ mice even though we cannot find Cyclin O expression in the adenomas, at difference with what we found in our studies in human CRC tissues. We can only find Cyclin O expression in the histopathologically normal epithelial cell layer surrounding the adenoma.

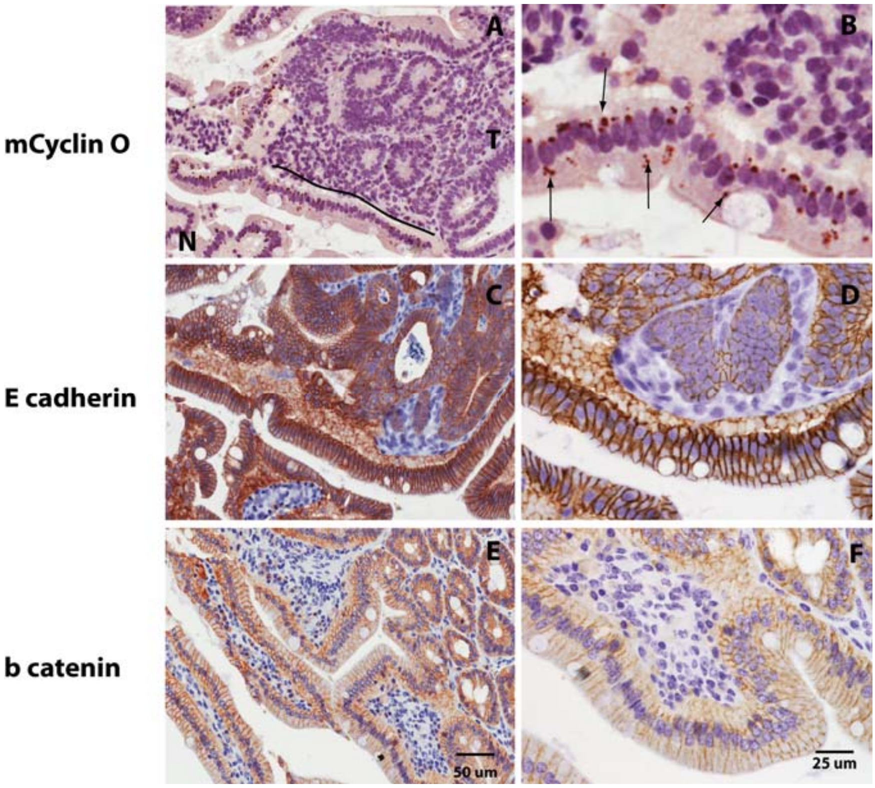

Figure R27. Expression of Cyclin O in the normal epithelial cells surrounding the adenomas in APC$^{min/+}$ mice. The expression of Cyclin O (A, B Cyclin O indicated with arrows) was observed in the normal epithelium (N) surrounding an adenoma (T). In the same cells, E cadherin (C, D) and ß-catenin (E, F) expression appears normal. All proteins were detected by IHC using the colorimetric substrate DAB.

R3.4. Cyclin O is expressed in morphogically normal epithelial cells of APC$^{min/+}$ mice

We could also detect Cyclin O expression in the cytoplasm of morphologically normal epithelial cells of the small intestine of APC$^{min/+}$ mice (Figure R28). We could observe Cyclin O expression in neighbouring villi forming a cluster where the whole villus is positive for Cyclin O expression, whereas moving to the neighbouring villi further away the Cyclin O expression was no longer detectable. The morphological features of those regions and the expression pattern of E-cadherin and ß-catenin are indistinguishable from the Cyclin O negative areas (Figure R29). We hypothesise that the expression zones in histologically normal appearing small intestine could mark epithelium in a very early state of adenomatous transformation.

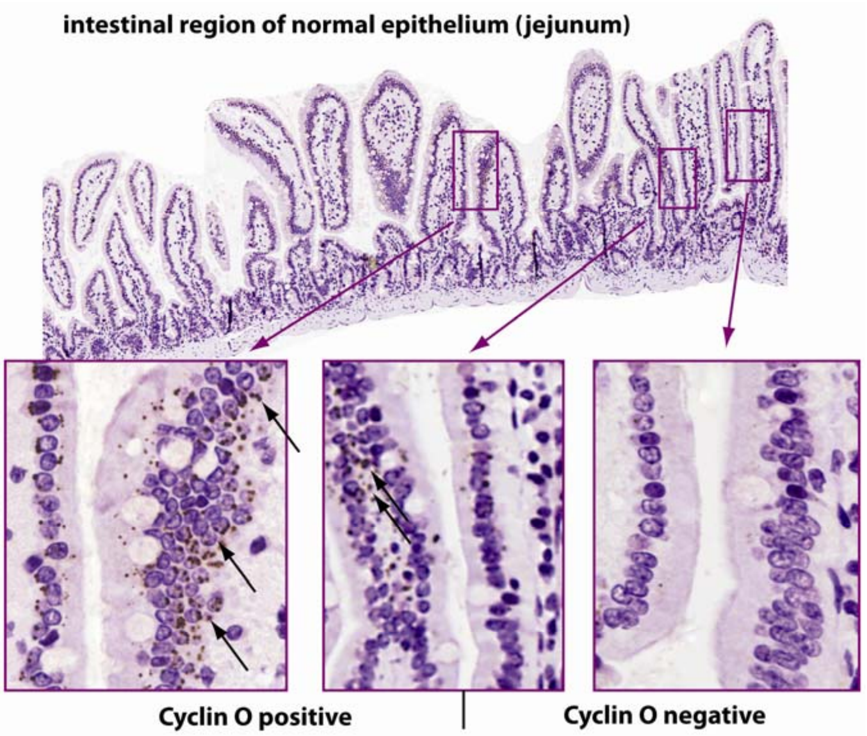
intestinal region of normal epithelium (jejunum)
Cyclin O positive
Cyclin O negative

Figure R28. Cyclin O expression in morphologically normal epithelial cells of APC$^{min/+}$ mice. Cyclin O protein was detected by IHC in intestinal epithelial cells of the jejunum part using the C2 antibody and the PowerVision^{TM} system with the colorimetric substrate DAB.

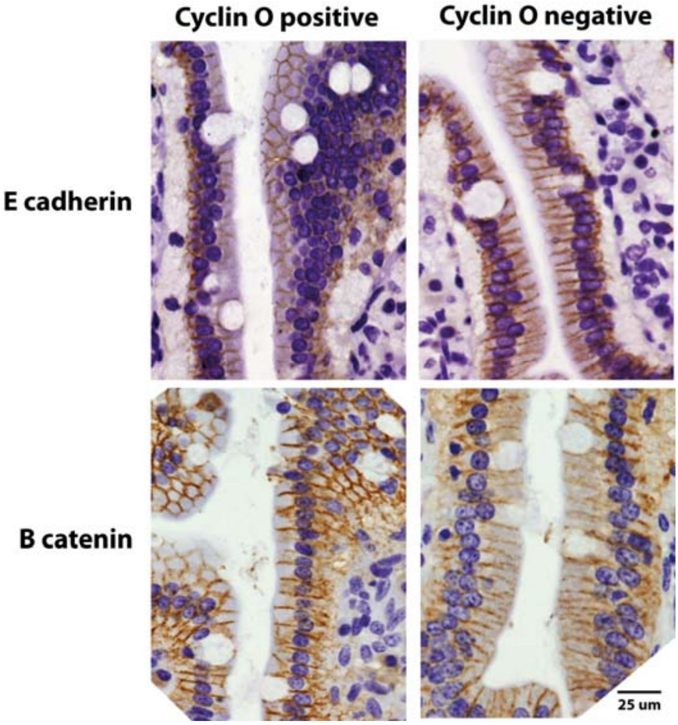
Cyclin O positive
Cyclin O negative
E cadherin
B catenin
25 um

Figure R29. E cadherin and ß-catenin expression in morphologically normal epithelial cells of APC$^{min/+}$ mice. E cadherin and ß-catenin stainings correspond to the same areas found Cyclin O positive or Cyclin O negative in the morphologically normal epithelial cells.

Discussion

D1. Expression of Cyclin O in normal human and mouse intestinal tissue

From two microarray analysis for Cyclin O mRNA expression using the Oncomine database, we could demonstrate that Cyclin O mRNA is not detected or expressed at very low levels in normal human colon. The expression pattern of Cyclin O in mouse intestinal tissue had been analysed by semi-quantitative RT-PCR in our laboratory. We could as well observe a very low Cyclin O expression level in the mouse intestine. Additionally we confirmed these results by IHC (section R1.1.).

The results suggest that Cyclin O is only expressed under specific circumstances. In fact, a characteristical feature of most cyclins is that they are only synthesised when they are required to perform their function, as it is observed during the cell cycle progression. Hence, Cyclin O could be expressed in a transient manner during the induction of apoptosis in intestinal epithelial cells. Apoptotic cells are difficult to detect because they are rapidly removed from any tissue. The apoptotic rate of intestinal epithelial cells is very high compared to any other tissue: in mice, 1400 cells per villus are shed every day [174], but they are detached from the villi or the superficial epithelium from the colon and get lost in the intestinal lumen, which further difficults their detection.

We can also not exclude that the Cyclin O gene could be active at some point of the embryonic development.

D1.1 Cyclin O protein is overexpressed in human CRC

We studied the expression levels of Cyclin O in human colorectal cancer specimens and we found that the Cyclin O protein is overexpressed in the majority of CRC related samples both in premalignant lesions (polyps and adenomas) as well as in full blown adenocarcinomas and their metastasis, representing early and late stages of the tumour development (Sections R1.2, 1.3 and 1.5).

We observed that the Cyclin O protein is homogenously overexpressed in all the cells of the lesion already from the early stages of the epithelial cell transformation, indicating that a deregulated Cyclin O expression might give a general advantage to all the transforming cells in order to gain malignant properties. Accordingly, the deregulated expression of Cyclin O could represent an essential mutation because no Cyclin O negative cancer cells could be observed within positive tumours.

However, we could also find CRC samples that do not express Cyclin O, indicating that the deregulated expression of Cyclin O is not essential for all developing tumours in order to transform or maintain their malignant properties.

How the Cyclin O expression could be initially triggered and how the deregulated Cyclin O function could give an advantage to the transforming cancer cells can have different explanations.

The development of sporadic CRC can be caused by different risk factors, such as certain types of diets but also the age [175]. The permanent exposion to certain genetic and environmental factors can cause cellular stress and damage to the epithelial cells and their DNA. Damaged cells within a tissue are either repaired or killed by apoptosis. If both of these mechanisms fail, the damaged cell can continue to proliferate and give rise to more mutated cells and finally lead to the development of the CRC.

Our group has previously demonstrated that the Cyclin O expression is induced in several cell types, such as thymocytes and mouse embryonic fibroblasts (MEF) in the presence of DNA damage. We have previously demonstrated that the presence and activation of the tumour suppressor p53 is necessary to induce Cyclin O expression in MEFs in response to DNA damage [160] (Brunet Roig, M., *L'activador de Cdk2 relacionat amb l'apoptosi*, doctoral thesis, 2006).

Accordingly, the expression of Cyclin O in CRC cells could have been initially triggered due to the accumulation of prooncogenic DNA lesions. In the presence of DNA damage in an intestinal epithelial cell, p53 would be activated in order to induce the transcription of genes important for cell cycle arrest, DNA repair and apoptosis. The expression of the p53 target Cyclin O could have been initially induced in order to participate in the induction of apoptosis if the DNA damage is too severe. In this way, most of the damaged epithelial cells would either be repaired or removed by apoptosis. However, under conditions of permanent cellular stress, it is conceivable that some Cyclin O expressing damaged cells might be able to escape the DNA repair or apoptosis induction through unknown mechanisms and could continue to proliferate and give rise to a pool of mutated cells able to survive and accumulate gene mutations. Consequently, these mutated cells would continue to express Cyclin O but would have gained resistance to the proapoptotic functions of Cyclin O (Figure D1). In fact, evasion of apoptosis accounts to one of the six essential alterations defined by Hanahan and Weinberg that collectively dictate malignant growth [161]. In agreement with this, in the laboratory we have evidence that overexpression of Cyclin O in p53-proficient, DNA-damage sensitive cell lines, such as U2OS (human osteosarcoma) or WEHI7.2 (mouse T-cell lymphoma) leads to massive cell death by apoptosis. However, clones resistant to the pro-apoptotic effect of Cyclin O can be isolated. At variance with the parental cells, these cells are now resistant to most apoptotic stimuli, particularly DNA-damage-induced apoptosis (Roig, Roset, Cabellos, Gil-Gomez, unpublished).

However, we have also found CRC cases that do not show overexpression of Cyclin O which could indicate that in these cases the resistance to apoptosis has been gained through a different mechanism.

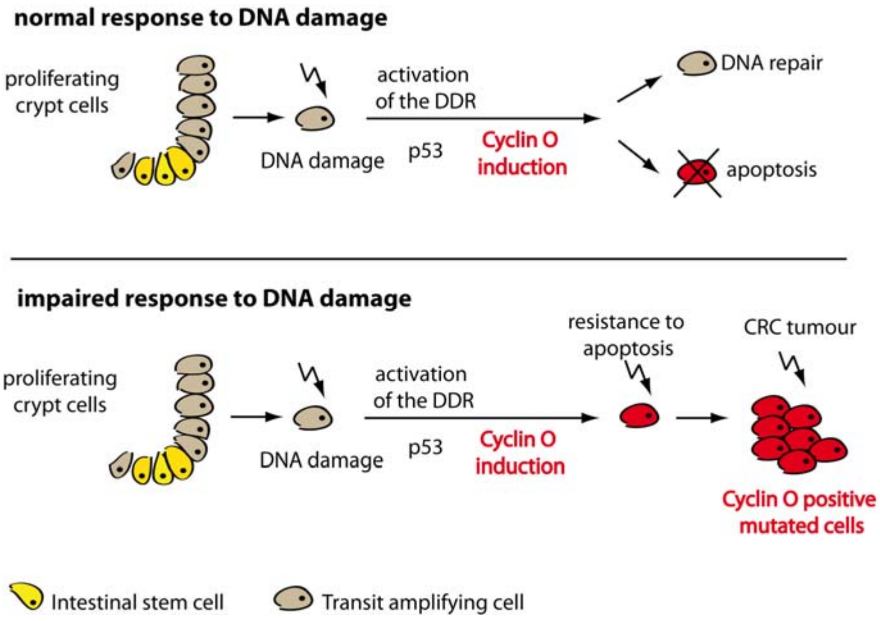
normal response to DNA damage
proliferating crypt cells
activation of the DDR
DNA damage
p53
Cyclin O induction
DNA repair
apoptosis
impaired response to DNA damage
proliferating crypt cells
activation of the DDR
DNA damage
p53
Cyclin O induction
resistance to apoptosis
CRC tumour
Cyclin O positive mutated cells
Intestinal stem cell
Transit amplifying cell

Figure D1. Overexpression of Cyclin O in CRC. The Cyclin O overexpression might have been triggered by DNA damage and might have been continued due to the gain of apoptosis resistance.

We could detect different Cyclin O expression levels in the CRC tissues independently of the stage of tumour development. Different factors could account for enhanced levels of Cyclin O in CRC cells.

One reason could be chromosomal instability. The most frequently mutated gene in sporadic CRC is the tumour suppressor gene *APC* whose mutational inactivation causes the permanent activation of the Wnt signalling pathway leading to uncontrolled proliferation and transcription of different Wnt target genes. Nevertheless, APC is a multifunctional protein that has been also described to play a role in chromosome segregation during mitosis. Mutations at APCs C-terminal end have been suggested to cause chromosomal instability and aneuploidy, representing a hallmark of many CRCs [176] [177]. Accordingly, it could be possible that in some CRC tumour cells the chromosome 5, where the *CCNO* gene is located, could be present in more than two copies leading to a higher expression of the Cyclin O protein in these cells (Figure D2).

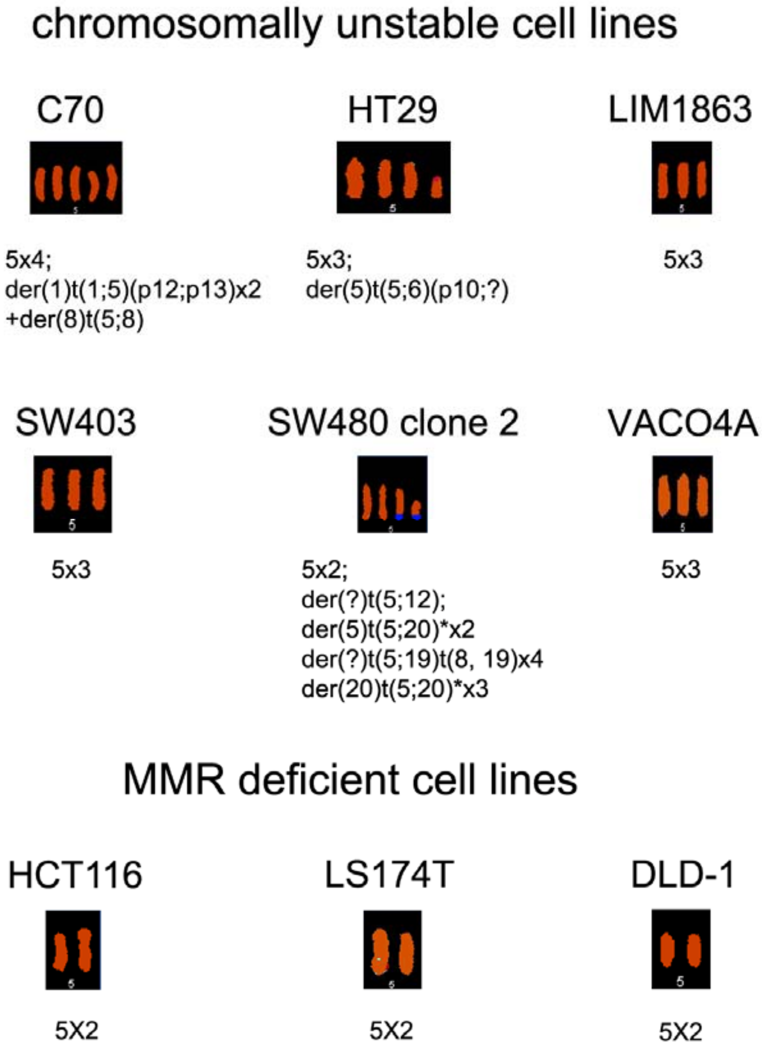
chromosomally unstable cell lines
C70
HT29
LIM1863
5
5x4;
der(1)t(1;5)(p12;p13)x2
+der(8)t(5;8)
5x3;
der(5)t(5;6)(p10;?)
5x3
SW403
SW480 clone 2
VACO4A
5x3
5x2;
der(?)t(5;12);
der(5)t(5;20)*x2
der(?)t(5;19)t(8, 19)x4
der(20)t(5;20)*x3
5x3
MMR deficient cell lines
HCT116
LS174T
DLD-1
5X2
5X2
5X2

Figure D2. Number of chromosme 5 in different CRC cell lines and chromosomal aberrations involving Chromosome 5 analysed by SKY.
(Adapted from www.path.cam.ac.uk/-pawefish/ColonCellLineDescriptions)

Another reason for the elevated Cyclin O expression levels could be that once Cyclin O expression is triggered, the cell is unable to decrease the protein levels because of failures in the mechanisms of Cyclin O degradation.

Cyclin D1, another member of the cyclin protein family, has been observed to be overexpressed in different cancers and tumour derived cell lines. One study suggests that overexpression of Cyclin D1 can occur due to the disruption of Cyclin D1 proteolysis [178]. They described that active Cyclin D1 is phosphorylated by GSK3ß in order to favour its nuclear export and proteolysis during S phase [179]. Lin *et al* suggest that the Cyclin D1 proteolysis could have been circumvented in cancer due to the impairment of the proteolytic mechanism.

We observed the appearance of putative phosphorylated forms of the Cyclin O protein in cell lysates of human Cyclin O transfected HEK293T cells (R1.3., Figure R7). On the contrary, in lysates of fresh normal epithelium and colon adenocarcinomas, we were not able to detect similar forms for Cyclin O, neither in the cytoplasmic nor in the nuclear fraction. This observation could indicate that Cyclin O would not be degraded in these mutated cells and therefore accumulates. The absence of Cyclin O degradation could occur either due to mutations in phosphorylation sites controlling its stability or due to mutations in upstream proteolytic mechanisms, such as the inhibition of the GSK3ß activity. In our laboratory, we have evidences that the stability of Cyclin O is triggered, at least in part, by phosphorylation by GSK3ß (Brunet Roig, M., *L'activador de Cdk2 relacionat amb l'apoptosi*, doctoral thesis, 2006).

However, we cannot exclude that the phosphorylated forms could not be detected due to technical reasons.

D1.2. Cyclin O expression in fresh samples of CRC patients

We obtained fresh tumour samples from CRC patients and could confirm the Cyclin O overexpression that we have previously shown in the TMA analysis. We aimed to compare the Cyclin O expression levels detected by western blotting and IHC. However, the expression pattern in the same tissue samples analysed by western blot and IHC did not match.

One reason for the differences could be the loss of protein during the preparation of the subcellular fractions for the western blotting.

Another reason for this difference could lay in the different cellular composition of the tissue samples. We could observe by IHC that the tumour cells overexpress the Cyclin O protein. Additionally the cancerous tissue is composed of extracellular matrix and different Cyclin O negative cells, such as cancer-associated fibroblasts, endothelial cells or infiltrating immune cells. During the progression of the cancer, the surrounding ECM containing stromal cells also evolves dynamically and creates a microenvironment important to provide the tumour with signals for growth, angiogenesis or metastasis [180]. Nevertheless, the growth and development of tumour associated stroma is different depending on the individual cancerous tissue.

We suggest that the variable amount of ECM and Cyclin O negative stromal cells in the tumour samples contributed differently amongst the tumours to the total amount of protein in the subcellular fractions and by comparing equal amounts of total protein would not reflect the real Cyclin O protein expression in the tumour cells. The evaluation of Cyclin O expression levels by IHC, although it is only semiquantitative, it is probably the more accurate technique because we can distinguish between Cyclin O expressing tumour cells and other tumour associated Cyclin O negative cell types, such as infiltrating immune cells or stromal cells.

We have observed a deregulated Cyclin O expression in samples of normal mucosa both in the TMA analysis and in the fresh tumour samples. We did not expect to find Cyclin O overexpressed in these samples because normal intestinal mucosa has been found to not express Cyclin O. However, we know that these samples are taken at variable distances from the primary tumour and therefore even if histologically they appear as normal mucosa, they could have already started to accumulate lesions. Accordingly, we hypothesise that Cyclin O expression would be a very early indicator of epithelial cell transformation to CRC.

In order to proof this hypothesis, we intended to find a border between transformed, morphologically normal Cyclin O-positive and morphologically normal Cyclin O negative epithelium in the peritumoral epithelium. We analysed by IHC fresh normal mucosa samples that were taken at increasing distances with respect to the primary tumour location. However, none of the samples showed to be Cyclin O negative (not shown).

On the one hand, this could indicate that the peritumoral mucosa samples could not be taken far enough from the primary tumour to find “molecularly healthy” epithelium.

On the other hand, Cyclin O expression can be triggered by a wide range of cellular stressful agents (Ortet, L., *Signalling of Cyclin O complexes through eIF2α phosphorylation*, doctoral thesis, 2010). Hence, the Cyclin O expression in the normal mucosa samples could have been triggered as a consequence of the manipulation of the sample during surgery. Since the surgeon starts resecting the tumour until we could process the sample, typically took more than 4 hours. During this period the tissue suffers severe hypoxia as a consequence of the clamping of the blood vessels needed to resect the tumour.

D1.3. Cyclin O expression correlates with a longer cancer specific survival of CRC patients

The correlation of Cyclin O expression in the TMA samples to the patients' clinical parameters revealed that Cyclin O expression in the CRC tissue samples correlates with a longer cancer specific survival for CRC patients in TNM stages III or IV (section R1.4).
These results suggest that Cyclin O expression could indicate, for instance, a better response to the adjuvant or paliative chemo/radiotherapy compared to Cyclin O negative CRC tumours. Because the same correlation holds true when Cyclin O is expressed in the polyps and adenomas that represent earlier stages of the tumour development, we also suggest that this selection for a specific type of cancer cell could have taken place early during cancer progression.

Cyclin O has been described to be implicated in the DDR. Our Cyclin O expression studies in CRC show findings similar to the ATM expression studies from Grabsch *et al*. They describe that the expression of an activated form of ATM protein is high in different solid tumours at early stages of tumour development. A decrease in ATM protein levels in colon tumours has been correlated with a decreased survival. Additionally, Grabsch *et al* described that CRC patients with ATM expressing tumours who received adjuvant therapy showed an overall longer survival than patients with ATM negative tumours indicating that CRC expressing DDR proteins could be better treatable [181].

In CRC it has been described that a decreasing degree of differentiation, such as a loss of regular arrangement of tumour cells and increasing cellular atypia among other factors, correlate with a poorer prognosis for the CRC patient. Therefore, we hypothesise that the deregulated Cyclin O expression could correlate with a more differentiated and better treatable tumour cell type. Primary tumours are heterogeneous and can contain zones with different degrees of differentiation that make the histological tumour classification difficult. Halvorsen *et al* described that histological grading in CRC should be based on the predominating differentiation degree in order to estimate a clinical prognosis [182].

In order to correlate the degree of differentiation with the Cyclin O expression, we chose Cytokeratin 20 as a marker of differentiation. Cytokeratin 20 is a type I intermediate filament (IF) found to be expressed in mature enterocytes and Goblet cells of the intestinal mucosa. It has been proposed as a diagnostic marker valuable in distinguishing different types of carcinomas and has also been suggested to be a suitable histological marker of differentiation because of its differentiation-specific expression that has been described to be retained in malignant tumours [183] [184].

However, we did not find any significant correlation between Cytokeratin 20 and Cyclin O expression. We should take into account that the TMA samples that we have analysed represent only a very small, randomly chosen portion of the whole tumour. Because a tumour can contain areas with different degrees of differentiation, it would be better to analyse a bigger area of the primary tumour. Therefore, from our result we cannot draw any conclusion about the correlation of Cyclin O expression and a more differentiated tumour type.

Since CRC patients with CRC stage III or IV undergo surgery followed by chemotherapy or radiotherapy, we hypothesise that Cyclin O positive CRC tumours could respond better to the chemotherapeutic treatment than the Cyclin O negative tumours.

Contradictorily, CRC patients with stages I or II and positive Cyclin O expression in the normal peritumoral colon mucosa samples were found to have a trend towards a shorter cancer specific survival.

We have shown that Cyclin O is not expressed in normal intestinal epithelium. A positive Cyclin O expression in the peritumoral epithelium could therefore indicate that some of these cells would be early transforming cancer cells that undergo mutational changes but appear still as histologically normal epithelial cells. If they are early transforming CRC cells, it could indicate that not all the transformed tissue has been removed during the surgery. CRC patients in stage I do not receive chemotherapeutic treatment after the surgery and the benefit of the chemotherapy in patients with stage II is controversial. Therefore, if this tissue was not removed, a recurrence of CRC would be more likely and the prognosis worse. Accordingly, a Cyclin O negative normal mucosa sample would indicate that the cancerous tissue has been completely removed.

D1.4. Cyclin O expression is maintained during metastasis

During the initiation and progression of CRC the cell acquires driver mutations in different genes, such as *APC*, *KRAS* or *TP53*. Malignant full blown CRC tumours have the ability to invade the tissues underlying the colorectal epithelium and some cells within the tumour eventually acquire the ability to migrate and seed other organs. Specific gene mutations that are responsible for the appearance of metastasis are difficult to define. However, none of the driver mutations have been specifically associated with the ability of cancer cells to metastasise [185]. It has been described that every progressive step, such as from adenoma to carcinoma or metastasis in the development of CRC has a cell of origin, a founder cell. In the progression from adenoma to carcinoma for example, the carcinoma founder cell contains the mutations that were present in the adenoma and accumulates additional mutations that are necessary in order to progress to the carcinoma state. Following this model, any mutations that were present in the adenocarcinoma state can be also found in the metastatic cells [186]. We have found Cyclin O positive metastatic CRC cells in the lymph nodes and in the liver. Why the Cyclin O expression is maintained during metastasis could occur either because the resistance to the pro-apoptotic functions of Cyclin O could be an essential tumour cell ability and therefore is maintained in metastatic cells or that an unidentified mutation driving the Cyclin O overexpression was present in the primary tumour and will consequently be maintained in the metastatic founder cell and consequently in all metastatic cells.

D1.5. MOCS2 is a putative target gene of Cyclin O in CRC

The MOCS2 enzyme is involved in the synthesis of molibdopterin which is a cofactor for enzymes, such as Xanthine oxidase or Aldehyde oxidase involved in the detoxification of xenobiotics [170]. We hypothesised that the increased activity of these enzymes could be related to the resistance of colorectal tumours to some chemotherapeutic drugs.

Xanthine oxidase has been found at increased levels in different human cancers but its role in the development of CRC is not well characterised.

Allopurinol, a structural analog of hypoxanthine, is a Xanthine oxidase inhibitor used in the treatment of inflammatory bowel disease because of its anti-inflammatory properties. The chronic inflammatory microenvironment in inflammatory bowel disease is characterised by immune dysregulation and elevated levels of reactive oxygen species (ROS) which can lead to colorectal cancer development. Allopurinol has been reported to decrease ROS production and to inhibit the oxidant dependent activation of the NFκB pathway [187].

A few studies describe a lower risk of developing CRC and an increased survival rate for patients with advanced CRC when the Xanthine oxidase inhibitor was administered, even though it had no major effect in the treatment of CRC [187].

MOCS2 has been identified as a putative target gene of Cyclin O. We analysed the expression of MOCS2 in the CRC TMAs and we could find a positive correlation between its expression pattern and the expression of Cyclin O. Furthermore we could find a trend towards a better cancer specific survival for patients with negative MOCS2 expression in the adenocarcinoma tissue (Figure R14).

We hypothesise that Cyclin O could enhance the enzymatic functions of Xanthine oxidase in CRC through the expression of its target gene *MOCS2*. Because of the putative implication of Xanthine oxidase in the resistance to chemotherapy, we would expect a worse prognosis for the CRC patient when Cyclin O is expressed.

The expression of Cyclin O in the CRC tumours correlates with a better prognosis for the CRC patients (Figure R9), but the expression of its target gene *MOCS2* correlates with a worse prognosis. This could indicate that the increase of MOCS2 expression in the tumours caused by Cyclin O is not strong enough in order to influence the patients prognosis significantly. It is also possible that Cyclin O promotes the expression of MOCS2 but it might not be functional in the tumour tissue for other reasons, such as substrate availability.

We can not exclude that in individual CRC cases with a high Cyclin O expression, the detoxificant function of Xanthine oxidase could be stronger and the administration of a Xanthine oxidase inhibitor, such as allopurinol could further improve the patients’ prognosis.

D1.6. The Cyclin O gene is not mutated in human CRCs

Evasion of apoptosis accounts to one of the six hallmarks of cancer. We would expect that a tumour cell in order to survive must be able to overcome the Cyclin O's proapoptotic functions. We observed that Cyclin O is overexpressed in CRC. Accordingly, the protein is present but, how could it have lost its proapoptotic function?

In order to know if the expressed protein could correspond to a mutated form, we decided to sequence the Cyclin O gene but from our results we conclude that the Cyclin O protein overexpressed in CRC corresponds to the WT form (section R1.7).

Cyclin O forms complexes with Cdk2 and induces intrinsic apoptosis via activation of Caspase 8 and the apoptosome [156]. Even if Cyclin O is not mutated in CRC, mutations of other members of the intrinsic apoptotic pathway downstream of Cyclin O could lead to apoptosis resistance in the transforming cell.

Caspases are fundamental proteases involved in apoptosis. Their mutational inactivation would turn mutated cells resistant against apoptosis. Caspase 8 or 3 are rarely mutated in CRC indicating that they might not be the reason for the apoptosis resistance [188]. Nevertheless, they could be permanently inactivated by inhibitory proteins (IAPs). In this way, Cyclin O would be expressed without being able to trigger apoptosis.

Another reason for Cyclin O to not induce apoptosis could be that it cannot form active complexes with its binding partner Cdk2. Cdk2 not only binds to Cyclin O but also to Cyclin E and A during cell cycle progression. Tumour cells are actively proliferating and in order to pass through the cell cycle, cyclin E and A could compete with Cyclin O for Cdk2. Cdk2 / cyclin E complexes have been described to be elevated in CRC and have been a target in several clinical trials [189] [190]. Cyclin E could be the preferred binding partner in CRC cells. Experiments with MEFs with down- or upregulated levels of Cyclin O did not show any change in their cell cycle profile, indicating that there is no competition or preference in Cdk2 binding between the different cyclins. Therefore, we suggest that the WT form of Cyclin O could bind to Cdk2 in CRC.

Most of the cyclins perform their function in the nucleus. We found Cyclin O to be present in the cytoplasm, but could not observe the protein present in the nucleus in CRC tissues. This suggests that either Cyclin O is not active in tumour cells and that it performs its function in the cytoplasm. However, the protein levels in the nucleus could be very low and therefore could be undetectable by IHC or western blotting. It is also possible that Cyclin O gets imported and exported quickly from the nucleus.

In the samples from CRC patients, we frequently observed the Cyclin O protein expression in a punctate pattern. It has been suggested that Cyclin O is able under specific conditions of cellular stress to localize to cytoplasmic granules that are compatible with being stress granules (Ortet, L.; *Signalling of Cyclin O complexes through eIF2alpha phosphorylation*, doctoral thesis, 2010). It is possible that the Cyclin O protein when located to the stress granules in CRC cells looses its function. However, part of the protein could also be still present in the cytoplasm and stay functional.

D1.7. Significance of Cyclin O expression in CRC

Cancer cells expressing Cyclin O seem to have gained resistance to Cyclin Os proapoptotic function due to an unknown mechanism. Accordingly, we hypothesise that the downregulation of Cyclin O in CRC cells could possibly restore its sensitivity to apoptosis.

The most employed method to downregulate genes in human somatic cells is the use of RNA interference. Nevertheless, we did not succeed to downregulate Cyclin O using expression of different shRNAs expressed from plasmid or lentiviral vectors. Therefore, we decided to use a technique aimed to knock out the *CCNO* gene in a CRC cell line.

We intended to knock out Cyclin O by homologous recombination using recombinant AAVs that have been described to increase the targeting efficiency compared to conventional targeting constructs [163]. Cancer cells carry many different genomic aberrations and are often aneuploid. We chose the CRC cell line HCT116 to do the targeting experiment due to the fact that they are derived from a patient with HNPCC. CRC tumours from these patients are characterised by microsatellite instability (MMR) which leads to a mutator phenotype, but they are chromosomally stable and are euploid [58]. The HCT116 cell line has two copies of chromosome 5 (Figure D2) and overexpresses Cyclin O (not shown).

Targeting efficiencies ranging between 0,4 and 13 % have been described for this technique. We reached 3 % for the targeting of the first *Cyclin O* allele which is within this range. Even though our southern blotting analysis revealed that the heterozygous targeted clone had undergone a rearrangement in the vicinity of the *CCNO* locus we have evidences that the Cyclin O gene has been knocked out correctly, because we could confirm the correct targeting and the subsequent Cre-mediated excision of the *neo* cassette by PCR.

We did not succeed in identifying a clone carrying a homozygous targeting of the gene. One possible reason could be that a complete loss of Cyclin O could lead to a decreased proliferation rate or to the death of the targeted cell. Cyclin O is a proapoptotic protein and its loss has been shown to prevent apoptosis induction. Therefore, cell death in the absence of Cyclin O would be unexpected. However, the consequences of its loss in a malignant cell could be different, since the mRNA expression profile of Cyclin O overexpressing WEHI7.2 cells is completely different from the WT cells (data not shown).

Recently, several alternatives to the use of AAV-encoded targeting constructs to target genes in somatic cells have been described. The use of zinc finger nucleases (ZFN) [191] or TALEN [192] could be worth to try in the case of Cyclin O. Combined strategies are also possible, for example to use shRNA constructs in the heterozygous clone.

D2. Consequences of Cyclin O deficiency for mouse intestinal development

D2.1. Intestinal crypts are smaller in young Cyclin O deficient mice

The intestine is a constantly self renewing tissue where the stem cells are located in the crypts and represent the source of all the differentiated intestinal cell types. Studying the intestinal morphology of the Cyclin O deficient mice, we observed that 20-days old Cyclin O knockout mice have smaller intestinal crypts compared to their wildtype littermates. This difference was overcome in 2 and 6 months-old adult Cyclin O deficient mice.

It has been described that mice lack intestinal crypt structures at the time of birth and only contain differentiated epithelial cells in the villi that have been formed at late embryogenesis. These differentiated intestinal villus cells are short lived and have to be renewed from a proliferating source soon after birth, which makes the rapid crypt formation during the first days after birth essential to ensure a fully functional intestinal tissue [193]. The murine differentiated villus cells at birth are able to maintain their intestinal digestive activity approximately 10-14 days. Around postnatal day 7, the intestinal stem cells and the proliferating progenitors shape the mature crypts which become progressively deeper as the submucosa grows out while the number of crypt units steadily increases by crypt fission. In order to make crypt formation most efficient it remains unclear whether the intestinal stem cells divide symmetrically first to provide a pool of stem cells and then asymmetrically to give rise as well to the non-stem cells, populating the crypt or if the stem cells divide asymmetrically from the beginning [194 195].

We suggest that the smaller crypt size could appear due to an influence of Cyclin O deficiency on the proliferation either of the proliferating progenitors or the intestinal stem cells forming the mature crypts.

We have found less proliferating crypt cells in 2 and 6 months old adult Cyclin O deficient mice compared to age matched WT mice. According to this result, it is likely that the young Cyclin O deficient mice at birth also have less proliferating crypt cells or a decreased proliferation rate and, therefore, need longer time in order to form the mature crypts compared to WT mice.

A reduced number of intestinal stem cells or a failure in the stem cell division could also explain the slower formation of the crypts. Different cell markers to identify intestinal stem cells have been described, such as Lgr5 (CBCs) or Bmi1 (+4 positioned cells). However, up to this point we have not adressed experiments aimed to find out whether Cyclin O deficiency has influence on the number or appearance of intestinal stem cells.

The smaller crypts found in young Cyclin O KOs could influence the capacity of the intestinal tissue to perform its digestive function. The crypt cells of young Cyclin O deficient mice might not provide enough differentiating cells to rapidly renew the intestinal epithelium. This could explain why young Cyclin O deficient mice have a growth deficiency which they overcome when they reach adulthood (Nuñez, M, Balsiger, A., Gil Gomez, G., data not shown).

D2.2. Cyclin O deficient mice have less proliferating intestinal crypt cells

We observed less proliferating crypt cells in 2 and 6 months old Cyclin O deficient mice compared to WT mice, whereas the numbers of proliferating cells in heterozygote and WT mice are comparable. The reduced number of intestinal proliferating cells in Cyclin O deficient mice could be a consequence of different effects of Cyclin O on the normal crypt-axis homeostasis:

1. A direct effect on the proliferation of the stem cells and / or on the early transit amplifying compartment
2. Enhancement of spontaneous apoptosis
3. A decreased anoikis
4. An enhanced differentiation

The Wnt signalling pathway is the main responsible pathway for the proliferation of intestinal crypt cells and the maintenance of the intestinal stem cells. Cyclin O could interact in some parts with the members of this pathway and support the proliferative functions or the maintenance of the stem cells. Consequently, the absence of Cyclin O could lead to a decreased proliferation of the intestinal crypt cells or to the loss of the intestinal stem cells.

Cyclin O has been previously described to be required for the intrinsic apoptotic pathway in lymphoid cells. It has been demonstrated that under intrinsic apoptotic stimuli Cyclin O binds and activates Cdk2 and its *de novo* synthesis precedes apoptosis induction whereas its downregulation abrogates the induced apoptosis [160].

Under normal conditions, there are 2 different forms of apoptosis appearing in the intestinal epithelium.

The “spontaneous” apoptosis takes place in the crypts on the stem and early transit amplifying cells. This type of apoptosis occurs at a low rate and even though the mechanisms are not yet clear it is thought to control the number of cells entering the crypt-villus axis. Knock out mice for the proapoptotic protein Bax or antiapoptotic protein Bcl2 show similar levels of spontaneous apoptosis compared to WT mice suggesting that they have little effect in this process and on the normal homeostasis of the intestinal epithelium [139].

Cyclin O deficiency leads to an abrogation of its intrinsic induced apoptosis in other cells, such as activated T-cells (unpublished results). Accordingly, if Cyclin O is implicated in the apoptosis induction in the crypt cells, Cyclin O deficiency would result in an increase in the number of cells of the crypt. We counted the total numbers of crypt cells and also compared the crypt sizes of adult Cyclin O deficient and WT mice and could not find any difference indicating that the crypts are completely formed. Therefore, the implication of Cyclin O in the spontaneous apoptosis that could cause less proliferating crypt cells is not likely.

Intestinal cell shedding is another form of apoptosis in the intestine occurring at the tip of the villi in order to get rid of terminally differentiated cells. During this process, called anoikis, the intestinal cells that reach the tip of a villus get pushed out of the epithelial layer and get apoptosis because of loss of cell-cell and cell-extracellular matrix contacts. It is not clear if apoptotic stimuli are already induced before the cell is shed into the lumen [139].

If the apoptotic stimuli are induced in a differentiated cell before leaving the villus, Cyclin O deficiency could lead to a decreased apoptosis induction and consequently the cell could stay longer within the villus epithelium. This could cause a reduced migration along the crypt villus axis and a reduced proliferation of crypt cells in order to readjust the homeostasis of the system.

Another explanation for the presence of a decreased number of proliferating cells in the intestinal crypts in Cyclin O deficient mice could be that the proliferating cells differentiate earlier. We found that the total crypt cell numbers and size between adult WT and Cyclin O deficient mice were similar. Besides, the intestinal epithelium of Cyclin O deficient mice has an overall similar morphological appearance compared to the WT mice. If the proliferating crypt cells would die by apoptosis and not migrate upwards in order to differentiate, the villus structure would appear distorted. However, we could not find a difference in the number of one of the differentiated cell types, the Goblet cells. We have not checked yet if the most abundant cell type in the intestine, the enterocytes are present at normal numbers in Cyclin O deficient mice.

D3. Implication of Cyclin O deficiency in adenoma formation in a mouse model of CRC, the APC$^{min/+}$ mouse

We crossed Cyclin O deficient mice to APC$^{min/+}$ mice, a standard mouse model that recapitulates the first steps in the generation of CRCs in order to investigated if partial loss of Cyclin O could sinergize with the loss of APC in the development of intestinal neoplasms.

D3.1. Influence of Cyclin O on adenoma number and size in APC$^{min/+}$ mice

We analysed Cyclin O$^{+/+}$ APC$^{min/+}$ and Cyclin O$^{+/-}$ APC$^{min/+}$ mice for the incidence and growth of intestinal adenomas and found a statistically significant increase of the number of adenomas that develop in the Cyclin O$^{+/-}$ compared to Cyclin O$^{+/+}$ APC$^{min/+}$ mice. Additionally the adenomas from Cyclin O$^{+/-}$ APC$^{min/+}$ mice appeared to grow bigger compared to the Cyclin O$^{+/+}$ APC$^{min/+}$ mice.

Kwong *et al* crossed the DDR deficient Atm knockout mice to APC$^{min/+}$ mice in order to study the implication of the Atm kinase in the formation of intestinal cancer. Upon complete Atm deletion, APC$^{min/+}$ mice developed two-fold more intestinal adenomas than the Atm heterozygous or WT APC$^{min/+}$ mice. They also found an increased incidence of colon adenomas with Atm deficiency. Additionally, the diameter of the adenomas significantly increased upon Atm deletion in APC$^{min/+}$ mice [196].

We have evidences that Cyclin O also modulates the DDR through activation of ATM by an uncharacterised mechanism (Nuñez, M, Gil-Gomez, unpublished data).

Comparing our results to the findings of Kwong *et al*, we could observe a higher adenoma multiplicity in Cyclin $O^{+/-}$ $APC^{min/+}$ mice whereas Kwong *et al* described that Atm heterozygosity affected the adenoma size but not the multiplicity in $APC^{min/+}$ mice. Upon complete Atm deletion, both adenoma growth and multiplicity differed singificant from $Atm^{+/+}$ $APC^{min/+}$ mice. The adenomas from Cyclin $O^{+/-}$ $APC^{min/+}$ mice appeared to grow bigger, but we could not reach statistically significant difference.

In order to initiate adenoma growth, it has been described that a proliferating $APC^{min/+}$ crypt cell has to loose its APC heterozygosity (LOH). A defect in the DDR, such as a decreased expression of Cyclin O could facilitate the aquisition of a second APC mutation and lead to a higher adenoma incidence because of an inefficient DDR and/or a decrease in apoptosis.

We could not investigate the adenoma incidence in Cyclin $O^{-/-}$ $APC^{min/+}$ mice, because of the high mortalilty rate due to hydrocephalus caused by the Cyclin deficiency. 80 % of the Cyclin $O^{-/-}$ $APC^{min/+}$ mice die due to hydrocephalus before reaching a sufficient age in order to analyse intestinal adenoma incidence (unpublished).

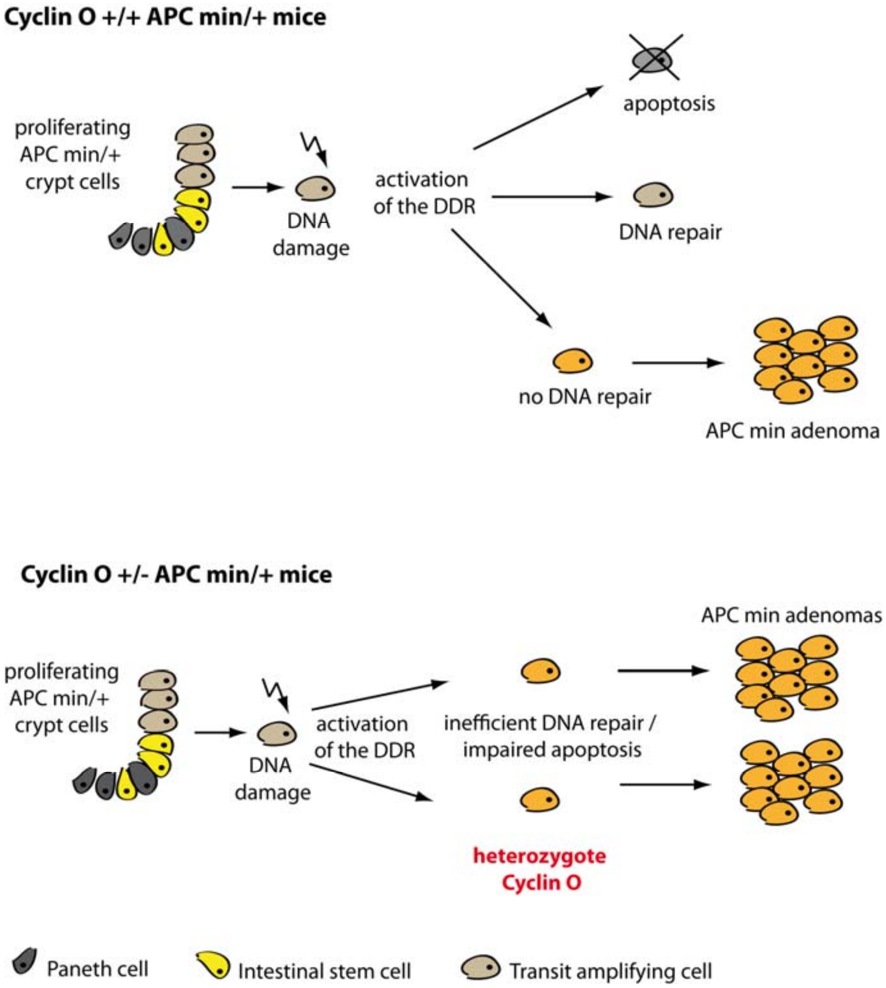
Cyclin O +/+ APC min/+ mice
proliferating APC min/+ crypt cells
DNA damage
activation of the DDR
apoptosis
DNA repair
no DNA repair
APC min adenoma
Cyclin O +/- APC min/+ mice
proliferating APC min/+ crypt cells
DNA damage
activation of the DDR
inefficient DNA repair / impaired apoptosis
APC min adenomas
heterozygote Cyclin O
Paneth cell
Intestinal stem cell
Transit amplifying cell

Figure D4. Model of Appearance of more adenomas in Cyclin O$^{+/-}$ APC$^{min/+}$ mice.

D3.2. Cyclin O deficient adenomas show more malignant features

We analysed morphological and histological differences between the adenomas of Cyclin $O^{+/+}$ $APC^{min/+}$ and Cyclin $O^{+/-}$ $APC^{min/+}$ mice and we observed an increased abundance of mesenchymal cells in the adenomas of Cyclin $O^{+/-}$ $APC^{min/+}$ mice (section R3.2).

The importance of the tumour stroma in the development of the tumour has been demonstrated as it creates a dynamic microenvironment that is able to communicate signals to the tumour cells. In this way, the tumour stroma is able to promote the tumours initiation, growth and invasive capacities. Cancer associated fibroblasts (CAF) and tumour pericytes are the best known cell types within the tumour stroma. CAFs can stimulate tumour cell proliferation by expressing growth factors, enzymes and cytokines. Additionally it has also been described that CAFs are able to support the tumour cell in gaining invasive and metastatic abilities [180 185 197].

Vimentin is a type III intermediate filament and it is ubiquitously expressed by cells of mesenchymal origin, such as fibroblasts, endothelial cells and smooth muscle cells. The upregulation of vimentin expression in tumour cells has been associated with an aggressive phenotype and metastasis in different carcinomas, such as breast cancer or melanomas [173].

In a high throughput study, expression of vimentin in the tumour stroma of human adenocarcinoma samples has been demonstrated to correlate with a poor prognosis for the patient [172].

The number of vimentin-expressing stromal cells is increased in adenomas of Cyclin $O^{+/-}$ $APC^{min/+}$ mice. Accordingly, Cyclin $O^{+/-}$ $APC^{min/+}$ adenomas contain more stroma compared to the adenomas of Cyclin $O^{+/+}$ $APC^{min/+}$ mice. This increase in stroma in Cyclin $O^{+/-}$ $APC^{min/+}$ mice and the less compact appearance could contribute to the overall bigger adenoma size in this group. Whether these adenomas have a higher aggressive phenotype cannot be concluded from our observations. We suggest that the reduced levels of Cyclin O expression due to Cyclin O heterozygosity could cause the selection of a different adenomatous cell phenotype. It could also influence the proliferation capacity of the adenomatous cells. Additionally, Cyclin O heterozygosity could have an influence on the proliferation or apoptosis rate of the CAFs.

D3.3. Cyclin O is expressed in normal epithelial cells surrounding the adenomas and in morphological normal epithelium

We found that the Cyclin O protein is expressed in normal epithelial cells surrounding the adenomas and in groups of intestinal villi not related to adenoma locations of the small intestine of Cyclin $O^{+/+}$ $APC^{min/+}$ and Cyclin $O^{+/-}$ $APC^{min/+}$ mice (section R3.4). The Cyclin O expression appeared randomly in both genotypes in the differentiated epithelial cells outside of the crypts. We have observed the expression of Cyclin O in normal human colon mucosa that under normal conditions does not express the Cyclin O protein. We hypothesised that Cyclin O expressed in normal mucosa of CRC patients could possibly indicate very early lesions in CRC.

Chen *et al* studied early alterations in gene expression in adenomas of $APC^{min/+}$ mice and used WT tissue as a control. They identified 5 different genes that were upregulated in the adenomas and in regions of histologically normal appearing mucosa that were not related to the adenoma location in $APC^{min/+}$ mice. They suggested that the same genes could as well be altered in human CRC [198].

We could not observe the Cyclin O expression in the adenomatous cells of Cyclin $O^{+/+}$ $APC^{min/+}$ and Cyclin $O^{+/-}$ $APC^{min/+}$ mice, but it was expressed in some parts of the normal appearing epithelium. We did not observe Cyclin O expression in the intestinal tissue of WT mice. This resembles the same observations that Chen *et al* made and could indicate that the Cyclin O expression marks morphologically normal appearing early lesions.

Following the “bottom up histogenesis” and the adenoma growth model in $APC^{min/+}$ mice of Oshima *et al* [91], the initiator cells of an adenoma are the proliferating crypt cells. We hypothesised that the Cyclin O expressing cells represent very early adenomatous lesions, but we observed the Cyclin O expression in the more differentiated cells outside of the crypts.

If the Cyclin O expressing differentiated epithelial cells represent very early transforming cancer cells, in order to grow a tumour, they would have to dedifferentiate into a more proliferative cancerous phenotype. The initiation of tumour growth by dedifferentiation and acquisition of stem-cell–like properties in differentiated villus cells has been described by Schwitalla *et al* [199]. Upon permanent activation of ß-catenin and the NF-κB pathway, they found actively proliferating aberrant foci along the villus epithelium resembling crypt structures. These structures were able to form adenomatous crypts and to invade the subepithelium. Accordingly, they demonstrated that villus cells can reaquire stem cell properties by dedifferentiation when Wnt signalling is elevated in a NF-κB-dependent manner [199].

We did not observe crypt-like structures formed by the Cyclin O expressing cells in the villus. Additionally, we observed a similar ß-catenin expression located to the epithelial cell membrane in Cyclin O positive and negative villus cells. We did not observe a ß-catenin accumulation in the Cyclin O expressing cells.
However, we can not exclude that the Cyclin O expression has been triggered before the ß-catenin accumulation in these cells is detectable.

D4. Concluding remarks

Colorectal cancer is one of the four most frequently occurring cancers worldwide. Both, hereditary and environmental factors contribute to the development of CRC. Most colorectal neoplasms develop sporadically [46], although familiar predisposition genes have been identified.

Under continuous cellular stress, an intestinal epithelial cell can suffer damage of different cell components including its DNA. In the presence of DNA damage, epithelial cells activate the DDR in order to repair the DNA or to induce apoptosis if the damage is too severe. If both mechanisms fail, the damaged cell continues to proliferate and can accumulate further mutations.

In our laboratory, we have described that Cyclin O is induced after DNA damage through the transcription factor p53. Following induction, Cyclin O has been shown to bind to Cdk2 in order to induce the activation of the apical Caspase-8. Consequent cleavage of Bid to tBid by the active Caspase-8 triggers the mitochondrial pathway that leads to apoptosis [160] [156].

The evasion of apoptosis accounts to one of the six hallmarks of cancer [200]. In this thesis, we describe the overexpression of Cyclin O in CRC cells of early and late stages of the tumour development as well as in metastatic cells. We hypothesise that the CRC cells have gained resistance to the proapoptotic functions of Cyclin O.

We could demonstrate that the Cyclin O expression correlates to a longer cancer specific survival of CRC patients in stages III and IV. We suggest that the Cyclin O expression could lead to a more differentiated type of tumour that could be better treatable.

From a microarray analysis in our laboratory, we identified *MOCS2* as a downstream target gene of Cyclin O and hypothesised that the Cyclin O directed MOCS2 expression in CRC could turn the cancer cells more resistant to chemotherapeutic treatment. Oppositely to our hypothesis, we could show that the Cyclin O mediated MOCS2 expression does not worsen the CRC patient’s prognosis.

We have studied the consequences of Cyclin O deficiency in mouse intestinal tissue and could find a reduction in the number of proliferating crypt cells. We observed as well a reduced crypt size of young Cyclin O deficient mice which could be caused by a reduced proliferating capacity during the first postnatal days when the mature crypts are formed. We have not identified yet how the absence of Cyclin O could cause less proliferating cells in the intestinal mouse tissue.

We crossed Cyclin O deficient mice to $APC^{min/+}$ mice, a standard mouse model that recapitulates the first steps in the generation of CRCs in order to investigate if Cyclin O deficiency could synergize with the loss of APC in the development of intestinal neoplasms. We could show that Cyclin $O^{+/-}$ $APC^{min/+}$ mice develop more adenomas than Cyclin $O^{+/+}$ $APC^{min/+}$ mice. Our findings resemble the phenotype observed for $Atm^{-/-}$ $APC^{min/+}$ mice, another protein implicated in the DDR [196]. However, we could still not identify what causes the higher abundance of adenomas in Cyclin $O^{+/-}$ $APC^{min/+}$ mice.

We could find the Cyclin O protein expressed in normal peritumoral CRC tissue and in morphologically normal intestinal epithelial cells of $APC^{min/+}$ mice. Because Cyclin O is normally not expressed in the intestinal epithelium, we hypothesise that the Cyclin O expressing cells could be very early transforming cancer cells. Acordingly, Cyclin O could possibly serve as an indicator of early lesions in CRC. However, the question of what has triggered the Cyclin O expression remains and if the Cyclin O positive epithelial cells are able to progress to later stages of CRC.

Conclusions

1. Cyclin O is not expressed in physiologically normal mouse and human intestinal tissue.
2. Cyclin O is overexpressed in human colorectal adenocarcinomas.
3. The Cyclin O overexpression appears during the early stages of the tumour development.
4. Positive Cyclin O expression correlates with a better cancer specific survival in CRC stages III and IV.
5. The Cyclin O expression is maintained in the metastasis of the colorectal adenocarcinomas.
6. MOCS2 is a putative target gene of Cyclin O.
7. The Cyclin O mediated expression of MOCS2 in adenocarcinomas does not worsen the prognosis of the patients.
8. The Cyclin O gene is not mutated in Colorectal adenocarcinomas.
9. Young Cyclin O deficient mice have small crypts but the defect is overcome in adults.
10. Cyclin O deficient mice have less proliferating intestinal crypt cells.
11. Cyclin $O^{+/-}$ $APC^{min/+}$ mice develop more and bigger intestinal adenomas than Cyclin $O^{+/+}$ $APC^{min/+}$ mice.
12. Cyclin O is expressed in the normal intestinal epithelial cells surrounding the adenomas and in regions of normal intestinal epithelium in $APC^{min/+}$ mice.

Bibliography

1. Sancho, E., Batlle, E. & Clevers, H. Signaling pathways in intestinal development and cancer. *Annu Rev Cell Dev Biol* **20**, 695-723 (2004).

2. Noah, T.K., Donahue, B. & Shroyer, N.F. Intestinal development and differentiation. *Exp Cell Res* **317**, 2702-2710 (2011).

3. Hauck, A.L.*, et al.* Twists and turns in the development and maintenance of the mammalian small intestine epithelium. *Birth Defects Res C Embryo Today* **75**, 58-71 (2005).

4. Clevers, H. & Batlle, E. SnapShot: The Intestinal Crypt. *Cell* **152**, 1198-1198 (2013).

5. Batlle, E. A new identity for the elusive intestinal stem cell. *Nat Genet* **40**, 818-819 (2008).

6. Sato, T.*, et al.* Paneth cells constitute the niche for Lgr5 stem cells in intestinal crypts. *Nature* **469**, 415-418 (2011).

7. Sancho, E., Batlle, E. & Clevers, H. Live and let die in the intestinal epithelium. *Curr Opin Cell Biol* **15**, 763-770 (2003).

8. Gordon, J.I. & Hermiston, M.L. Differentiation and self-renewal in the mouse gastrointestinal epithelium. *Curr Opin Cell Biol* **6**, 795-803 (1994).

9. Bach, S.P., Renehan, A.G. & Potten, C.S. Stem cells: the intestinal stem cell as a paradigm. *Carcinogenesis* **21**, 469-476 (2000).

10. Potten, C.S., Kellett, M., Roberts, S.A., Rew, D.A. & Wilson, G.D. Measurement of in vivo proliferation in human colorectal mucosa using bromodeoxyuridine. *Gut* **33**, 71-78 (1992).

11. Potten, C.S., Hendry, J.H. & Moore, J.V. Estimates of the number of clonogenic cells in crypts of murine small intestine. *Virchows Arch B Cell Pathol Incl Mol Pathol* **53**, 227-234 (1987).

12. Brittan, M. & Wright, N.A. Stem cell in gastrointestinal structure and neoplastic development. *Gut* **53**, 899-910 (2004).

13. Paulus, U., Loeffler, M., Zeidler, J., Owen, G. & Potten, C.S. The differentiation and lineage development of goblet cells in the murine small intestinal crypt: experimental and modelling studies. *J Cell Sci* **106 (Pt 2)**, 473-483 (1993).

14. Ayabe, T.*, et al.* Secretion of microbicidal alpha-defensins by intestinal Paneth cells in response to bacteria. *Nat Immunol* **1**, 113-118 (2000).

15. Bevins, C.L., Martin-Porter, E. & Ganz, T. Defensins and innate host defence of the gastrointestinal tract. *Gut* **45**, 911-915 (1999).

16. Bjerknes, M. & Cheng, H. The stem-cell zone of the small intestinal epithelium. I. Evidence from Paneth cells in the adult mouse. *Am J Anat* **160**, 51-63 (1981).

17. Barker, N. & Clevers, H. Tracking down the stem cells of the intestine: strategies to identify adult stem cells. *Gastroenterology* **133**, 1755-1760 (2007).

18. Sangiorgi, E. & Capecchi, M.R. Bmi1 is expressed in vivo in intestinal stem cells. *Nat Genet* **40**, 915-920 (2008).

19. Barker, N.*, et al.* Identification of stem cells in small intestine and colon by marker gene Lgr5. *Nature* **449**, 1003-1007 (2007).

20. Sato, T.*, et al.* Single Lgr5 stem cells build crypt-villus structures in vitro without a mesenchymal niche. *Nature* **459**, 262-265 (2009).

21. Tian, H.*, et al.* A reserve stem cell population in small intestine renders Lgr5-positive cells dispensable. *Nature* **478**, 255-259 (2011).

22. Takeda, N.*, et al.* Interconversion between intestinal stem cell populations in distinct niches. *Science* **334**, 1420-1424 (2011).

23. MacDonald, B.T., Tamai, K. & He, X. Wnt/beta-catenin signaling: components, mechanisms, and diseases. *Dev Cell* **17**, 9-26 (2009).

24. Tanaka, S.S., Kojima, Y., Yamaguchi, Y.L., Nishinakamura, R. & Tam, P.P. Impact of WNT signaling on tissue lineage differentiation in the early mouse embryo. *Dev Growth Differ* **53**, 843-856 (2011).

25. Logan, C.Y. & Nusse, R. The Wnt signaling pathway in development and disease. *Annu Rev Cell Dev Biol* **20**, 781-810 (2004).

26. Reya, T. & Clevers, H. Wnt signalling in stem cells and cancer. *Nature* **434**, 843-850 (2005).

27. Clevers, H. Wnt/beta-catenin signaling in development and disease. *Cell* **127**, 469-480 (2006).

28. Davidson, G.*, et al.* Casein kinase 1 gamma couples Wnt receptor activation to cytoplasmic signal transduction. *Nature* **438**, 867-872 (2005).

29. Tamai, K.*, et al.* LDL-receptor-related proteins in Wnt signal transduction. *Nature* **407**, 530-535 (2000).

30. Zeng, X.*, et al.* Initiation of Wnt signaling: control of Wnt coreceptor Lrp6 phosphorylation/activation via frizzled, dishevelled and axin functions. *Development* **135**, 367-375 (2008).

31. Cadigan, K.M. & Waterman, M.L. TCF/LEFs and Wnt signaling in the nucleus. *Cold Spring Harb Perspect Biol* **4** (2012).

32. Taketo, M.M. Mouse models of gastrointestinal tumors. *Cancer Sci* **97**, 355-361 (2006).

33. Korinek, V.*, et al.* Constitutive transcriptional activation by a beta-catenin-Tcf complex in APC-/- colon carcinoma. *Science* **275**, 1784-1787 (1997).

34. Myant, K. & Sansom, O.J. Wnt/Myc interactions in intestinal cancer: partners in crime. *Exp Cell Res* **317**, 2725-2731 (2011).

35. van de Wetering, M., *et al.* The beta-catenin/TCF-4 complex imposes a crypt progenitor phenotype on colorectal cancer cells. *Cell* **111**, 241-250 (2002).

36. Korinek, V., *et al.* Depletion of epithelial stem-cell compartments in the small intestine of mice lacking Tcf-4. *Nat Genet* **19**, 379-383 (1998).

37. He, T.C., *et al.* Identification of c-MYC as a target of the APC pathway. *Science* **281**, 1509-1512 (1998).

38. Muncan, V., *et al.* Rapid loss of intestinal crypts upon conditional deletion of the Wnt/Tcf-4 target gene c-Myc. *Mol Cell Biol* **26**, 8418-8426 (2006).

39. Pinto, D., Gregorieff, A., Begthel, H. & Clevers, H. Canonical Wnt signals are essential for homeostasis of the intestinal epithelium. *Genes Dev* **17**, 1709-1713 (2003).

40. Bettess, M.D., *et al.* c-Myc is required for the formation of intestinal crypts but dispensable for homeostasis of the adult intestinal epithelium. *Mol Cell Biol* **25**, 7868-7878 (2005).

41. Pasquale, E.B. Eph-ephrin bidirectional signaling in physiology and disease. *Cell* **133**, 38-52 (2008).

42. Batlle, E., *et al.* Beta-catenin and TCF mediate cell positioning in the intestinal epithelium by controlling the expression of EphB/ephrinB. *Cell* **111**, 251-263 (2002).

43. Solanas, G., Cortina, C., Sevillano, M. & Batlle, E. Cleavage of E-cadherin by ADAM10 mediates epithelial cell sorting downstream of EphB signalling. *Nat Cell Biol* **13**, 1100-1107 (2011).

44. Herath, N.I. & Boyd, A.W. The role of Eph receptors and ephrin ligands in colorectal cancer. *Int J Cancer* **126**, 2003-2011 (2010).

45. Edwards, B.K., *et al.* Annual report to the nation on the status of cancer, 1975-2006, featuring colorectal cancer trends and impact of interventions (risk factors, screening, and treatment) to reduce future rates. *Cancer* **116**, 544-573 (2010).

46. Siegel, R., Naishadham, D. & Jemal, A. Cancer statistics, 2012. *CA Cancer J Clin* **62**, 10-29 (2012).

47. Phillips, K.A.*, et al.* Trends in colonoscopy for colorectal cancer screening. *Med Care* **45**, 160-167 (2007).

48. Morson, B.C. The evolution of colorectal carcinoma. *Clin Radiol* **35**, 425-431 (1984).

49. de la Chapelle, A. Genetic predisposition to colorectal cancer. *Nat Rev Cancer* **4**, 769-780 (2004).

50. Fearon, E.R. & Vogelstein, B. A genetic model for colorectal tumorigenesis. *Cell* **61**, 759-767 (1990).

51. Pancione, M., Remo, A. & Colantuoni, V. Genetic and epigenetic events generate multiple pathways in colorectal cancer progression. *Patholog Res Int* **2012**, (2012).

52. Powell, S.M.*, et al.* APC mutations occur early during colorectal tumorigenesis. *Nature* **359**, 235-237 (1992).

53. Polakis, P. The adenomatous polyposis coli (APC) tumor suppressor. *Biochim Biophys Acta* **1332**, F127-147 (1997).

54. Fodde, R. & Khan, P.M. Genotype-phenotype correlations at the adenomatous polyposis coli (APC) gene. *Crit Rev Oncog* **6**, 291-303 (1995).

55. Rustgi, A.K. The genetics of hereditary colon cancer. *Genes Dev* **21**, 2525-2538 (2007).

56. Liu, B.*, et al.* Analysis of mismatch repair genes in hereditary non-polyposis colorectal cancer patients. *Nat Med* **2**, 169-174 (1996).

57. Huang, J.*, et al.* APC mutations in colorectal tumors with mismatch repair deficiency. *Proc Natl Acad Sci U S A* **93**, 9049-9054 (1996).

58. Muller, A. & Fishel, R. Mismatch repair and the hereditary non-polyposis colorectal cancer syndrome (HNPCC). *Cancer Invest* **20**, 102-109 (2002).

59. Umar, A., *et al.* Revised Bethesda Guidelines for hereditary nonpolyposis colorectal cancer (Lynch syndrome) and microsatellite instability. *J Natl Cancer Inst* **96**, 261-268 (2004).

60. Parsons, R., *et al.* Microsatellite instability and mutations of the transforming growth factor beta type II receptor gene in colorectal cancer. *Cancer Res* **55**, 5548-5550 (1995).

61. Rampino, N., *et al.* Somatic frameshift mutations in the BAX gene in colon cancers of the microsatellite mutator phenotype. *Science* **275**, 967-969 (1997).

62. Lynch, H.T., *et al.* Review of the Lynch syndrome: history, molecular genetics, screening, differential diagnosis, and medicolegal ramifications. *Clin Genet* **76**, 1-18 (2009).

63. de la Chapelle, A. Microsatellite instability. *N Engl J Med* **349**, 209-210 (2003).

64. Heinen, C.D., Richardson, D., White, R. & Groden, J. Microsatellite instability in colorectal adenocarcinoma cell lines that have full-length adenomatous polyposis coli protein. *Cancer Res* **55**, 4797-4799 (1995).

65. Kinzler, K.W. & Vogelstein, B. Lessons from hereditary colorectal cancer. *Cell* **87**, 159-170 (1996).

66. Ichii, S., *et al.* Inactivation of both APC alleles in an early stage of colon adenomas in a patient with familial adenomatous polyposis (FAP). *Hum Mol Genet* **1**, 387-390 (1992).

67. van Es, J.H., Giles, R.H. & Clevers, H.C. The many faces of the tumor suppressor gene APC. *Exp Cell Res* **264**, 126-134 (2001).

68. Knudsen, A.L., Bisgaard, M.L. & Bulow, S. Attenuated familial adenomatous polyposis (AFAP). A review of the literature. *Fam Cancer* **2**, 43-55 (2003).

69. Groden, J., *et al.* Identification and characterization of the familial adenomatous polyposis coli gene. *Cell* **66**, 589-600 (1991).

70. Nishisho, I., *et al.* Mutations of chromosome 5q21 genes in FAP and colorectal cancer patients. *Science* **253**, 665-669 (1991).

71. Senda, T., Iizuka-Kogo, A., Onouchi, T. & Shimomura, A. Adenomatous polyposis coli (APC) plays multiple roles in the intestinal and colorectal epithelia. *Med Mol Morphol* **40**, 68-81 (2007).

72. Half, E., Bercovich, D. & Rozen, P. Familial adenomatous polyposis. *Orphanet J Rare Dis* **4**, 22 (2009).

73. Rowan, A.J., *et al.* APC mutations in sporadic colorectal tumors: A mutational "hotspot" and interdependence of the "two hits". *Proc Natl Acad Sci U S A* **97**, 3352-3357 (2000).

74. Levy, D.B., *et al.* Inactivation of both APC alleles in human and mouse tumors. *Cancer Res* **54**, 5953-5958 (1994).

75. Sparks, A.B., Morin, P.J., Vogelstein, B. & Kinzler, K.W. Mutational analysis of the APC/beta-catenin/Tcf pathway in colorectal cancer. *Cancer Res* **58**, 1130-1134 (1998).

76. Arrington, A.K., *et al.* Prognostic and Predictive Roles of KRAS Mutation in Colorectal Cancer. *Int J Mol Sci* **13**, 12153-12168 (2012).

77. Shibata, D., Schaeffer, J., Li, Z.H., Capella, G. & Perucho, M. Genetic heterogeneity of the c-K-ras locus in colorectal adenomas but not in adenocarcinomas. *J Natl Cancer Inst* **85**, 1058-1063 (1993).

78. Jen, J., *et al.* Molecular determinants of dysplasia in colorectal lesions. *Cancer Res* **54**, 5523-5526 (1994).

79. Baker, S.J., *et al.* p53 gene mutations occur in combination with 17p allelic deletions as late events in colorectal tumorigenesis. *Cancer Res* **50**, 7717-7722 (1990).

80. Edge, S.B. & Compton, C.C. The American Joint Committee on Cancer: the 7th edition of the AJCC cancer staging manual and the future of TNM. *Ann Surg Oncol* **17**, 1471-1474 (2010).

81. Lewis, A.M. & Martin, R.C. The treatment of hepatic metastases in colorectal carcinoma. *Am Surg* **72**, 466-473 (2006).

82. Liljegren, A.*, et al.* Prevalence and incidence of hyperplastic polyps and adenomas in familial colorectal cancer: correlation between the two types of colon polyps. *Gut* **52**, 1140-1147 (2003).

83. Shih, I.M.*, et al.* Top-down morphogenesis of colorectal tumors. *Proc Natl Acad Sci U S A* **98**, 2640-2645 (2001).

84. Preston, S.L.*, et al.* Bottom-up histogenesis of colorectal adenomas: origin in the monocryptal adenoma and initial expansion by crypt fission. *Cancer Res* **63**, 3819-3825 (2003).

85. Fodde, R.*, et al.* A targeted chain-termination mutation in the mouse Apc gene results in multiple intestinal tumors. *Proc Natl Acad Sci U S A* **91**, 8969-8973 (1994).

86. Dietrich, W.F.*, et al.* Genetic identification of Mom-1, a major modifier locus affecting Min-induced intestinal neoplasia in the mouse. *Cell* **75**, 631-639 (1993).

87. Haines, J.*, et al.* Genetic basis of variation in adenoma multiplicity in ApcMin/+ Mom1S mice. *Proc Natl Acad Sci U S A* **102**, 2868-2873 (2005).

88. Paulsen, J.E.*, et al.* Qualitative and quantitative relationship between dysplastic aberrant crypt foci and tumorigenesis in the Min/+ mouse colon. *Cancer Res* **61**, 5010-5015 (2001).

89. Coletta, P.L.*, et al.* Lymphodepletion in the ApcMin/+ mouse model of intestinal tumorigenesis. *Blood* **103**, 1050-1058 (2004).

90. You, S.*, et al.* Developmental abnormalities in multiple proliferative tissues of Apc(Min/+) mice. *Int J Exp Pathol* **87**, 227-236 (2006).

91. Oshima, H., Oshima, M., Kobayashi, M., Tsutsumi, M. & Taketo, M.M. Morphological and molecular processes of polyp formation in Apc(delta716) knockout mice. *Cancer Res* **57**, 1644-1649 (1997).

92. Cortina, C., *et al.* EphB-ephrin-B interactions suppress colorectal cancer progression by compartmentalizing tumor cells. *Nat Genet* **39**, 1376-1383 (2007).

93. Romagnolo, B., *et al.* Intestinal dysplasia and adenoma in transgenic mice after overexpression of an activated beta-catenin. *Cancer Res* **59**, 3875-3879 (1999).

94. Harada, N., *et al.* Intestinal polyposis in mice with a dominant stable mutation of the beta-catenin gene. *EMBO J* **18**, 5931-5942 (1999).

95. Tanaka, T., *et al.* A novel inflammation-related mouse colon carcinogenesis model induced by azoxymethane and dextran sodium sulfate. *Cancer Sci* **94**, 965-973 (2003).

96. Rosenberg, D.W., Giardina, C. & Tanaka, T. Mouse models for the study of colon carcinogenesis. *Carcinogenesis* **30**, 183-196 (2009).

97. Kroemer, G., *et al.* Classification of cell death: recommendations of the Nomenclature Committee on Cell Death 2009. *Cell Death Differ* **16**, 3-11 (2009).

98. Melino, G. The Sirens' song. *Nature* **412**, 23 (2001).

99. Kerr, J.F., Wyllie, A.H. & Currie, A.R. Apoptosis: a basic biological phenomenon with wide-ranging implications in tissue kinetics. *Br J Cancer* **26**, 239-257 (1972).

100. Sulston, J.E. Post-embryonic development in the ventral cord of Caenorhabditis elegans. *Philos Trans R Soc Lond B Biol Sci* **275**, 287-297 (1976).

101. Brenner, S. The genetics of Caenorhabditis elegans. *Genetics* **77**, 71-94 (1974).

102. Ellis, H.M. & Horvitz, H.R. Genetic control of programmed cell death in the nematode C. elegans. *Cell* **44**, 817-829 (1986).

103. Danial, N.N. & Korsmeyer, S.J. Cell death: critical control points. *Cell* **116**, 205-219 (2004).

104. Kumar, S. Caspase function in programmed cell death. *Cell Death Differ* **14**, 32-43 (2007).

105. Galluzzi, L., *et al.* To die or not to die: that is the autophagic question. *Curr Mol Med* **8**, 78-91 (2008).

106. Thorburn, A. Apoptosis and autophagy: regulatory connections between two supposedly different processes. *Apoptosis* **13**, 1-9 (2008).

107. Klionsky, D. An overview of autophagy: Morphology, mechanism and regulation. *Antioxid Redox Signal* (2013).

108. Bernard, A. & Klionsky, D.J. Autophagosome formation: tracing the source. *Dev Cell* **25**, 116-117 (2013).

109. Golstein, P. & Kroemer, G. Cell death by necrosis: towards a molecular definition. *Trends Biochem Sci* **32**, 37-43 (2007).

110. Festjens, N., Vanden Berghe, T. & Vandenabeele, P. Necrosis, a well-orchestrated form of cell demise: signalling cascades, important mediators and concomitant immune response. *Biochim Biophys Acta* **1757**, 1371-1387 (2006).

111. Yuan, J., Shaham, S., Ledoux, S., Ellis, H.M. & Horvitz, H.R. The C. elegans cell death gene ced-3 encodes a protein similar to mammalian interleukin-1 beta-converting enzyme. *Cell* **75**, 641-652 (1993).

112. Martinon, F. & Tschopp, J. Inflammatory caspases: linking an intracellular innate immune system to autoinflammatory diseases. *Cell* **117**, 561-574 (2004).

113. Park, H.H. Structural features of caspase-activating complexes. *Int J Mol Sci* **13**, 4807-4818 (2012).

114. Shi, Y. Mechanisms of caspase activation and inhibition during apoptosis. *Mol Cell* **9**, 459-470 (2002).

115. Peter, M.E. & Krammer, P.H. The CD95(APO-1/Fas) DISC and beyond. *Cell Death Differ* **10**, 26-35 (2003).

116. Tinel, A. & Tschopp, J. The PIDDosome, a protein complex implicated in activation of caspase-2 in response to genotoxic stress. *Science* **304**, 843-846 (2004).

117. Cain, K., Bratton, S.B. & Cohen, G.M. The Apaf-1 apoptosome: a large caspase-activating complex. *Biochimie* **84**, 203-214 (2002).

118. Degterev, A., Boyce, M. & Yuan, J. A decade of caspases. *Oncogene* **22**, 8543-8567 (2003).

119. Uegaki, K.*, et al.* Structure of the CAD domain of caspase-activated DNase and interaction with the CAD domain of its inhibitor. *J Mol Biol* **297**, 1121-1128 (2000).

120. Jin, Z. & El-Deiry, W.S. Overview of cell death signaling pathways. *Cancer Biol Ther* **4**, 139-163 (2005).

121. Vaux, D.L. & Silke, J. Mammalian mitochondrial IAP binding proteins. *Biochem Biophys Res Commun* **304**, 499-504 (2003).

122. Richter, B.W. & Duckett, C.S. The IAP proteins: caspase inhibitors and beyond. *Sci STKE* **2000**, pe1 (2000).

123. Salvesen, G.S. & Duckett, C.S. IAP proteins: blocking the road to death's door. *Nat Rev Mol Cell Biol* **3**, 401-410 (2002).

124. Lomonosova, E. & Chinnadurai, G. BH3-only proteins in apoptosis and beyond: an overview. *Oncogene* **27 Suppl 1**, S2-19 (2008).

125. Cheng, E.H.*, et al.* BCL-2, BCL-X(L) sequester BH3 domain-only molecules preventing BAX- and BAK-mediated mitochondrial apoptosis. *Mol Cell* **8**, 705-711 (2001).

126. Brunelle, J.K. & Letai, A. Control of mitochondrial apoptosis by the Bcl-2 family. *J Cell Sci* **122**, 437-441 (2009).

127. Roset, R., Ortet, L. & Gil-Gomez, G. Role of Bcl-2 family members on apoptosis: what we have learned from knock-out mice. *Front Biosci* **12**, 4722-4730 (2007).

128. Kuwana, T., *et al.* BH3 domains of BH3-only proteins differentially regulate Bax-mediated mitochondrial membrane permeabilization both directly and indirectly. *Mol Cell* **17**, 525-535 (2005).

129. Reubold, T.F. & Eschenburg, S. A molecular view on signal transduction by the apoptosome. *Cell Signal* **24**, 1420-1425 (2012).

130. Renault, T.T., Floros, K.V. & Chipuk, J.E. BAK/BAX activation and cytochrome c release assays using isolated mitochondria. *Methods* (2013).

131. Fulda, S. & Debatin, K.M. Extrinsic versus intrinsic apoptosis pathways in anticancer chemotherapy. *Oncogene* **25**, 4798-4811 (2006).

132. Lee, E.W., Seo, J., Jeong, M., Lee, S. & Song, J. The roles of FADD in extrinsic apoptosis and necroptosis. *BMB Rep* **45**, 496-508 (2012).

133. Pobezinskaya, Y.L. & Liu, Z. The role of TRADD in death receptor signaling. *Cell Cycle* **11**, 871-876 (2012).

134. Hensley, P., Mishra, M. & Kyprianou, N. Targeting caspases in cancer therapeutics. *Biol Chem* (2013).

135. Dickens, L.S., *et al.* A death effector domain chain DISC model reveals a crucial role for caspase-8 chain assembly in mediating apoptotic cell death. *Mol Cell* **47**, 291-305 (2012).

136. Li, H., Zhu, H., Xu, C.J. & Yuan, J. Cleavage of BID by caspase 8 mediates the mitochondrial damage in the Fas pathway of apoptosis. *Cell* **94**, 491-501 (1998).

137. Dickens, L.S., Powley, I.R., Hughes, M.A. & MacFarlane, M. The 'complexities' of life and death: death receptor signalling platforms. *Exp Cell Res* **318**, 1269-1277 (2012).

138. Silke, J. & Strasser, A. The FLIP Side of Life. *Sci Signal* **6**, pe2 (2013).

139. Watson, A.J. & Pritchard, D.M. Lessons from genetically engineered animal models. VII. Apoptosis in intestinal

epithelium: lessons from transgenic and knockout mice. *Am J Physiol Gastrointest Liver Physiol* **278**, G1-5 (2000).

140. Martinou, J.C. & Green, D.R. Breaking the mitochondrial barrier. *Nat Rev Mol Cell Biol* **2**, 63-67 (2001).

141. Ilic, D.*, et al.* Extracellular matrix survival signals transduced by focal adhesion kinase suppress p53-mediated apoptosis. *J Cell Biol* **143**, 547-560 (1998).

142. Valentijn, A.J., Metcalfe, A.D., Kott, J., Streuli, C.H. & Gilmore, A.P. Spatial and temporal changes in Bax subcellular localization during anoikis. *J Cell Biol* **162**, 599-612 (2003).

143. Gilmore, A.P. Anoikis. *Cell Death Differ* **12 Suppl 2**, 1473-1477 (2005).

144. Malumbres, M.*, et al.* Cyclin-dependent kinases: a family portrait. *Nat Cell Biol* **11**, 1275-1276 (2009).

145. Malumbres, M. & Barbacid, M. Mammalian cyclin-dependent kinases. *Trends Biochem Sci* **30**, 630-641 (2005).

146. Adams, P.D. Regulation of the retinoblastoma tumor suppressor protein by cyclin/cdks. *Biochim Biophys Acta* **1471**, M123-133 (2001).

147. Satyanarayana, A. & Kaldis, P. Mammalian cell-cycle regulation: several Cdks, numerous cyclins and diverse compensatory mechanisms. *Oncogene* **28**, 2925-2939 (2009).

148. Yu, D.S. & Cortez, D. A role for CDK9-cyclin K in maintaining genome integrity. *Cell Cycle* **10**, 28-32 (2011).

149. Lu, Z. & Hunter, T. Ubiquitylation and proteasomal degradation of the p21(Cip1), p27(Kip1) and p57(Kip2) CDK inhibitors. *Cell Cycle* **9**, 2342-2352 (2010).

150. Sherr, C.J. & Roberts, J.M. CDK inhibitors: positive and negative regulators of G1-phase progression. *Genes Dev* **13**, 1501-1512 (1999).

151. Pavletich, N.P. Mechanisms of cyclin-dependent kinase regulation: structures of Cdks, their cyclin activators, and Cip and INK4 inhibitors. *J Mol Biol* **287**, 821-828 (1999).

152. Kaldis, P. The cdk-activating kinase (CAK): from yeast to mammals. *Cell Mol Life Sci* **55**, 284-296 (1999).

153. Shen, T. & Huang, S. The role of Cdc25A in the regulation of cell proliferation and apoptosis. *Anticancer Agents Med Chem* **12**, 631-639 (2012).

154. Morgan, D.O. Principles of CDK regulation. *Nature* **374**, 131-134 (1995).

155. Golsteyn, R.M. Cdk1 and Cdk2 complexes (cyclin dependent kinases) in apoptosis: a role beyond the cell cycle. *Cancer Lett* **217**, 129-138 (2005).

156. Granes, F., Roig, M.B., Brady, H.J. & Gil-Gomez, G. Cdk2 activation acts upstream of the mitochondrion during glucocorticoid induced thymocyte apoptosis. *Eur J Immunol* **34**, 2781-2790 (2004).

157. Gil-Gomez, G., Berns, A. & Brady, H.J. A link between cell cycle and cell death: Bax and Bcl-2 modulate Cdk2 activation during thymocyte apoptosis. *EMBO J* **17**, 7209-7218 (1998).

158. Brady, H.J., Gil-Gomez, G., Kirberg, J. & Berns, A.J. Bax alpha perturbs T cell development and affects cell cycle entry of T cells. *EMBO J* **15**, 6991-7001 (1996).

159. Williams, O., Gil-Gomez, G., Norton, T., Kioussis, D. & Brady, H.J. Activation of Cdk2 is a requirement for antigen-mediated thymic negative selection. *Eur J Immunol* **30**, 709-713 (2000).

160. Roig, M.B.*, et al.* Identification of a novel cyclin required for the intrinsic apoptosis pathway in lymphoid cells. *Cell Death Differ* **16**, 230-243 (2009).

161. Hanahan, D. & Weinberg, R.A. The hallmarks of cancer. *Cell* **100**, 57-70 (2000).

162. Kim, J.S., Bonifant, C., Bunz, F., Lane, W.S. & Waldman, T. Epitope tagging of endogenous genes in diverse human cell lines. *Nucleic Acids Res* **36**, e127 (2008).

163. Rago, C., Vogelstein, B. & Bunz, F. Genetic knockouts and knockins in human somatic cells. *Nat Protoc* **2**, 2734-2746 (2007).

164. Sastry, L., Johnson, T., Hobson, M.J., Smucker, B. & Cornetta, K. Titering lentiviral vectors: comparison of DNA, RNA and marker expression methods. *Gene Ther* **9**, 1155-1162 (2002).

165. Xu, Y.*, et al.* Excision of selectable genes from transgenic goat cells by a protein transducible TAT-Cre recombinase. *Gene* **419**, 70-74 (2008).

166. Sharma, R.C., Murphy, A.J., DeWald, M.G. & Schimke, R.T. A rapid procedure for isolation of RNA-free genomic DNA from mammalian cells. *Biotechniques* **14**, 176-178 (1993).

167. Ramsby, M.L. & Makowski, G.S. Differential detergent fractionation of eukaryotic cells. Analysis by two-dimensional gel electrophoresis. *Methods Mol Biol* **112**, 53-66 (1999).

168. Rhodes, D.R.*, et al.* Oncomine 3.0: genes, pathways, and networks in a collection of 18,000 cancer gene expression profiles. *Neoplasia* **9**, 166-180 (2007).

169. Sabates-Bellver, J.*, et al.* Transcriptome profile of human colorectal adenomas. *Mol Cancer Res* **5**, 1263-1275 (2007).

170. Pritsos, C.A. & Gustafson, D.L. Xanthine dehydrogenase and its role in cancer chemotherapy. *Oncol Res* **6**, 477-481 (1994).

171. Reiss, J. & Johnson, J.L. Mutations in the molybdenum cofactor biosynthetic genes MOCS1, MOCS2, and GEPH. *Hum Mutat* **21**, 569-576 (2003).

172. Ngan, C.Y.*, et al.* Quantitative evaluation of vimentin expression in tumour stroma of colorectal cancer. *Br J Cancer* **96**, 986-992 (2007).

173. Satelli, A. & Li, S. Vimentin in cancer and its potential as a molecular target for cancer therapy. *Cell Mol Life Sci* **68**, 3033-3046 (2011).

174. Yuan, J. & Kroemer, G. Alternative cell death mechanisms in development and beyond. *Genes Dev* **24**, 2592-2602 (2010).

175. Vargas, A.J. & Thompson, P.A. Diet and nutrient factors in colorectal cancer risk. *Nutr Clin Pract* **27**, 613-623 (2012).

176. Fodde, R.*, et al.* Mutations in the APC tumour suppressor gene cause chromosomal instability. *Nat Cell Biol* **3**, 433-438 (2001).

177. Fearnhead, N.S., Wilding, J.L. & Bodmer, W.F. Genetics of colorectal cancer: hereditary aspects and overview of colorectal tumorigenesis. *Br Med Bull* **64**, 27-43 (2002).

178. Lin, D.I.*, et al.* Phosphorylation-dependent ubiquitination of cyclin D1 by the SCF(FBX4-alphaB crystallin) complex. *Mol Cell* **24**, 355-366 (2006).

179. Alt, J.R., Cleveland, J.L., Hannink, M. & Diehl, J.A. Phosphorylation-dependent regulation of cyclin D1 nuclear export and cyclin D1-dependent cellular transformation. *Genes Dev* **14**, 3102-3114 (2000).

180. Pietras, K. & Ostman, A. Hallmarks of cancer: interactions with the tumor stroma. *Exp Cell Res* **316**, 1324-1331 (2010).

181. Grabsch, H.*, et al.* Expression of DNA double-strand break repair proteins ATM and BRCA1 predicts survival in colorectal cancer. *Clin Cancer Res* **12**, 1494-1500 (2006).

182. Halvorsen, T.B. & Seim, E. Degree of differentiation in colorectal adenocarcinomas: a multivariate analysis of the influence on survival. *J Clin Pathol* **41**, 532-537 (1988).

183. Moll, R., Lowe, A., Laufer, J. & Franke, W.W. Cytokeratin 20 in human carcinomas. A new histodiagnostic marker detected by monoclonal antibodies. *Am J Pathol* **140**, 427-447 (1992).

184. Moll, R. [Cytokeratins as markers of differentiation. Expression profiles in epithelia and epithelial tumors]. *Veroff Pathol* **142**, 1-197 (1993).

185. Calon, A.*, et al.* Dependency of colorectal cancer on a TGF-beta-driven program in stromal cells for metastasis initiation. *Cancer Cell* **22**, 571-584 (2012).

186. Jones, S.*, et al.* Comparative lesion sequencing provides insights into tumor evolution. *Proc Natl Acad Sci U S A* **105**, 4283-4288 (2008).

187. Puntoni, M.*, et al.* A randomized, placebo-controlled, preoperative trial of allopurinol in subjects with colorectal adenoma. *Cancer Prev Res (Phila)* **6**, 74-81 (2013).

188. Olsson, M. & Zhivotovsky, B. Caspases and cancer. *Cell Death Differ* **18**, 1441-1449 (2011).

189. Gladden, A.B. & Diehl, J.A. Cell cycle progression without cyclin E/CDK2: breaking down the walls of dogma. *Cancer Cell* **4**, 160-162 (2003).

190. Loeb, K.R. & Chen, X. Too much cleavage of cyclin E promotes breast tumorigenesis. *PLoS Genet* **8**, (2012).

191. Mussolino, C. & Cathomen, T. On target? Tracing zinc-finger-nuclease specificity. *Nat Methods* **8**, 725-726 (2011).

192. Gaj, T., Gersbach, C.A. & Barbas, C.F., 3rd. ZFN, TALEN, and CRISPR/Cas-based methods for genome engineering. *Trends Biotechnol* (2013).

193. Itzkovitz, S., Blat, I.C., Jacks, T., Clevers, H. & van Oudenaarden, A. Optimality in the development of intestinal crypts. *Cell* **148**, 608-619 (2012).

194. Totafurno, J., Bjerknes, M. & Cheng, H. The crypt cycle. Crypt and villus production in the adult intestinal epithelium. *Biophys J* **52**, 279-294 (1987).

195. Dehmer, J.J.*, et al.* Expansion of intestinal epithelial stem cells during murine development. *PLoS One* **6**, (2011).

196. Kwong, L.N., Weiss, K.R., Haigis, K.M. & Dove, W.F. Atm is a negative regulator of intestinal neoplasia. *Oncogene* **27**, 1013-1018 (2008).

197. Medema, J.P. & Vermeulen, L. Microenvironmental regulation of stem cells in intestinal homeostasis and cancer. *Nature* **474**, 318-326 (2011).

198. Chen, L.C.*, et al.* Alteration of gene expression in normal-appearing colon mucosa of APC(min) mice and human cancer patients. *Cancer Res* **64**, 3694-3700 (2004).

199. Schwitalla, S.*, et al.* Intestinal tumorigenesis initiated by dedifferentiation and acquisition of stem-cell-like properties. *Cell* **152**, 25-38 (2013).

200. Hanahan, D. & Weinberg, R.A. Hallmarks of cancer: the next generation. *Cell* **144**, 646-674 (2011).